Disease-causing dysfunctions of barttin, an accessory subunit of ClC-K chloride channels

Von der Naturwissenschaftlichen Fakultät
der Gottfried Wilhelm Leibniz Universität Hannover
zur Erlangung des Grades

Doktorin der Naturwissenschaften

-Dr. rer. nat.-

genehmigte Dissertation
von

Audrey Gertruda Huberdina Janssen, M.Sc.
geboren am 8. Juli 1980, in Venray, Niederlande

2008

Referent: Prof. Dr. Christoph Fahlke
Korreferent: Prof. Dr. Anaclet Ngezahayo
Prüfer: Prof. Dr. Symeon Papadopoulos

Tag der Promotion: 15-August-2008

Contents

1. Introduction.. 1

1.1 Membrane proteins in the kidney and the inner ear.. 3
  1.1.1 Kidney.. 3
  1.1.2 Inner ear.. 4

1.2 Bartter Syndrome.. 5

1.3 ClC chloride channel / transporter family... 6
    1.3.1 ClC-1, ClC-2, ClC-Ka, ClC-Kb and barttin... 7
    1.3.2 ClC-3, ClC-4 and ClC-5.. 9
    1.3.3 ClC-6, ClC-7 and ostm1.. 10

1.4 ClC protein structure.. 10
    1.4.1 Structure of the transmembrane core... 10
    1.4.2 Structure of the cytoplasmic domain... 13

1.5 Barttin... 14
    1.5.1 The PY motif... 14
    1.5.2 Disease-causing barttin mutations... 15

1.6 Aim of this thesis.. 17

2. Materials and methods.. 19

2.1 Chemicals and materials.. 21

2.2 Alignment... 21

2.3 Molecular biology.. 21

2.3.1 Vectors.. 21

2.3.2 Mutagenesis.. 22

2.3.2.1 Primers and constructs.. 22

2.3.2.2 Quikchange: site directed mutagenesis.. 23

2.3.2.3 Polymerase Chain Reaction.. 24

2.3.3 Transformation.. 24

2.3.4 Plasmid recovery.. 25

2.3.4.1 Plasmid recovery.. 25

2.3.4.2 DNA concentration measurement.. 25

2.3.5 Agarose gel electrophoresis.. 25

2.3.6 DNA restriction.. 26

2.3.7 Gel extraction.. 26

2.3.7.1 Gel extraction.. 26

2.3.7.2 Glassmilk preparation.. 26

2.3.8 Ligation.. 27

2.3.9 DNA sequencing.. 27

2.3.9.1 DNA sequencing.. 27

2.3.9.2 Ethanol precipitation of sequenced DNA.. 28

2.3.10 LB medium, agar plates and antibiotics.. 28

2.3.11 Competent bacteria.. 28

2.4 Cell culture of mammalian cells.. 29

2.4.1 Cell lines, growth and splitting.. 29

2.4.2 Transfection.. 29

2.4.2.1 Lipofectamine.. 30

2.4.2.1 Calcium phosphate precipitation.. 30

2.4.3 Stable transfected MDCK cells.. 30

2.4.4 Freezing cells.. 31

2.4.5 Thawing cells.. 31

2.5 Electrophysiology.. 31

2.5.1 Cells.. 31

2.5.2 Setup.. 31

2.5.3 Microelectrodes... 32
2.5.4 Measure and reference electrode... 32
2.5.5 Gigaseal.. 32
2.5.6 Whole cell configuration and solutions..33
2.5.7 Data analysis...33

2.6 Fluorescence..34

2.7 Confocal imaging... 34
2.7.1 Experiments on fixed cells..34
2.7.2 Experiments on living cells.. 35

2.8 Protein Biochemistry...36
2.8.1 SDS polyacrylamide gel electrophoresis...36
2.8.2 2x SDS loading buffer.. 36
2.8.3 Western blotting..37
2.8.4 Deglycosylation.. 37
2.8.5 Scanning of fluorescent proteins on SDS gels...38
2.8.6 Biotinylation... 39
2.8.6.1 Complete cell biotinylation..39
2.8.6.2 Basolateral or apical cell membrane biotinylation..........................40

3. Results..45

3.1 The amino acid sequence is conserved in the amino terminal part of barttin.............. 47

3.2 Barttin mutants enable ClC-Kb exit from the endoplasmic reticulum.........................48
3.2.1 WT and mutant barttin enable complex glycosylation of ClC-Kb................48
3.2.2 Q32X and G47R barttin decrease ClC-Kb channel expression......................50

3.3 Most barttin mutants transport ClC-Kb to the plasma membrane................................51

3.3.1 G10S, E88X and WT barttin stimulate ClC-Kb insertion into the plasma membrane........ 51
3.3.2 Only Q32X barttin is inable to induce ClC-Kb membrane insertion............. 56
3.3.3 E88X barttin lacks the sorting mechanism of WT barttin............................. 58

3.4 Loss of protopore activation by most barttin mutants.. 59
3.4.1 Only E88X induces currents like WT barttin in human ClC-K isoforms.......59
3.4.2 All barttin mutants but Q32X invert the voltage dependence of activation of rat V166E ClC-K1..61

4. Discussion.. 67

4.1 Effect on endoplasmatic reticulum exit and channel stability......................................69

4.2 Insertion into the surface membrane.. 71
4.2.1 Intracellular versus Membrane localisation...71
4.2.2 Apical versus basolateral membrane insertion.. 72

4.3 Channel activation by WT and mutant barttin.. 73
4.3.1 Human isoforms...73
4.3.2 Rat ClC isoforms.. 74

4.4 Conclusions.. 75

4.5 Further research.. 75

5. Abstract 79

5.1 Abstract and keywords, Englisch.. 81
5.2 Zusammenfassung und Stichwörter, German...82

6. References 85

7. Acknowledgements 93

8. Curriculum vitae 95

9. List of publications 97

List of Figures and Tables

Figures

1.1 Membrane proteins in a cell from the thick ascending limb of Henle.......................... 4
1.2 Dendrogram of human ClC genes... 7
1.3 Representation of a ClC protein and the position of its 4 conserved regions................12

2.1 Scheme of the Quikchange reaction...23
2.2 Scheme of apical biotinylation of MDCKII cells grown on filters.............................. 41

3.1 Structure and conservation of barttin... 47
3.2 ClC-Kb is complex glycosylated only in the presence of barttin.................................48
3.3 All barttin mutants induce complex glycosylation of ClC-Kb.....................................49
3.4 G47R and Q32X lower the amount of ClC-Kb opposed to WT barttin........................51
3.5 Confocal images of fixed MDCK cells expressing WT or mutant CFP tagged barttin.51
3.6 Confocal images of fixed MDCK cells expressing YFP tagged ClC-Kb alone or with WT or mutant barttin CFP...52
3.7 Confocal images of living MDCK cells.. 52
3.8 Horizontal and vertical confocal images of living MDCK cells grown on dishes.......53
3.9 Confocal images and vertical slides of stably WT or E88X barttin CFP transfected polarized MDCK cells...55
3.10 Q32X does not colocalise in the membrane with rClC-K1..55
3.11 Only Q32X barttin is impaired in ClC-Kb membrane insertion................................ 57
3.12 E88X barttin lacks epithelial sorting.. 58
3.13 Only E88X barttin induces currents in human ClC-K channels as WT barttin...........59
3.14 Activation of the ClC-Kb protopore by WT, E88X and G47R barttin...................... 60
3.15 GK$^{V}/_{L}$GP motif in ClC-K channels.. 61
3.16 All barttin mutants but Q32X invert rat V166E ClC-K1 voltage dependence of activation.. 62
3.17 Barttin mutations, except G10S and E88X, affect the current amplitude of V166E ClC-K1.. 63

3.18 Non-stationary noise analysis of V166E rClC-K1 alone or in the presence of WT, R8L, G10S, G47R or E88X barttin.. 64

Tables

1.1 Mutations found in the *BSND* gene resulting in Bartter Syndrome type IV................. 16

2.1 Oligonucleotides used for Quikchange or pcr mutagenesis.. 22
2.2 Consistence of running and stacking gel of denaturing SDS gels.................................36
2.3 Reaction conditions for a deglycosylation assay...38

Abbreviations

A	Ampere
aa	amino acids
9-AC	9-anthracene-carboxylic acid
APS	Ammoniumpersulphate
ATPase	adenosine triphosphate-dependent ion pump
bp	basepairs
BP	Bandpassfilter
BS	Bartter Syndrome
BSA	Bovine serum albumine
CBS	Cystathionin-β-Synthase
CFP	Cyan fluorescent protein
CFTR	Cystic fibrosis transmembrane conductance regulator
ClC	Chloride channel
CMV	Cytomegalovirus
CPP	2-(p-chlorophenoxy)propionic acid
dG	Gibb's free energy
DIDS	4,4'-diisothiocyanatostilbene-2,2'-disulphonic acid
DMEM	Dulbecco´s Modified Eagle´s Medium
DNA	Desoxyribonucleic acid
dNTP	deoxyribonucleotide triphosphate
DTT	DL-dithiothreitol
EDTA	Ethylenediaminetetraacetic acid
EGTA	Ethylene glycol-bis(2-aminoethylether)-N,N,N',N'-tetraacetic acid
ER	Endoplasmic reticulum
E_{rev}	Reversal potential
E. coli	Escherichia coli
F	Faraday's constant ($9.648 * 10^4$ Coulombs mol^{-1})
FBS	Fetal Bovine Serum
HEPES	N-(2-hydroxyethyl)piperazine-N'-2-ethane sulfonic acid
IBS	Infantile Bartter Syndrome
IRES	Internal Ribosome Entry Site

kDa	kilodalton
k.o.	knock out
LB medium	Luria-Bertani-medium
MDCK	Madin-Darby Canine Kidney cells
MEM	Modified essential medium
MOPS	3-(N-morpholino)propanesulfonic acid
OD	Optical Density
p	Significance
p_o	Absolute open probability
PBS	Phosphate buffer saline
PCR	Polymerase Chain Reaction
R	Gas constant (8.315 J^{-1} K^{-1} mol^{-1})
R	rat
SAM	S-adenosylmethionine
SDS	Sodium dodecylsulphate
SP	Shortpassfilter
TEMED	N,N,N'-tetramethyl-ethylene diamine
T_m	Melting temperature
TAE	Tris-acetate-EDTA buffer
UV	Ultraviolet light
V	Voltage
WT	Wild type
YFP	Yellow fluorescent protein

1. Introduction

Bartter syndrome type IV is a disease that leads to deafness and mild to severe kidney insufficiency. It is important to understand the origin of this disease because although it is rare it is also very intrusive. This disease is part of a group of renal diseases (tubulopathies), Bartter syndromes. Type IV is the only Bartter syndrome that is accompanied by sensorineural deafness and is caused by mutations in the *BSND* gene, which encodes for barttin. This thesis aims to contribute to the molecular understanding of this disease via a detailed study of the barttin protein. The following sections will briefly introduce the relevant ion channels and transporters as they exist in the inner ear and the kidney.

1.1 Membrane proteins in the kidney and inner ear

1.1.1 Kidney

The membrane proteins affected in Bartter diseases are all present in the kidney in the thick ascending limb of Henle, which explains the kidney problems in these patients. Figure 1.1 shows a scheme of a cell from the thick ascending limb of Henle. Sodium and chloride ions are actively reabsorbed, thus creating an osmotic gradient that allows water reabsorbtion into the body (Hunter 2001). The energy for this active absorption is supplied by the breakdown of ATP molecules by the ubiquitous Na^+, K^+-ATPase. This protein is present in the basolateral membrane on the external surface of the tubule. It transports sodium ions out of the cell into the external fluid and potassium ions into the cell, thus reducing the intracellular sodium concentration and raising the potassium concentration. The sodium gradient provides the driving force for the NKCC2 co-transporter. This apical membrane protein imports Na^+, K^+ and two Cl^- ions. The excess of potassium and chloride ions leaves the cell via ion channels. ROMK (apical localisation) circulates potassium back to the lumen while chloride permeates through ClC-Kb on the basolateral side of the cell (Hunter 2001).

The exit of chloride on the basolateral side and potassium at the apical side of the cell creates a lumen-positive electrical potential, driving paracellular transport of calcium, magnesium and some sodium from lumen into the blood. The calcium sensing receptor (CaSR) is activated by high concentrations of extracellular calcium or magnesium. It inhibits ROMK and possibly NKCC2 and Na^+, K^+-ATPase, which in turn leads to a decreased NaCl reabsorption and thus an increased calcium and magnesium excretion (Hebert 2003; Zelikovic 2003).

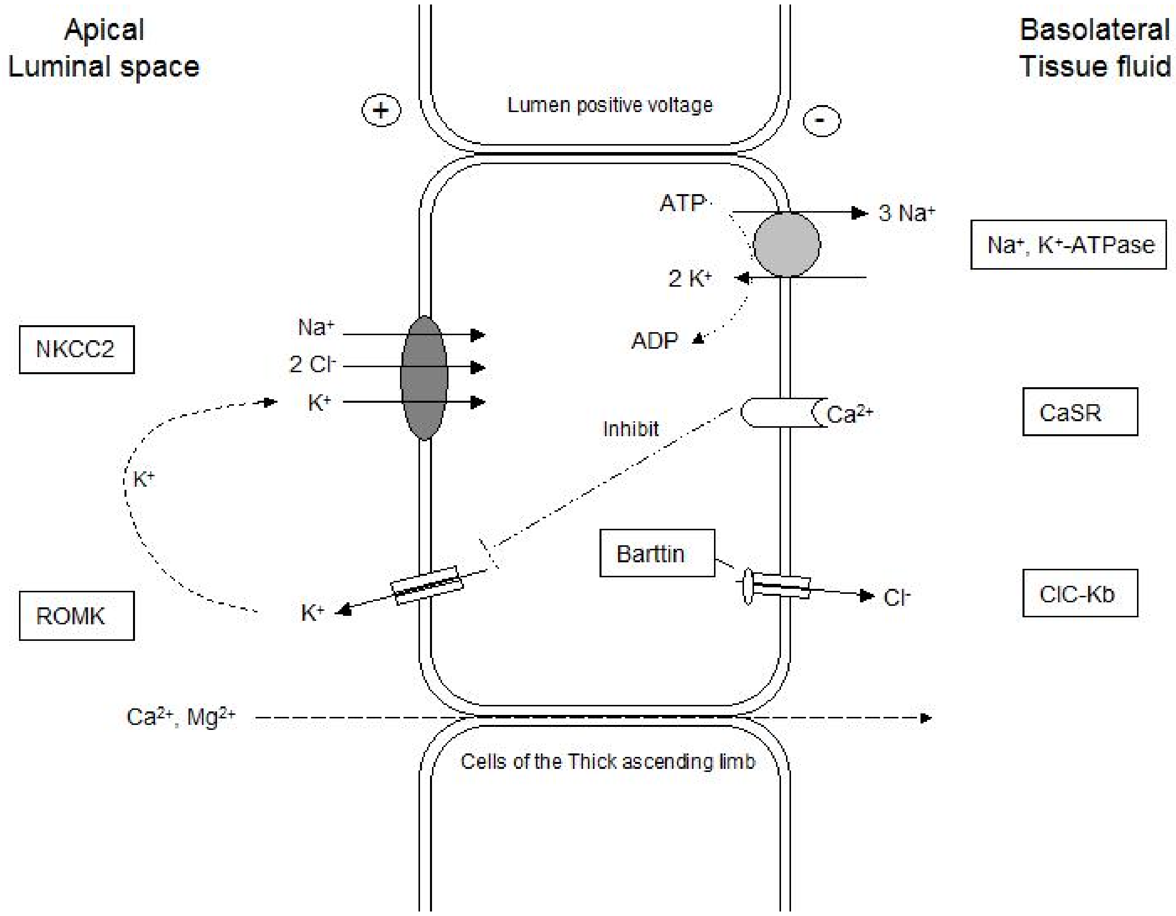
Apical
Luminal space
Basolateral
Tissue fluid
+
Lumen positive voltage
-
ATP
3 Na+
Na+, K+-ATPase
2 K+
ADP
NKCC2
Na+
2 Cl-
K+
CaSR
Ca2+
Inhibit
K+
Barttin
ROMK
K+
Cl-
ClC-Kb
Ca2+, Mg2+
Cells of the Thick ascending limb

Figure 1.1 Membrane proteins in a cell from the thick ascending limb of Henle (Hunter 2001; Hebert 2003; Zelikovic 2003; D'Souza-Li 2006).

The second human ClC-K isoform, ClC-Ka, is expressed on the apical and basolateral sides of cells in the thin ascending limb which makes this section of the kidney highly permeable to sodium and chloride but not to water. This is opposed to the thin descending limb which exhibits a high osmotic permeability for water but less to chloride (Uchida, Sasaki et al. 1995).

1.1.2 Inner ear

Bartter syndrome type IV also results in deafness, caused by disfunction of the ClC-K channels in the potassium secreting tissue in the inner ear. In the stria vascularis in the inner ear, a similar mechanism as in the thick ascending limb of Henle can be found. Na^+, K^+-ATPase transports potassium out of the intersitium into the cell while reducing the intracellular sodium concentration. NKCC1 is present on the same cell side where it imports Na^+, K^+ and two Cl^- ions while excess intracellular chloride recirculates back to the interstitium through both ClC-Ka and ClC-Kb. Potassium is released from the cell through potassium channels (KCNQ1/KCNE1) into the endolymph, leading to the high potassium level that is necessary for the excitability of the sensory hair cells (Hunter 2001). Genetic defects in several channels and transporters that are critical for the maintenance of high potassium in the endolymph are associated with deafness (Birkenhager, Otto et al. 2001; Estévez, Boettger et al. 2001; Hunter 2001). ClC-K chloride channels are vital in both kidney and the inner ear since the accumulation of chloride in the cell would oppose further ion uptake (Hunter 2001).

1.2 Bartter syndrome

Bartter syndrome type IV is one of five renal diseases (tubulopathies) that belong to the group of Bartter syndromes that were first described by Frederic C. Bartter in 1962 (Bartter, Pronove et al. 1962). These tubulopathies are characterized by renal salt wasting, elevated renin and aldosterone levels with normal or low blood pressures and a low amount of potassium in the blood leading to an elevated blood pH (hypokalemic metabolic alkalosis) (Brennan, Landau et al. 1998).

Bartter types I, II, III and IV show autosomal recessive inheritance and are caused by inactivating mutations in the sodium potassium chloride co-transporter NKCC2 (*SLC12A1*), the potassium channel ROMK (*KCNJ1*), chloride channel ClC-Kb (*CLCNKB*) and barttin (*BSND*) which is an accessory protein of ClC-K chloride channels, respectively. Type V is caused by a gain of function mutation in the calcium sensing receptor CaSR, resulting in an abnormal low amount of calcium in the blood, leading to autosomal dominant hypocalcaemia (D'Souza-Li 2006; Kitananka, Sato et al. 2006). Two Bartter syndrome type IV patients have been reported to have no mutations in barttin but in both the ClC-Ka and ClC-Kb chloride channel (Schlingmann, Konrad et al. 2004; Nozu, Inagaki et al. 2008).

Bartter syndromes type I and II are neonatal / antenatal / infantile Bartter syndromes (IBS, also reported as hyperprostaglandin E syndrome). Type III is the classic form that starts at early infancy. It is often difficult to distinguish this type from other Bartter variants and Gitelman´s syndrome (Zelikovic 2003), which is caused by mutations in the thiazide-sensitive Na^+-Cl^- cotransporter NCCT (*SLC12A3*) (Brennan, Landau et al. 1998; Fukuyama, Hiramatsu et al. 2004). Type IV is IBS with sensorineural deafness (Kitananka, Sato et al. 2006). IBS is considered to be the most severe Bartter variant (Konrad, Vollmer et al. 2000; Miyamura, Matsumoto et al. 2003; Zelikovic 2003).

Bartter syndrome type IV is rare, occuring at one of a million live births (Hunter 2001). The affected *BSND* gene was found on chromosome 1p (Brennan, Landau et al. 1998; Vollmer, Jeck et al. 2000; Birkenhager, Otto et al. 2001). Patients are reported to have at least some of the following symptoms: too much amniotic fluid in the pregnant uterus (mild or severe polyhydramnios), triangular face, large eyes, protruding ears, rapid breathing (tachypnea, more than 20 breaths per min.) and retractions, renal salt wasting, to much aldosterone production due to an increased renin level (hyper-reninemic hyperaldosteronism), hypokalemic metabolic alkalosis, impaired renal function, bilateral sensorineural deafness, large volumes of urine (polyuria), failure to thrive (lack of growth, flourish), abnormal deposition of calcium salts in the nephron (nephrocalcinosis), muscle weakness, (severe) muscle hypotonia, developmental delay. Interestingly no balance problems were reported (Estévez, Boettger et al. 2001). The absence of hypomagnesaemia in antenatal Bartter syndrome could be explained by additional stimulation of magnesium reabsorption in the distal convoluted tubule, induced by the high level of aldosterone that is typical in this disease (Hebert 2003; Zelikovic 2003).

A common polymorphism of ClC-Kb, the T481S substitution, activates the channel (Jeck, Waldegger et al. 2004) and has been suggested to be involved in hypertensive blood pressure (Jeck, Waldegger et al. 2004) however this has been debated (Kokubo, Iwai et al. 2005; Fava, Montagnana et al. 2007). It has also been shown to protect against hearing loss (Frey, Lampert et al. 2006). Common genetic ClC-Ka variants have been reported to be associated to salt sensitive hypertension (Barlassina, Dal Fiume et al. 2007). Two *BSND* polymorphisms, V43I and G284D, resulted in a partial loss of function and smaller human ClC-K currents. E255Q barttin is shown to function like WT (Sile, Vanoye et al. 2006; Sile, Gillani et al. 2007). V43I barttin was suggested to protect against hypertension (Sile, Vanoye et al. 2006) however, this did not seem to be the case (Sile, Gillani et al. 2007).

1.3 ClC chloride channel / transporter family

ClC-K chloride channels belong to the ClC family which consists of two subclasses; plasma membrane chloride channels (ClC-0, 1, 2, Ka and Kb) and vesicular Cl^-/H^+ exchangers (ClC-3 to ClC-7). Their gating can be converted by strategic mutations, which makes the boundary between the two types thin (Pusch, Zifarelli et al. 2006; Sile, Vanoye et al. 2006). There are many differences between members of this family but most of them have anion over cation selectivity and a block of chloride current by larger anions like I^-, SCN^- and other organic anions. There is a strong coupling between ion conduction and gating. The permeating chloride ion influences the open probability by binding in the pore (Dutzler, Campbell et al. 2002). There are two known accessory proteins in the human ClC family; barttin which acts on ClC-K channels and Ostm-1 which interacts with ClC-7 (Lange, Wartosch et al. 2006).

ClC proteins are found in bacteria, yeast, plants and animals (Maulet, Lambert et al. 1999). Prokaryotic ClC genes form a distinct branch in the ClC family. Some prokaryotes have no ClC genes while others might have up to two, leading to proteins which should reside in the outer membrane since they lack intracellular membranes (Jentsch, Friedrich et al. 1999). The kidney contains 8 of the 9 ClC proteins found in humans (Briet, Vargas-Poussou et al. 2005) and only lacks ClC-1 (Uchida 2000; Uchida and Sasaki 2005). ClC-5, ClC-Ka, ClC-Kb and barttin are primarily expressed in the kidney where they participate in urinary concentration, transepithelial salt transport and endosomal acidification (Sile, Vanoye et al. 2006). Figure 1.2 displays a dendrogram of human ClC genes that are sorted into three groups with less than 30% homology between them. Also shown are the organs in the proteins can be found, the function of the protein and the disease that is caused by mutations (Jentsch, Friedrich et al. 1999; Fahlke 2001).

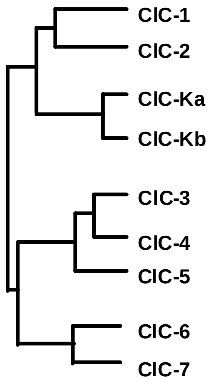

	expression	function	disease
ClC-1	skeletal muscle	stabilization of membrane potential	myotonia congenita
ClC-2	ubiquitous	cell volume regulation?, limitation of intracellular [Cl^-], transepithelial Cl^- -transport	idiopathic generalized epilepsie***
ClC-Ka	kidney, inner ear	transepithelial Cl^- -transport	diabetes insipidus in k.o. mice*
ClC-Kb	kidney, inner ear	transepithelial Cl^- -transport	Bartter‘s syndrome Type III
ClC-3	ubiquitous	cell volume regulation, acidification of endosomes or synaptic vesicles	
ClC-4	ubiquitous	?	
ClC-5	kidney, brain, liver, gut	acidification of intracellular vesicles	Dent‘s disease
ClC-6	ubiquitous	?	
ClC-7	ubiquitous	acidification of lysosomes or reabsorbtion lacune from osteoclasts	osteopetrosis **

Figure 1.2 Dendrogram of human ClC genes (in protein nomentclature). Shown are their organs of expression, probable function of the protein and disease in case of mutations. The figure is modified from (Jentsch, Friedrich et al. 1999) by (Blanz and Zdebik 2004) while * = (Matsumura, Uchida et al. 1999; Akizuki, Uchida et al. 2001), ** = (Lange, Wartosch et al. 2006), *** = (Haug, Warnstedt et al. 2003).

1.3.1 ClC-1, ClC-2, ClC-Ka, ClC-Kb and barttin

This branch of channels reside in the plasma membrane (Blanz and Zdebik 2004). ClC-1 is primarily expressed in skeletal muscle (Jentsch, Friedrich et al. 1999; Blanz and Zdebik 2004) where it is essential for the electrical stability of the muscle plasma membrane. Activation takes place upon depolarisation. In contrast to other cell types, the muscle cells resting conductance is dominated by the chloride conductance. Chloride thus plays a similar role as the potassium conductance in other cells and stabilizes the resting potential. A loss of chloride conductance impairs the repolarization of action potentials, so that sodium channels can recover from their inactivation when the membrane potential is still slightly depolarized, leading to a train of action potentials upon a single stimulus. Disfunction of ClC-1 results in myotonia congenita, a defect in muscle relaxation which can be inherited as an autosomal recessive (Becker type) or autosomal dominant (Thomsen type) disease (Jentsch, Friedrich et al. 1999).

ClC-2 is activated by acidic extracellular pH, cell swelling or strong hyperpolarization. ClC-2 is expressed early in development and has been speculated to be important in several cell types (Jentsch, Friedrich et al. 1999). ClC-2 knock out (k.o.) mice suffer from degenerated retina and germinal epithelial (Blanz and Zdebik 2004). Mutations in ClC-2 are associated with idiopathic generalized epilepsy in humans (Haug, Warnstedt et al. 2003).

ClC-Ka, ClC-Kb and barttin are expressed in plasma membranes from cells in the kidney and the inner ear. Human ClC-K isoforms are 90% homologue, which is more than the approximate 80% homology to their rat homologues ClC-K1 and ClC-K2. ClC-K channels were also found in rabbit, mouse, *Oeochromis mossambicus* (tilapia) and *Xenopus leavis* (Jentsch, Friedrich et al. 1999; Waldegger and Jentsch 2000; Uchida and Sasaki 2005). Early attempts to characterize the functional properties of ClC-K2, ClC-Ka and ClC-Kb but not of ClC-K1 in heterologues expression systems failed. Though ClC-K1 was able to give small currents in the absence of barttin, only after the discovery of barttin the two human isoforms could be functionally expressed (Estévez, Boettger et al. 2001; Krämer, Bergler et al. 2008). These ClC channels have little voltage dependence (Blanz and Zdebik 2004). ClC-K1 in oocytes showed no gating and opened at any membrane voltage, though the channel is slightly outward rectifying, chloride ions were able to pass in both directions. This enables a high chloride permeability in the thin ascending limb (Uchida, Sasaki et al. 1995). ClC-K1 k.o. mice suffer from diabetes insipidus (Matsumura, Uchida et al. 1999; Akizuki, Uchida et al. 2001), mutations in ClC-Kb (Simon, Bindra et al. 1997; Konrad, Vollmer et al. 2000; Waldegger and Jentsch 2000; Fukuyama, Hiramatsu et al. 2004) lead to Bartter syndrome type III and in barttin to Bartter syndrome type IV. Disfunction of one of the channels results in kidney disease. If both channels together or barttin is affected there is additional deafness.

The *BSND* gene is transcribed in the thin limb and the thick ascending limb of the loop of Henle in the kidney and in the dark cells of the inner ear (Birkenhager, Otto et al. 2001). The barttin protein that it encodes, colocalizes with ClC-Ka and Kb (Birkenhager, Otto et al. 2001; Miyamura, Matsumoto et al. 2003). In *Xenopus leavis* (Maulet, Lambert et al. 1999) and rat (Kieferle, Fong et al. 1994) ClC-K RNA transcripts were solely found in the kidney, while in transgenic mice the ClC-Kb promoter was sufficient for the expression of enhanced green fluorescent protein (EGFP) in specific cell types of both the kidney and the inner ear (Kobayashi, Uchida et al. 2002). Although Vandewalle *et al.* located ClC-K isoforms predominantly to basolateral membranes of the thick ascending limb and other parts of the nephron (Vandewalle, Cluzeaud et al. 1997; Jentsch, Friedrich et al. 1999; Uchida and Sasaki 2005) usually ClC-K1 and ClC-Ka were found in the thin ascending limb of Henle's loop on apical and basolateral plasma membranes, consistent with the high chloride ion permeation of this nephron segment (Uchida, Sasaki et al. 1995; Hebert 2003; Uchida and Sasaki 2005). Though rClC-K1 and barttin were also reported to be expressed throughout the distal nephron predominantly in the cortical thick ascending limb, distal convolute tubule and the cortical collecting tubule (Kieferle, Fong et al. 1994; Waldegger, Jeck et al. 2002). Several studies also differed in the localization of rClC-K2 and ClC-Kb however a commonality is the location of the protein at the basolateral side of epithelial cells of the thick ascending limb and at other more distally located nephron segments (Kieferle, Fong et al. 1994; Uchida 2000; Waldegger and Jentsch 2000; Akizuki, Uchida et al. 2001; Birkenhager, Otto et al. 2001; Estévez, Boettger et al. 2001; Hunter 2001; Waldegger, Jeck et al. 2002).

1.3.2 ClC-3, ClC-4 and ClC-5

Amino acid sequences of ClC-3, 4 and 5 are 80% homologous. There is only 35% homology to the other branches of the ClC-channel and transporter family (Jentsch, Friedrich et al. 1999; Blanz and Zdebik 2004). Bacterial ClCec-1, ClC-3, ClC-4 and ClC-5 are estimated to exchange Cl^- to H^+ in a ratio of 2:1 which may partially dissipate the proton gradient generated by H^+-ATPases (Pusch, Zifarelli et al. 2006; Sile, Vanoye et al. 2006; Matsuda, Filali et al. 2008). These Cl^-/H^+ exchangers are mostly expressed in endosomes. The H^+-ATPase imports protons into the vesicle, creating a charge import that has to be neutralised by chloride import (Blanz and Zdebik 2004).

ClC-3 and ClC-4 are expressed in numerous tissue, including brain and kidney (Jentsch, Friedrich et al. 1999). ClC-3 k.o. mice suffer from degeneration of the hippocampus and the retina. This protein is of importance in the acidification of synaptic vesicles (Blanz and Zdebik 2004). Expression of ClC-3 has proven difficult and conflicting electrophysiological results were yielded (Jentsch, Friedrich et al. 1999). In mouse it was preferentially expressed in the nervous system, intestine and kidney but was also present in liver, lung, skeletal muscle and heart (Schmieder, Lindenthal et al. 2001).

ClC-5 is primarily expressed in renal cells with a high rate of endocytosis. It is thought to colocalize with the proton pump in intracellular vesicles however conflicting results were obtained. A cell surface localization of 4-8% was detected (Schmieder, Bogliolo et al. 2007). Disruption of the ClC-5 gene leads to Dent's disease (Jentsch, Friedrich et al. 1999; Uchida 2000; Blanz and Zdebik 2004; Briet, Vargas-Poussou et al. 2005), an X-linked disorder that results in low-molecular-weight proteinuria, higher phosphate secretion (Blanz and Zdebik 2004) and hypercalciuria which can lead to secondary symptoms like kidney stones, nephrocalcinosis and renal failure (Jentsch, Friedrich et al. 1999). In k.o. mice, endosomes took longer to acidify which could explain a decrease in endocytosis (Blanz and Zdebik 2004; Sile, Vanoye et al. 2006). Low molecular weight proteins can normally pass through the glomerular filter, into the primary urine. By endocytosis they are reabsorbed by proximal tubular cells and are targeted to lysosomes for degradation. These vesicles are acidified after budding from the plasma membrane and during trafficking to the lysosomes. Acidification is performed by a proton pump, transporting protons and thus charge into the vesicle. ClC-5 is necessary to limit the positive voltage across the vesicle membrane so that this does not limit the acidification process (Jentsch, Friedrich et al. 1999).

1.3.3 ClC-6, ClC-7 and ostm-1

The amino acid sequences of ClC-6 and ClC-7 are 40% identical, but only 25-30% to the other ClC branches. Both are expressed ubiquitously and are present early in mouse development (Jentsch, Friedrich et al. 1999). Ostm-1 is an accessory protein for ClC-7. Mutations in the OSTM1 or ClC-7 gene, result in severe osteopetrosis and lysosomal storage disease. In k.o. mice also retinal and central nervous system degeneration was found, which is related to lysosomal storage disease. The proteins colocalize in late endosomes and lysosomes and in the ruffled border of bone-reabsorbing osteoclasts. Lysosomes are exocytosed in the ruffled border, thus releasing hydrolases in the acidic resorption lacune. An acidic pH activates the hydrolases which dissolve the anorganic parts of the bone. ClC-7 deficient osteoclasts are disrupted in this acidification resulting in more bone growth than reabsorbtion (Blanz and Zdebik 2004; Lange, Wartosch et al. 2006).

1.4 ClC protein structure

1.4.1 Structure of the transmembrane core

The ClC study started over 30 years ago when Miller discovered and characterised (Miller 1982) the chloride channel in the electric organ of the *Torpedo marmorata* (ClC-0), its expression cloning resulted in the first gene identified to encode for a voltage-gated chloride channel (Jentsch, Steinmeyer et al. 1990). Miller predicted them to have two parallel independent pores (a double barrelled channel) (Dutzler, Campbell et al. 2002). ClC proteins have indeed been shown to be dimers, both subunits containing an ion translocation pore (Meyer and Dutzler 2006). They consist of 18 membrane helices. This was difficult to distinguish by protein biochemistry due to their orientation and not complete spanning of the membrane. The human cytoplasmic c-terminus consists of two CBS domains which seem to be essential for function and could be involved in targeting of the protein (Jentsch, Friedrich et al. 1999; Dutzler, Campbell et al. 2002). CBS domains were first found in the enzyme cystathionine-β-synthetase, hence the name CBS.

The X-ray structure of the Cl^--H^+-antiporter from *Escherichia coli* (*E. coli* with the ecCLC protein) provides a structural framework for the membrane spanning domain (Dutzler, Campbell et al. 2002; Meyer and Dutzler 2006; Pusch, Zifarelli et al. 2006) though it lacks a cytoplasmic tail. The X-ray structures of *Salmonella enterica* serovar *typhimurium* and *E. coli* reveal two identical pores, each formed by a separate subunit from this dimeric membrane protein. The individual subunits are formed by two roughly repeated halves that span the membrane in opposite orientations. Each subunit forms its own independent pore and selectivity filter by contributing residues from different parts of the protein to form a selectivity filter for chloride ions in the centre of the membrane. In this regard ClC chloride proteins resemble porins, aquaporins and bacteriorhodopsin rather than the cation channel family (Dutzler, Campbell et al. 2002; Dutzler 2006; Meyer and Dutzler 2006).

ClC channels have high rates of selective ion conduction and a regulatory domain that controls the opening and closing of the pore in response to external stimuli (Meyer and Dutzler 2006). There is a fast gate that operates on the single pores and a common slow gate affecting both pores simultaneously (Jentsch, Friedrich et al. 1999). Gating of the individual pore occurs in proximity of the selectivity filter while the mechanism of the common gate is currently not understood (Meyer and Dutzler 2006).

The ion binding site of one subunit is formed by 4 different regions which are highly conserved in the ClC family; GSGIP, G(K/R)EGP, GXFXP and a tyrosine. These sequences occur at the polypeptide loops at the N-terminus of α-helices that point with there N-terminus to the binding site and create an electrostatic favourable environment for anion binding, because of the aminoterminal positive end charge (Dutzler, Campbell et al. 2002; Dutzler 2006).

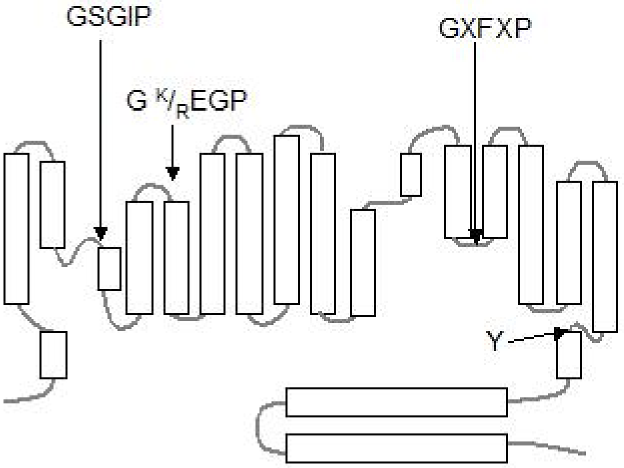

Figure 1.3 Representation of a ClC protein and the position of its 4 conserved regions (Dutzler 2006).

GKxGPxxH is present in all ClC family members as a GKEGP motif, except in ClC-K. The human ClC-K isoforms have a valine instead of the glutamate, as does rat ClC-K1. Rat ClC-K2 exhibits a leucine at this place (Fahlke, Yu et al. 1997). The fast gate of ClC-0 appeared to stay open when the glutamic acid was mutated to alanine (Traverso, Elia et al. 2003) while the reversed mutation in ClC-K1 results in a strong voltage dependent gating (Uchida and Sasaki 2005). The WT rClC-K1 channel also has a fast and slow gate (Fischer, Janssen et al. 2008). GKEGP is shown to influence ion selectivity and gating (Waldegger and Jentsch 2000) which might explain the lack of time-dependent gating in ClC-K channels (Sile, Vanoye et al. 2006). Crystallographic studies on the *E. coli* ClC protein showed the ClC selectivity filter as a narrow region containing three chloride binding sites that can be occupied simultaneously in the open conformation, but only two in the closed state. The most external binding site is occupied by a conserved glutamate side residue (present in the GKEGP motif) when it is deprotonated. When protonated, the side chain moves out of the pathway, allowing the third chloride to bind. This movement might correlate with fast gating in eukaryotic ClC channels and gives some explanation for the coupling of external pH and channel activation. Mutation of the external glutamic acid makes channels unable to close and transporters lose their ability to transport protons.

An intracellular facing glutamate is present in ClC transporters and is identified to be critical for H^+ translocation but not for chloride permeation. ClC channels exhibit a valine instead of a glutamate at the hologe position (Jentsch, Friedrich et al. 1999; Dutzler, Campbell et al. 2002; Blanz and Zdebik 2004; Dutzler 2006; Sile, Vanoye et al. 2006).

Some ClC channel blockers and activators have been identified. NPPB (5-nitro-2-(3-phenylpropylamino)-benzoate) inhibits ClC-K1 (Lui, Morimoto et al. 2002). Phenylbenzofuran carboxilic acid derivates inhibit ClC-Ka and Kb but no other ClC proteins (Pusch, Zifarelli et al. 2006; Liantonio, Picollo et al. 2008). DIDS (4,4'-diisothiocyanatostilbene-2,2'-disulphonic acid), 9-AC (9-anthracene-carboxylic acid) and derivates of CPP (2-(p-chlorophenoxy)propionic acid) block ClC-0 and ClC-1 (Pusch, Zifarelli et al. 2006), ClC-K1, ClC-Ka and Kb (Uchida, Sasaki et al. 1995; Fong 2004; Liantonio, Pusch et al. 2004; Picollo, Liantonio et al. 2004; Liantonio, Picollo et al. 2006; Pusch, Zifarelli et al. 2006; Sile, Vanoye et al. 2006). CPP had no effect on ClC-2 or ClC-5 (Fong 2004; Pusch, Zifarelli et al. 2006).Fenamates can activate or inhibit ClC-K channels in a dose-dependent manner. Both isoforms are activated by niflumic acid (10-100µmol/l) whereas flufenamic acid derivates or high concentration niflumic acid inhibit ClC-Ka and maybe ClC-Kb (Liantonio, Pusch et al. 2004; Liantonio, Picollo et al. 2006; Sile, Vanoye et al. 2006; Liantonio, Picollo et al. 2008).

1.4.2 Structure of the cytoplasmic domain

In vertebrates, the c-terminal cytoplasmic tail can range from 160 to 315 amino acids, this difference in length is due to the different lengths of the linker between the two CBS domains and the sequence after the last CBS domain (the C-peptide) (Meyer and Dutzler 2006). Human ClC proteins contain 2 CBS domains but most prokaryotic homologues lack a long cytoplasmic c-terminus and CBS domains, though some contain up to two (Jentsch, Friedrich et al. 1999). The role of these domains is still largely unknown but they seem to be involved in the gating mechanism and may bind ATP, thereby regulating the ion permeation and transport. They have been suggested to be involved in ClC protein function, cellular localization, protein trafficking and might act as sensors for cellular energy status (Meyer and Dutzler 2006; Sile, Vanoye et al. 2006). In ClC-1 the carboxy terminus is shown to be necessary for channel function but not for intracellular trafficking (Hebeisen, Biela et al. 2004).

X-ray crystallography clarified the structure of the cytoplasmic tail of the *Torpedo marmorata* chloride channel which revealed two CBS subdomains with tight interaction. The 96 amino acid mobile linker between these domains was disordered in the crystals and the C-peptide was removed before crystallization. The domains were monomeric in crystals, opposed to a dimeric structure of the transmembrane ClC pore domain and CBS dimerisation in solution. This monomerisation could be a result of the high salt concentration present during crystalization (Meyer and Dutzler 2006).

1.5 Barttin

Barttin has been predicted to have two putative membrane spanning domains at the amino terminal side of the protein and a long cytoplasmic tail. Both termini are intracellular. The first membrane helix is a putative signal peptide (Birkenhager, Otto et al. 2001; Waldegger, Jeck et al. 2002). It has been shown that ClC-K1 and Kb are retained in the ER (Scholl, Hebeisen et al. 2006) and ClC-K2 in the golgi apparatus (Hayama, Rai et al. 2003) in the absence of barttin while membrane insertion and current amplitudes are higher in the presence of this β-subunit. The N-terminal part of barttin until amino acid (aa) 61 or 71 is necessary for ClC-Kb chloride currents while a smaller part of barttin consisting of the first 54-57aa is sufficient for ClC-Kb membrane staining in confocal images. ClC-K1 already increased current amplitudes in the presence of the first 54aa of barttin. Though, 61-71aa were needed to change the single channel amplitude of V166E rClC-K1 like WT barttin, the complete c-terminal tail of barttin influenced the absolute open probability of this channel. The cytoplasmic tail in the absence of the two transmembrane domains was not able to increase ClC-Kb or ClC-K1 currents or to traffick to the plasmamembrane (Scholl, Hebeisen et al. 2006). These data emphasize the importance of the two transmembrane helices of barttin in comparison to the cytoplasmic tail.

1.5.1 The PY motif

Renal ClC channels have been shown to interact with protein ubiquitin ligases from the neural precursor cell-expressed developmentally down-regulated 4 (Nedd4) family. Mammalian ClC-5 contains a proline rich peptide sequence (PPLPPY) resembling a PY motif found in the apical epithelial sodium channel (ENaC), which is well characterized as an interaction site of Nedd4 and related WW domain proteins. ClC-5 interacts with Nedd4-2 which modulates its cell membrane expression. This is dependent on an intact PY motif which was shown to be involved in ClC-5 internalisation. No PY motif is present in amphibian xClC-5 (Estévez, Boettger et al. 2001; Kamynina and Staub 2002; Sile, Vanoye et al. 2006; Schmieder, Bogliolo et al. 2007).

Nedd4-2 may regulate cell surface expression of ClC-Ka/barttin channels. Coexpression of Nedd4-2 decreased ClC-Ka/barttin induced currents and cell surface expression in *Xenopus* oocytes which was dependent upon an intact PY motif in the barttin c-terminus (amino acids 94 to 98). This effect could be reversed by co-expression of serum and glucocorticoid inducible kinases (SGK1, SGK3 but not SGK2). SGK phosphorylates Nedd4-2, thus inactivating this ubiquitin ligase. SGK1 transcription is under regulation of hormones like glucocorticoids, mineralcorticoids, insulin and IGF-1. Like SGK1, SGK3 is also activated by IGF1, insulin and oxidative stress (Embark, Böhmer et al. 2004; Sile, Vanoye et al. 2006). SGK1 k.o. mice are like normal mice under regular conditions, but have an insufficient adaptation to a salt free diet. ClC-Ka also posesses a SGK1 consensus site (Embark, Böhmer et al. 2004).

Y98A barttin contains a disrupted PY motif and has been reported to give intense staining of the plasma membrane and no intracellular retention, opposed to WT barttin which showed additional intracellular staining. This implicates a higher stability of the mutated barttin (Hayama, Rai et al. 2003). This particular mutation also enhances the stimulatory effect of barttin on ClC-Kb channels, similar as for the Na^+ channel ENaC and the ClC-5 chloride channel (Estévez, Boettger et al. 2001; Kamynina and Staub 2002).

1.5.2 Disease-causing barttin mutations

Table 1.1 shows the known mutations in the *BSND* gene that cause Bartter syndrome type IV, the age of the patient when diagnosed, the amount of weeks of pregnancy and whether or not the disease resulted in end-stage renal failure. Remarkably a homozygous loss of the start codon described by Ozlu *et al.* resulted in unilateral sensorineural deafness. The heterozygous Q32X G47R mutation leads to mild perinatal clinical features, similar to those of a patient with homozygous G47R. However, there was severe renal failure that was probably caused by the Q32X deletion. Patients homozygous for G47R were usually diagnosed late because of their mild symptoms. Although the symptoms are more severe than for G47R, G10S mutations also do not lead to major long-term deterioration in kidney function. Extraordinary was the 10 year old male described in García-Nieto *et al.* who, at the age of 1 year, suffered from 70% hearing loss (García-Nieto, Flores et al. 2006). In a correspondence with George Deschênes it was cleared that R8L mutated patients did not suffer renal endstage failure.

Table 1.1 Mutations found in the *BSND* gene resulting in Bartter syndrome type IV.

Mutation	Age at discovery	Born (weeks)	End-stage renal failure	Literature
Substitution in splice site	birth	33	26 months	[A]
Loss exon	3 months	30	Chronic renal failure	[B] F708 [C] IV-1
	birth	30	Chronic renal failure	[B] F708 [C] IV-2
Loss of start codon	49 days	30	Chronic renal failure	[J]
	birth	37	Chronic renal failure	[A]
	birth	28	Chronic renal failure	[B] F314 [C] V-1
	birth	33	4 years	[B] F730 [C] VI-1
	birth	31	Chronic renal failure	[B] F786 [C] II-1
	birth	27	Death 3.5 years	[B] F791 [C] III-1
	birth	31	Chronic renal failure	[B] F791 [C] III-2
R8L				[B]
R8W				[B]
G10S	Birth	38		[B] F542 [D,E] [F] V-1
	15 days	32		[B] F542 [D,E] [F] V-2
	15 days	31		[B] F542 [D,E] [F] V-3
	3.5 years	33		[B] F542 [D,E] [F] V-4
	15 years	33		[B] F542 [D,E] [F] V-5
G47R	20 years			[G]
	28 years	40		[H]
	10 years	36		[I]
	-	31		[I]
	21 years	32		[I]
	14 years	normal		[I]
E88X	Soon after birth	31		[J]
Q32X+ G47R	1 year, 8 months	37	15 years	[K]

References are shown between brackets, the individual or family numbers are given immediately after the respective reference. References are: A=(Zaffanello, Taranta et al. 2006), B=(Birkenhager, Otto et al. 2001), C=(Jeck, Reinalter et al. 2001), D=(Brennan, Landau et al. 1998), E=(Shalev, Ohali et al. 2003), [F]= (Landau, Shalev et al. 1995), [G]= (Brum, Rueff et al. 2007), [H]= (Miyamura, Matsumoto et al. 2003), [I]= (García-Nieto, Flores et al. 2006), [J]= (Ozlu, Yapicioglu et al. 2006), [K]= (Kitananka, Sato et al. 2006)

1.6 Aim of this thesis

Barttin is an accessory subunit of ClC-K chloride channels and is affected in patients suffering from Bartter syndrome type IV. The goal of this thesis was to understand how disease causing mutations in the *BSND* gene affect the barttin protein in its trafficking to the membrane and its ClC-K chloride channel activating properties. All previously reported mutations were investigated: R8L, R8W, G10S, Q32X, G47R and E88X barttin. The experiments in this thesis were performed in mammalian cell lines, either a human embryonic kidney cell line (tsA201) or Madin-Darby Canine Kidney (MDCK). All known *BSND* mutations were subject to confocal imaging to visualise trafficking. Electrophysiology was performed for functionality assays while protein biochemistry gave additional information on trafficking properties. The two human ClC-K isoforms, ClC-Ka and Kb, were evaluated as well as the V166E mutated rat ClC-K1.

2. Materials and methods

2.1 Chemicals and materials

All chemicals and solutions were at least purity p.A. and were obtained from companies; Sigma-Aldrich (Germany), BioRad (Muenchen), Gibco (Eggenstein), Merck (Darmstadt), Fluka (Neu-Ulm), Roth (Karlsruhe), New England Biolabs (Frankfurt), Serva (Heidelberg) and Calbiochem (Bad Soden). Materials were from Millipore (Eschborn), Eppendorf (Hamburg), Schott Glaswerke (Mainz), Roth (Karlsruhe), Corning (New York, USA), Qiagen (Hilden), Ibidi GmbH (Muenchen) and Kimberley-Clarke (Roswell, USA). Deionised water was prepaired at 18.2 MΩ in a milliQ plus from Millipore (USA).

2.2 Alignment

Alignments were made with use of Vector NTI Advance 10 (Invitrogen). *BSND* genes found in different species had gi numbers; bornean urangutan 55732534, chimpanzee 114556813, human 54035724, rhesus monkey 109005014, cow 76613782, chicken 50751652, zebrafish 125832290, platypus 149519268, gray short-tailed opossum 126306077, mouse 54035723, rat 54035682, rabbit 83638321. Genes for ClC alignment of human ClC proteins and rat ClC-K1 and ClC-K2 had gi numbers; ClC-1 544024, ClC-2 5597006, ClC-3 1705903, ClC-4 4502871, ClC-5 4557473, ClC-6 1705910, ClC-7 12644301, ClC-Ka 1705857, ClC-Kb 1705859, ClC-K1 1754526, ClC-K2 1705861.

2.3 Molecular biology

2.3.1 Vectors

pcDNA3.1(-) or (+) was used for the human barttin encoding gene. The human ClC isoform ClC-Kb was present in pRcCMV while ClC-Ka was either in pcDNA3.1(-) or pSVL. Rat ClC-K1 was encoded as a V166E mutant in the pSVL vector or as WT in pRcCMV. The hClC-1/hClC-Kb concatamer was present in the pRcCMV vector. pLeu is a plasmid that encodes for the CD8 antigen. Cells transfected with this plasmid could be identified with polystyrene beads coated with anti-CD8 antibody (Jurman, Boland et al. 1994). pRcCMV YFP hClC2 and pcDNA3.1(+) CFP EAAT3 were used for confocal imaging.

pRcCMV and pcDNA 3.1 have the expressed gene under control of the cytomegalovirus (CMV) promoter (Invitrogen, Groningen, Netherlands) while pSVL contains the simian virus 40 late promoter. Barttin was expressed as a CFP fusion protein. The channels were either expressed as YFP fusion proteins and were either cotransfected with pLeu or contained an Internal Ribosome Entry Site (IRES) just before the coding region of the CD8 antigen present on the same plasmid as the channel.

2.3.2 Mutagenesis

2.3.2.1 Primers and constructs

Table 2.1 shows the primers used for mutagenesis, these were synthesized by Sigma-Aldrich (Hamburg, Germany) and were constructed with help from the site www.bioinformatics.org/primerx/. The region to be mutated was copied to this site and a primer was designed. The primer was checked in Vector NTI Advance 10 (Invitrogen) for a low amount of loops, one or more cytosine or guanine at both ends, 25 to 45 bases, melting temperature of ≥78°C, the mutation in the middle of the primers and no or small negative dG (Gibb's free energy). The Gibb's free energy should not be (too) negative since this means there is not a lot of energy needed for the primer to bind to itself when there is a palindrome.

Table 2.1. Oligonucleotides used for Quikchange or pcr mutagenesis (5´ to 3´): s = sense, as = antisense.

Construct	s/as	Sequence
pcDNA3.1(+) R8L Barttin CFP	s	TCTGCGGCCGCCATGGCTGACGAGAAGACCTTCCTGATC
	as	GTCAGAGTCAGCAGGGACGAAG
pcDNA3.1(+) R8W Barttin CFP	s	CTGCGGCCGCCATGGCTGACGAGAAGACCTTCTGGAT
	as	GTCAGAGTCAGCAGGGACGAAG
pcDNA3.1(+) G10S Barttin CFP	s	CTGCGGCCGCCATGGCTGACGAGAAGACCTTCCGGATCTCCTTC
	as	GTCAGAGTCAGCAGGGACGAA
pcDNA3.1(-) Q32X Barttin CFP	s	CCCACTGCTTACTGGCTTATC
	as	AAAAAGGATCCGGCCGATCATGG
pcDNA3.1(+) G47R Barttin CFP	s	CCCACTGCTTACTGGCTTATCG
	as	GGCACATGCACCAGATGATGCCCCGGATC
pcDNA3.1(+) E88X Barttin CFP	s	GGAGAATGGGCTTGCTGCGGATCCGAAGAGCCCCAGTCCC
	as	GGGACTGGGGCTCTTCGGATCCGCAGCAAGCCCATTCTCC

Mutations R8L, R8W, G10S and G47R were made by pcr with pcDNA3.1(+) Barttin CFP as template. The desired mutation was cleaved out of the pcr (R8L, R8W, G10S with NotI and NspI, G47R with NheI and NspI) and ligated into the mentioned vector.

pcDNA3.1(+) E88X Barttin CFP Barttin CFP was made by quikchange on pcDNA3.1(+) Barttin CFP with the mentioned primers and was than transformed. E88X barttin now contained a BamHI site inserted so that the Barttin protein behind amino acid 87 to the CFP protein could be cleaved out.

pcDNA3.1(-) Q32X Barttin CFP was made by addition of a BamHI site behind the 31 amino acid by use of a pcr. The part of barttin behind the 31 amino acid was now removed thus replacing barttin with barttin Q32X with use of NheI and BamHI. Some of these constructs were made by Ute Scholl and all pcred DNA was sequenced.

2.3.2.2 Quikchange: Site directed mutagenesis

Site directed mutagenesis by Quikchange (see Fig. 2.1) was performed with 50ng of template DNA together with 125ng sense primer, 125ng antisense primer, 2% (v/v) 10mM dNTP mixture (Eppendorf or Qiagen), 10% (v/v) 10X reaction buffer (Stratagene), the reaction was filled to 49µl with HPLC quality water (Fluka) after which 1µl of Pfu Turbo DNA polymerase (2.5U/µl, Stratagene) was added. The reaction mixture was placed in a thermocycler (Biometra or MJ Research) starting denaturation for 2 minutes at 95°C. Nineteen cycles were performed;

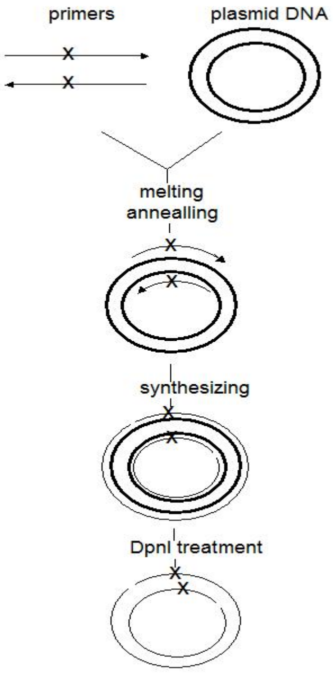

Figure 2.1 Scheme of the Quikchange reaction.

Denature	45 sec	95°C
Anneal	1 min	55°C
Synthesis	1 min/kbp	68°C

After these cycles the temperature was kept at 68°C for 10 more minutes for end synthesis. The sample was placed on ice for 2 minutes to cool the tube. 10 Units of DpnI (Fermentas or New England Biolabs) were added, which resulted in digested not mutated DNA since DpnI only digests methylated DNA. The DNA gained from bacteria is methylated, however the pcred synthesized DNA is not since this lacks the appropriate enzymes. The sample was incubated at 37°C for 1 hour. Competent bacteria were transformed so that the correct plasmid could be multiplied.

2.3.2.3 Polymerase Chain Reaction

Instead of Quikchange a polymerase chain reaction (pcr) could be performed with 100ng DNA, 10% 10x buffer (Qiagen), 2% (v/v) 10mM dNTP mixture (Eppendorf or Qiagen), 100ng sense primer, 100ng antisense primer, 1.4% Taq DNA polymerase (Qiagen) and the reaction was filled to the final volume with HPLC quality water (Fluka). The reaction mixture was performed in a thermocycler (Biometra or MJ Research) where, after denaturation at 94°C for 10 min, 35 cycles were performed;

Denature	1 min	94°C
Anneal	1 min	40-72°C (T_m-10°C)
Synthesis	3 min	72°C

Final synthesis took place at 72°C for 10min. The PCR product was purified by a pcr purification kit (Qiagen, Hilden) or was placed on a 1% agarose gel and gel extracted with a kit (Qiagen, Hilden), to remove primers, nucleotides, salt and DNA polymerase.

2.3.3 Transformation

5-10µl of ligation mixture, purified plasmid DNA or 15µl of quikchange mutated DNA was added to 40 or 75µl of one shot competent *Escherichia coli* (*E. coli*) bacteria (DH5α-T1), respectively. The slc110 *E. coli* strain was used to obtain not methylated DNA. After 20 minutes incubation on ice, the tube was transferred to a heatblock for 90 seconds at 42°C and then placed on ice for 2 minutes. The bacteria recovered by addition of 300µl of LB medium and a 1 hour incubation, shaking at 220U/min and 37°C. The bacteria were spun down for 0.5 min. at 3800g in a table centrifuge, the pellet was resuspended in a small part of the supernatant which was than transferred to an agar plate with the appropriate antibiotics to select for the desired plasmid. The plates were incubated upside down, to avoid condensed water on the colonies, overnight at 37°C. Each transfection a positive (50ng of a high copy plasmid with the same antibiotics resistance) and negative (autoclaved deionised water or nothing instead of DNA) control was used.

2.3.4 Plasmid recovery

2.3.4.1 Plasmid recovery

Small amounts of DNA were recovered from a 6 to 8ml overnight culture, grown at 37°C and shaken at 220U/min (Infors, Bottmingen, Schweiz), in LB medium with antibiotics. The protocol of the Qiaprep 8 Miniprep Kit (Qiagen, Hilden), or Qiaprep Spin Miniprep Kit (Qiagen, Hilden) with use of respectively a vacuum pump (KNF lab, Laboport) or table centrifuge, were followed. Larger quantities of DNA were recovered with the Qiagen (Hilden) HiSpeed Plasmid Maxi Kit (Qiagen, Hilden). A 2ml preculture was grown at 37°C for 8 hours, partly used to inoculate a large amount of medium with antibiotics (150-400ml) which was incubated overnight at 37°C and 200U/min. All steps were followed as recommended by the manufacturer. From all cultures a glycerol stock was frozen at –80°C before recovering the DNA, by addition of the same volume of 50% glycerol to the amount of culture to be stored.

2.3.4.2 DNA concentration measurement

DNA concentrations were measured diluted 1:100 in autoclaved deionised water. The optical density (OD) was measured at 260nm in a spectrophotometer that already calculated the concentration (Ultrospec 2100 pro from Amersham Biosciences) or was calculated manually. An OD_{260} of 1, represents 50µg/µl.

2.3.5 Agarose gel electrophoresis

Depending on the DNA fragments, agarose was dissolved in 1x TAE buffer (50x consists of 2M Trisbase, 5.95% (v/v) of 96% Acetic Acid, 10% (v/v) 0.5M EDTA pH8.0 or 3.72% (w/v) $Na_2EDTA*2H_2O$), at 1% (w/v) for fragments smaller than 1000 basepairs (bp) and at 2% (w/v) for fragments bigger than 1000bp. Ethidium Bromide was dissolved in the agarose gels at 0.01% (v/v). This was done to visualize DNA since it is an intercalating agent that fluoresces when exposed to UV-light. Lambda DNA/EcoRI+HindIII marker (Fermentas) or GeneRuler DNA Ladder Mix (Fermentas) were also loaded on the gel to estimate band sizes. Samples were dissolved in 6x Loading buffer (0.25% Bromophenol Blue, 0.25% Xylene cyanil FF, 30-40% glycerol this whole mixture was diluted with 260% (v/v) of 50%glycerol and 160 (v/v) deionised H_2O). Gels were run at 100V, scanned with a Gel-Doc 2000 Documentation system (Bio-Rad Laboratories GmbH, Muenchen) and bands were visualised and quantified with the Quantify One program (BioRad).

2.3.6 DNA Restriction

For fragments up to 3000bp 5µg and for bigger fragments 3µg of DNA was used. The appropriate amount of DNA was used together with 10% (v/v) 10x enzyme buffer, 1% (v/v) BSA (bovine serum albumine) or SAM (S-adenosylmethionine) if required, the reaction was filled to 48.5µl with autoclaved deionised H_2O and 1.5µl of enzyme (New England Biolabs) was used. For a double digest with compatible buffers the reaction was filled to 47µl and 2x 1.5µl of different enzymes were added. Sometimes the buffers of the different enzymes were not compatible and one digest was performed for 2 hours after which NaCl and the second enzyme could be added. If there were too different buffers to be used, the digest was PCR purified (Qiaquick PCR purification Kit, Qiagen, Hilden) or placed on an agarose gel and than gel extracted. After these purifications the DNA than was digested with the second enzyme in the appropriate buffer. Test restrictions were performed in a total of 20µl reaction of which 10% (v/v) was DNA and 5% (v/v) was enzyme.

2.3.7 Gel extraction

2.3.7.1 Gel extraction

DNA was extracted from agarose gels by a Qiaquick Gel Extraction Kit (Qiagen, Hilden) as recommended by the manufacturer. As an alternative, DNA fragments larger than 1000bp were purified with glassmilk. The DNA fragment was cut out of the agarose gel and weight. For the glassmilk purification the gel was dissolved in 3 volumes of sodium iodide solution (6M NaI, 10mM Na_2SO_3, 20 mM Tris HCl which was filtered) at 65°C for at least 5 minutes. The mixture was cooled and then mixed with 10µl vortexed glassmilk. The mixture was vortexed several times during a 10 minute incubation at room temperature. Centrifugation at 5900g for 10 seconds in a table centrifuge, pelleted the glassmilk. The pellet was washed with 600µl NEET wash solution (100mM NaCl, 1mM EDTA, 50 % Ethanol, 10mM Tris HCl (pH 7.5) stored at –20°C), by vortexing and centrifugation. The pellet was washed with 400µl NEET wash solution and after removal of the supernatant it was additionally centrifuged at 16100g. The supernatant was completely removed and the glassmilk was dried for 10 minutes of centrifugation at 30°C under vacuum (Concentrator 5301, Eppendorf). DNA was eluted from the glassmilk by addition of 30µl Elution Buffer (Qiagen, Hilden) and incubation for 10 minutes at 65°C. Centrifugation of 30 seconds at 16100g was needed to obtain the supernatant in a second tube. This was repeated once more to make sure there was no glassmilk left in the DNA fraction.

2.3.7.2 Glassmilk preparation

In 200-300ml of deionised water, 50g of silica (Sigma-Aldrich) was stirred for 1 hour. After 2min without movement the supernatant was transferred to a beaker and was standing for another minute. The supernatant was discarded and the rest was centrifuged for 5min at 1200g. The pellet was resuspended in 100ml 50% nitric acid (HNO_3) and was boiled for 1 hour under a hood. After cooling down and centrifugation as before, the silica was washed 4 to 6 times with deionised water until the pH was 7. The pellet was resuspended in deionised water to a 50% suspension and was frozen in 0.5ml aliquots at -20°C.

2.3.8 Ligation

Restriction fragments were run on a 1% agarose gel and were scanned with the Gel-Documentation system (Bio-Rad) where the bands were quantified with the Quantify One program. Ligations were composed of 1x the biggest plasmid fragment and 3x the inserted fragments, 2µl ligase buffer, up to 19µl of autoclaved deionised H_2O and 1µl T4 DNA ligase (Fermentas). Ligation took place overnight at RT or 18°C. After 24 hours it was transformed.

2.3.9 DNA sequencing

2.3.9.1 DNA sequencing

250ng of DNA, dissolved in HPLC quality water (Fluka), was used. To the DNA 10pmol of sense or antisense primer was added, 2 to 4 µl premix (Big Dye Terminator v1.1 Cycle Sequencing Kit, Applied Biosystems) and HPLC quality water (Fluka) to 10µl of total reaction volume. The sequencing pcr took place in a thermocycler with a heated lid for 25 cycles;

Denature	30 sec	96°C
Anneal	20 sec	45-52°C (T_m-5 to 10)
Synthesis	4 min	60°C

The sequence was purified with a DyeEx 2.0 Spin Kit from Qiagen or by ethanol precipitation.

DNA was placed 2 minutes at 90°C for denaturing and 5 minutes on ice after which the sequence was transferred to a PCR sequencing facility (Microbiology at the MHH) where DNA sequence was visualised (Genetic Analyser 3130 XL from Applied Biosystems). Some constructs were sequenced at the company GATC Biotech (Marseille, France).

2.3.9.2 Ethanol precipitation of sequenced DNA

Sequencing mixture was placed in a 0.5ml tube and was subsequently mixed with a mixture of 90µl HPLC quality water (Fluka) and 10µl 3M NaAc pH 4.6 and than with 250µl 100% Ethanol (stored at -20°C). Centrifugation took place for 20min at 16100g after which the ethanol was removed. The pellet was washed with 250µl 70% ethanol and centrifuged for 7min at 16100g. The supernatant was removed and the pellet was dried for 5min at 30°C under vacuum (Concentrator 5301, Eppendorf). The pellet was dissolved in 25µl of HPLC quality water (Fluka).

2.3.10 LB medium, agar plates and antibiotics

LB medium was made with 22,5g LB broth (Difco laboratories) in a final volume of 900ml with deionised water. After dissolving by stirring it was autoclaved immediately. For agar plates 22,5g LB broth (Difco laboratories) and 18g of Bacto Agar (Difco laboratories) were in a total volume of 900ml in deionised water, stirred and autoclaved. After cooling down to 60°C the appropriate antibiotic was added to the flask to give a final 1x solution. Plates were poured under a clean bench. Ampicilline (Applichem) was dissolved in autoclaved deionised water. A 1000x solution contained 100mg ml^{-1}, aliquots were stored at –20°C.

2.3.11 Competent bacteria

A culture of *E. coli* with an OD_{600} of 2.5 grown in medium without antibiotics was diluted in 100ml and was grown in the absence of antibiotics to its exponential phase at an OD_{600} of 0.5-0.6. Bacteria were harvested at 4°C, 3000g for 10min and were kept on ice from than on. The pellet was resuspended in 30ml TFB I (100mM RbCl, 50mM $MnCl_2*2\ H_2O$, 30mM KAc, 10mM $CaCl_2*2\ H_2O$, 15% (v/v) Glycerol, pH was set to 5.8) and was incubated for 20 to 90min on ice. Bacteria were harvested again at 4°C 3000g for 10min and were resuspended in 3ml TFB II (10mM MOPS, 10mM RbCl which is rubidium chloride, 75mM $CaCl_2*2\ H_2O$, 15% (v/v) Glycerol, pH was set to 8). These competent bacteria were aliquoted, frozen in liquid nitrogen and stored at -80°C.

2.4 Cell culture of mammalian cells

2.4.1 Cell lines, growth and splitting

TsA201 cells are a human embryonic kidney cell line, HEK293, stably transfected with simian virus 40 which enhances the transfection efficiency and makes this cell line ideal for transient transfections. MDCKII are Madin-Darby Canine Kidney cells.

TsA201 and MDCKII cells were grown in tissue culture dishes with 100mm diameter (Sarstedt), at 37°C and 5% CO_2. Medium used was Dulbecco´s Modified Eagle´s Medium (DMEM) supplemented with 2mM L-glutamine, 10% foetal bovine serum (FBS) and 1% penicillin and streptomycin (all Gibco, Invitrogen). The medium was filtered before use (0.22µm from Biochrom or TPP). Stably transfected MDCK cells were grown in medium supplemented with 0.5mg/ml Geneticin and were also splitted in this medium without use of trypsin.

To maintain tsA201 cells in culture, they were splitted every 2-4 days and were kept until around 20 passages. TsA201 cells were splitted by removing the old medium and adding 3ml fresh medium. After detaching the cells from the dish by forceful resuspension, they were transferred to other dishes containing 10ml of medium. MDCK II cells were splitted after one wash with PBS (Cambrex Bio Sciences Verviers, Belgium), by addition of 2ml 25% Trypsin with EDTA (Gibco, Invitrogen), incubation for 2 to 10 minutes, addition of 8ml fresh medium and forceful resuspension of the cells. Cells were transferred to new dishes with 10ml medium.

Transfected tsA201 cells for electrophysiology were typically splitted one day after transfection by removing the medium and addition of 3ml 25% Trypsin with EDTA (Gibco, Invitrogen). Forceful resuspension, detached the cells and made them single cells. In less then 2 minutes after addition of the Trypsin, 7ml of medium was added to the dish. After one time of resuspension, 1.5ml of cells was added to a 60mm diameter tissue culture dish (Falcon) containing 2ml of medium.

2.4.2 Transfection

TsA201 cells were transfected by calcium phosphate precipitation. By adding a DNA/$CaCl_2$ mixture in a controlled manner to a buffered saline/phophate solution, a precipitate develops that is taken up by cultured cells. These cells could also be transfected with lipofectamine, like was done for MDCKII cells.

2.4.2.1 Lipofectamine

Amounts of transfection solutions were calculated according to data supplied by the company, to ensure an optimal DNA to lipofectamine ratio. DNA and Optimem, lipofectamine and Optimem were mixed. After 5 minutes the DNA mixture and lipofectamine mixture were pooled and left at room temperature for 20 to 30min. Medium on the cells was exchanged to medium without antibiotics and the DNA/lipofectamine mixture was added. Cells were placed in the incubator and after 6-9 hours the medium was exchanged for medium with penicillin and streptomycin. MDCKII cells for living cell confocal microscopy were transfected with 0.25-1.2µg per plasmid whereas; 1.6-4µg was used for confocal images of fixed cells, grown on coverslips. Stable barttin MDCK cell lines were transfected with 0.5µg of ClC-Kb YFP in the presence of penicillin, streptomycin and geneticin.

2.4.2.2 Calcium phosphate precipitation

The desired amount of DNA and 10µl of Salmon Sperm DNA (Invitrogen) were pooled and than mixed in 500µl 250mM $CaCl_2$. This mixture was added to 500µl 2xHEBS by adding a few drops and shaking the tube, until everything was transferred. After 20-30 minutes at room temperature the mixture was added to the cells, dropwise and carefully moving the dish while doing this. Before transfection the medium was refreshed.

TsA201 cells for electrophysiology were transfected with 1 to 9µg of DNA, MDCKII cells for confocal imaging of fixed cells grown on coverslips were transfected with 0.2-6µg DNA from each plasmid. For electrophysiology 2µg of pLeu DNA was co-transfected, which encodes for the CD8 antigen, if this gene was not already present in one of the plasmid DNA´s (channel IRES CD8). Salmon Sperm DNA Solution (10mg/ml, Invitrogen) was diluted 10x in 10mM TrisHCl, pH 8.0, 1mM EDTA (TE buffer, Qiagen, Hilden). 2xHEBS consists of 274mM NaCl, 40mM HEPES, 12mM Dextrose, 10mM KCl, 1.4mM Na_2HPO_4 and was adjusted very accurately to pH 7.05. Both the $CaCl_2$ and HEBS solution were filtered.

2.4.3 Stable transfected MDCK cells

MDCK cells were grown to 70% confluency in 6 well plates. Cells were transfected by lipofectamine with 2µg of pcDNA 3.1 barttin or E88X barttin. One day after transfection the medium was changed to medium also containing 0.5mg/ml geneticin. Three wells with the most fluorescence were used to split to a big dish by incubation in trypsin. Cells were grown in the presence of 0.5mg/ml geneticin. Colonies were picked 3-10 days later and were continued to grow in 0.5mg/ml geneticin (Cheng, Glover et al. 2002).

2.4.4 Freezing cells

Medium was removed and cells were incubated for 3-5min in 3ml 25% Trypsin with EDTA (Gibco) in the incubator. Cells were detached, filled up to 10ml with medium and were mixed. Centrifugation was performed for 3min at 1500U/min. Cells were resuspended in 3ml of Freeze 1 and amounts of 0.7ml were aliquoted in cryo-tubes. The same amount of Freeze 2 was added and mixed. Cells were frozen at –80°C in a Nunc Box and transferred to liquid nitrogen the day after. A few days later one tube was thawed to see if the cells had survived.

Freeze 1 contains 4ml FBS and 6ml MEM. Freeze 2 contained 4ml FBS, 4ml MEM and 2ml cell culture tested DMSO. Both solutions are prepaired fresh and are sterile filtered.

2.4.5 Thawing cells

Cells frozen in liquid nitrogen were thawed under hot water until they separated from the wall of the tube and were poured in 10ml of medium. After centrifugation at 1500U/min cells were washed twice with 10ml medium. The last resuspension of the cells was transferred to a culture dish with 100mm diameter (Sarstedt).

2.5 Electrophysiology

2.5.1 Cells

TsA201 cells were used for whole-cell patch clamp recordings. To identify transfected cells, a bicistronic vector containing the coding region of the respective ClC-K channel and of the CD8 antigen (pRcCMV or pSVL-ClC-K-IRES-CD8) was used, or 2µg of a plasmid encoding the CD8 antigen was co-transfected. Cells were incubated 5 min before use together with polystyrene microbeads precoated with anti-CD8 antibodies (Dynabeads M-450 CD 8, Dynal, USA), and only cells decorated with microbeads were used for electrophysiological recordings. Barttin was co-transfected as CFP-fusion protein.

2.5.2 Setup

The Patch-Clamp stand was located on an air shock dampened table (TMC, Peabody, USA) and was protected for environmental background electricity by a Faraday cage. An inverted

Leica (usually with fluorescence detection) microscope was used to see the cells and a micromanipulator (SM1 Luigs & Neumann, Ratingen) to move the glass pipet to the cells. The measured signals were send to a Patch-Clamp amplifier (EPC10, HEKA Electronics, Lambrecht) and an AD/DA converter (LIH 1600, Luigs&Neumann SM-6).

The amplifier amplified, filtered and digitalised the signal from the preamplifier and than send the data over an interface to the computer. Data was visualised by Pulse v8.77 showing the measured signal on an oscilloscope module, the different applied protocols and it applied the first data analysis.

2.5.3 Microelectrodes

Pipettes were pulled from borosilicate glass capillaries (Harvard apparatus) with a micropipette puller (Sutter instrument co.) and then polished with a microforge (MF-830, Narishige Japan). This was done to make the pipets dust free and to smooth the edges. The pipettes had openings of 1.0-2.0µm. For non-stationary noise experiments the pipets were pulled and than coated with wax (Moyco), after which they were polished. This was done to minimize the background noise.

Just before use, the intracellular solution was placed in the pipet with a needle. The glasspipet was placed on a chloride treated silver wire and was fixed to the pipetholder. On one side of the pipetholder, underpressure could be applied to the pipet.

2.5.4 Measure and reference electrode

The electrodes are not polarizing Ag/AgCl-electrodes, which in solutions with chloride ions a reversible ionmovement enables. Chloride ions either go in solution from the electrode ($AgCl + e^- \rightarrow Cl^- + Ag$) or chloride ions attach to the white silver as AgCl ($Cl^- + Ag \rightarrow AgCl + e^-$). This reversible ion movement does not function with white metalelectrodes (polarisable electrodes). Both internal and reference electrode were silver wires that are treated with chloride solution.

2.5.5 Gigaseal

A 10ms long testpuls of 5mV was applied with a frequence of 66Hz to the measure pipet. When the pipet was placed in the bath solution a square current signal could be seen in the oscilloscope module. From this the pipetresistance could be measured, only pipets with a resistance of 1.0-2.2 MΩ were used. After correction of the offset, the pipet was moved to a single transfected cell. The pipet was placed on the cellmembrane which lowered the amplitude of the testpulse since the resistance increased. By carefully applying underpressure by suction, and sometimes temporarily applying a negative voltage, the resistance increased to 1GΩ ($1*10^9\Omega$ = Gigaseal). Series resistances were compensated 60-80% by an analog procedure, so the calculated voltage error due to access resistance was always less than 2 mV.

2.5.6 Whole cell configuration and solutions

In the whole-cell configuration all channels of a cell are observed. After establishing a gigaseal the cell was opened by suction and sometimes with use of a 100µs pulse of 400mV. All experiments in this thesis were performed in this configuration. When negatively charged ions go into the cell, this is shown as an outgoing current and a positive amplitude since this means a loss of positive charge on the inside of the cell. Negatively charged ions released from the cell thus give a negative current amplitude and is called an inward current.

The extracellular solution contained 140 mM NaCl, 4 mM KCl, 2 mM $CaCl_2$, 1 mM $MgCl_2$, and 5 mM HEPES, while the intracellular solution contained 120 mM NaCl, 2 mM $MgCl_2$, 5 mM EGTA (to quenche calcium ions) and 10 mM HEPES. Both solutions were adjusted to pH 7.4 with NaOH. Cells were clamped to 0mV.

2.5.7 Data analysis

Data was analyzed by a combination of PulseTools (HEKA Electronics, Lambrecht, Germany), SigmaPlot (Jandel Scientific; San Rafael, USA), Clampfit (Axon Instruments, Union City, USA) and ChanneLab2 (Synaptosoft). Data were shown with standard error of the mean. An unpaired Student t-test performed in Sigmaplot gave p, * $0.01 > p < 0.05$ and ** $p < 0.01$.

To obtain the instantaneous current amplitude for the relative activation curve, several steps to diverse voltages (steps of 20mV) were made for 200ms that were followed by a voltage to -120mV for 20ms. Short after the beginning of the -120mV step, the current amplitudes were measured for the preceding voltages. The instantaneous currents were plotted to the applied voltages in the previous step. The graph for each cell was fitted and cells were normalized by the most extreme value. Averaging more recordings gave the relative activation curve or instantaneous current amplitudes. Recordings were sampled with a 3.3kHz bessel filter and sampled at 10kHz.

Non-stationary noise analysis was performed to determine the absolute open probabilities and the unitary current amplitudes of V166E rClC-K1. Pulses were applied from -100 to -200mV after a preceding step to +75mV. This was repeated 300 times for each cell.

The mean current and variance (σ^2) were transferred from the Heka Pulse program to Sigmaplot where a current to time graph was made to select the noise data. From this data a variance to mean current graph was made that could be fitted by $\sigma^2 = iI - I^2/N$ (Hebeisen, Biela et al. 2004). The recording was transported by Channelab2 (Synaptosoft) and fitted in Clampfit 9.2 (Axon Laboratory) to obtain the current (I) at the time the pulse started. With the single channel amplitude (i) and the number of channels (N) given by the noise fit, it was possible to calculate the absolute open probably (p_o) at +75mV. This was done with formula $I=i*N*p_o$ so $p_o=I/(i*N)$ (Alvarez, Gonzalez et al. 2002). The relative activation curve could now be adjusted to the absolute activation curve. Noise was recorded at a sampling rate of 50kHz, filtered with a 3.3kHz bessel filter and digitally filtered by 1kHz. Different filter settings during recording were analyzed as were different digital filters, neither gave differences in the gating properties of V166E rClC-K1.

The i/V graph was fitted by $I= m*(E–E_{rev})$. M is the slope and therefore the conductance of the channel. E_{rev} is the reversal potential for chloride that was calculated at 22°C with the Nernst equation. $E_{rev}=(RT/F)*(\ln([I]_i /[I]_o))$ in which R is the Gas constant (8.315 J^{-1} K^{-1} mol^{-1}), T the absolute temperature in Kelvin (273.16 + Temperature in °C), F is Faraday’s constant ($9.648 * 10^4$ Coulombs mol^{-1}) and [I] is the concentration in the internal (i) or external (o) solution.

2.6 Fluorescence

Fluorescent ClC-K channels (YFP) and barttin (CFP) were used for SDS-PAGE gel electrophoresis and confocal imaging. Fluorescent proteins fluoresce because electrons are excited by energetic photons of a specific wavelength. Electrons in this excited level are unstable and loose there energy rapidly, to return to their ground energy state. The emitted energy is observed as fluorescence.

2.7 Confocal Imaging

Confocal microscopes have a pinhole that is placed before the photomultiplier and removes unwanted, out-of-focus fluorescence, giving an optical slice of a 3-dimensional image.

2.7.1 Experiments on fixed cells

Glasscoverslips (12mm, round, Roth, Karlsruhe, Germany) were flamed with ethanol and coated with poly-L-lysine (Sigma-Aldrich, Germany, diluted 1:10 in autoclaved deionised H_2O) for 10 minutes at room temperature so that cells would be able to attach to and grow on this surface. Coverslips were washed 3 times with excess autoclaved deionised water and were dried for 3 to 24 hours under the hood. MDCKII cells were transfected one day before splitting to coated glasscoverslips, with lipofectamine or the calcium phosphate precipitation method. After 24-48 hours cells were washed twice with PBS (17.56mM $Na_2HPO_4*2H_2O$, 2.46mM $NaH_2PO_4*2H_2O$, 149,7mM NaCl) and fixed for 10 minutes in PBS with 4% (w/v) paraformaldehyde. Three washes with TBS (10mM TrisHCl, 154mM NaCl, pH 7.5) were followed by mounting the cells in solution from the ProLong Antifade Kit (Invitrogen) onto an objectglass (Roth, Karlsruhe, Germany). This was dried overnight in the dark after which it was sealed with nailpollish and again dried overnight in the dark. Confocal imaging was carried out with a Zeiss LSM 510 scan head and an inverted Axiovert 200M microscope. A 63x objective was used. In the multitrack configuration CFP and YFP were recorded after each other. CFP was excited at 458nm and YFP at 514nm, which was applied through the objective (so at the bottom of the sample). After filtering, the emission of CFP and YFP was detected at 475-515nm or at 530nm and higher wavelengths, respectively.

MDCK cells were also grown on filters (Costar) so that the cells were really polarized. Cells were transfected one day after splitting and one day later they were fixed with paraformaldehyde. First they were washed three times with PBS (3mM KH_2PO_4, 22mM $Na_2HPO_4*2H_2O$, 0.7% NaCl, 1mM $MgCl_2$, 0.1mM $CaCl_2$, pH7.6-7.8) on both sides of the filter, than 4% (w/v) paraformaldehyde was added to both sides of the filter. After 10 minutes of incubation, cells were washed three times with TBS (10mM TrisHCl, 150mM NaCl, pH 7.5). Filters were placed top to bottom on confocal microscope dishes (Ibidi) and were stored for zero to 10 days before confocal imaging as described in section 2.7.2.

2.7.2 Experiments on living cells

MDCKII cells were splitted to special dishes for confocal microscopy (Ibidi) with about 150 µl of cells and 550 µl of medium. Transfection occurred the day after, with use of lipofectamine in medium without antibiotics, after 6-9 hours of transfection the medium was replaced by medium with penicillin and streptomycin. The live cell imaging system Fluoview FV1000 (Olympus) was used with an Olympus IX81 inverted motorized microscope (so with the light source and condenser on top). Stacks were made from bottom to top or the other way around to avoid visualising results due to bleaching , Kallman 10 line averaging and 10µs per pixel. CFP and YFP were excited at 440nm or 515nm, while emitted light was detected at 465-495nm or 535-565nm respectively. CFP EAAT3 (Cheng, Glover et al. 2002) is expressed apical (top (Koivisto, Hubbard et al. 2001)) while YFP ClC-2 (Peña-Münzenmayer, Catalán et al. 2005) is present in the basolateral membrane (sides and bottom).

2.8 Protein Biochemistry

2.8.1 SDS polyacrylamide gel electrophoresis

SDS polyacrylamide gel electrophoresis (SDS-PAGE) was performed with 6-15% gradient gels, Table 2.2 gives the consistence of the different mixtures used for these gels.

Table 2.2 Consistence of running and stacking gel of denaturing SDS gels.

solution	6% running	15% running	stacking
H_2O	2.65 ml	1.15 ml	3.05 ml
1.5 M Tris pH8.8	1.25 ml	1.25 ml	
1 M Tris pH6.8			1.2 ml
10% SDS	50 µl	50 µl	50 µl
protogel	1 ml	2.5 ml	650 µl
10% APS	50 µl	50 µl	25 µl
Temed	5 µl	5 µl	5 µl

Protogel is an acrylamide-bisacrylamide 37.5:1 mixture (Serva).

Ammoniumpersulphate (APS) was prepaired fresh as a 10% solution of ammoniumpersulphate (Serva) in deionised H_2O. Tris was tris (hydroxymethyl)-aminomethane while Temed was short for N,N,N'-tetramethyl-ethylene diamine (both from Serva). The high percentage gel was on closest side of a pump while the lower percentage was in a tube a bit further away. By a stirrer, the high percentage mixture was diluted gradually with the lower percentage which was than pumped between the gel glasses. Deionised water was placed on top so that polymerysation would take place, which was allowed for about 1 hour. The stacking gel was poured after removal of the water. Gels were run in 25mM Trisbase, 192mM Glycine and 3.5mM SDS, first at 100V and when samples had entered the running gel the voltage was turned up to 180V.

2.8.2 2x SDS loading buffer

A 0.5M TrisHCl 0.4% (w/v) SDS solution was prepaired by dissolving 6.05g Trisbase in 40ml deionised H_2O and adjusting the pH to 6.8 with HCl. The volume was adjusted to 100ml with deionised H_2O and filtered (0.22µm MillexGP from Millipore). 0.4g of SDS was dissolved. From this solution 25ml was used for the final buffer together with 20ml glycerol (measured as 25,26g), 4g SDS, 3.1g DTT and 1mg bromphenol blue (Serva). Deionised H_2O was added to a total volume of 100ml. The buffer was aliquoted while stirring and was stored at -20°C. Final concentrations were: 125mM TrisHCl, 4.1% SDS, 20% glycerol, 200mM DTT and 0.014mM bromphenol blue.

2.8.3 Western blotting

Gels were blotted onto PVDF (Bio-Rad, Muenchen, Germany) which was prewet in methanol. The membrane, gel, fiber pads and filter papers were all equilibrated in transfer buffer (25mM Trisbase of pH8.0-10.5, 192mM glycine) for at least 15 minutes. The black site from cassette holder was placed down, and the white site on the top. A pile from bottom to top was made with: fiber pad, filter paper, gel, membrane, filter paper, fiber pad. The cassette was placed in the electrode module with the black side to the black side and the white one to red. This way the negatively charged proteins are able to run to the positive side, into the membrane. Western blotting was performed overnight at 4°C and 30V or 1 hour at room temperature and 100V. There were always a stirrer and an icecube present in the buffer tank, to take care of the developing heat.

After 1 hour of blocking in 3% BSA in TBS (10mM Trisbase, 150mM NaCl, pH 7.5), the blot was washed 3 times for 5 minutes with TBS 0.1% Tween-20. The first antibody (Sigma-Aldrich, Hamburg, Germany) was directed against the N-terminal part of actin of which 10µg was used for one hour in 1% BSA in TBS. The blot was washed 3 times for 5 minutes in TBS 0.1% Tween-20 and than incubated for 1 hour with 3µl of the second antibody. This antibody was made by goat and was directed against rabbit, it was tagged with Cy5 (GE Healthcare, Munchen, Germany). After 3 washes of 5 minutes, the blot could be scanned for fluorescence in the fluorescence scanner (Typhoon, GE Healthcare, Muenchen, Germany) as described in section 2.8.6.

2.8.4 Deglycosylation

MDCKII cells were transfected with 2µg pRcCMV YFP ClC-Kb alone or together with 4µg pcDNA 3.1(+) Barttin CFP with use of lipofectamine. Cells were washed twice with PBS after 24 hours of transfection. Cells were scraped from the plate and transferred to a tube. Supernatant was discarded after centrifugation for 2min at 0.8g. Cell pellet was dissolved in 300µl of lysis buffer with protease inhibitors (150 mM NaCl, 10 mM HEPES, 1 % Triton X-100 and 1:100 Sigma protease inhibitor). Incubation was performed on ice for 1 hour with 6x vortexing in between. Centrifugation for 15 min at 4°C and 13000 rpm was performed and supernatant was transferred to a new tube. The OD at 280nm was measured in a spectrophotometer (Ultrospec 2100 pro from Amersham Biosciences) and samples were diluted to a similar OD. Samples were placed in 2x SDS Loading Buffer.

Samples were incubated at 25°C for one hour and aliquoted to different tubes. Endoglycosidase H (endo H) was added for deglycosylation of high mannose structures which indicates core glycosylation. N-glycosidase F (PNGase F) deglycosylates complex and core glycosylated proteins.

Table 2.3 Reaction conditions for a deglycosylation assay (volumes are given in µl).

Reaction	Sample	endoH	PNGase F	10x G7 reaction buf	10% NP-40	H_2O
endo H	10	0.2	-	1.1	-	-
controle H	10	-	-	1.1	-	0.2
PNGase F	10	-	0.2	0.47	1.33	-
controle P	10	-	-	0.47	1.33	0.2

The YFP ClC-K protein was not stable in the reaction buffer supplied with endo H (10x = 0.5M sodium citrate, pH 5.5) so buffer supplied with PNGase F was used (10x = 0.5M sodium phosphate, pH 7.5), at which pH endoH should still be functional (Maley, Trimble et al. 1989). Samples were treated as mentioned in Table 2.3, incubated for 4 hours at 25°C (Thermomixer comfort, Eppendorf) after which they were loaded onto a 6-15% polyacrylamide gradient gel. Gels were scanned in a fluorescence scanner (Typhoon, GE Healthcare Biosciences). All chemicals used were from New England Biolabs (Beverly, MA, USA).

2.8.5 Scanning of fluorescent proteins on SDS gels

The fluorescence scanner (Typhoon, GE Healthcare, Muenchen, Germany) scanned the fluorescent gels or blots for CFP, YFP or Cy5 with excitation at 457, 532 or 633nm and emission filters 520 BP40, 526 SP or 670 BP30 respectively. Bands were quantified by measurement of squares drawed around the area´s to be measured with ImageQuant 5.2 and background was manually subtracted. BP stands for bandpass which means that for 520 BP 40, 500 to 540 nm passes the filter. SP stands for short pass, so for 526 SP shorter wavelengths than 520nm will pass this filter. An unpaired t-test was performed with the Sigmaplot program and significances were * for $0.05 > p > 0.01$ while ** $p < 0.01$.

2.8.6 Biotinylation

Biotinylation (Daniels and Amara 1998; Cheng, Glover et al. 2002; Dhani, Mohammad-Panah et al. 2003; Kutub Ali and Bergson 2003; Icking, Amaddii et al. 2007) allows the separation of membrane inserted proteins from other proteins. Biotin binds to accessible proteins on the outside of the cell and is than purified. Sulfosuccinimidyl-6-(biotinamido)hexanoate (in short: sulfo-NHS-LC-biotin) reacts with primary amino groups (-NH_2) for example in the side chain of lysine (K) or N-terminus of a polypeptide and is not able to permeate the cell membrane. Biotinylated proteins are purified by binding to neutravidin agarose. Elution with 2x loading buffer disrupts the biotin-avidin complex (Lei, Nowbar et al. 2003). To make sure cells stayed intact during the procedure a western blot was made from the purified fraction and was checked for actin purification. Actin should only be present intracellular and thus should not be purified. Western blot analysis was performed for the amount of actin in cleared lysate which gives the possibility to adjust the measured fluorescence to the amount of cells used per experiment.

2.8.6.1 Complete cell biotinylation

MDCK cells were grown not confluent on plates (Dhani, Mohammad-Panah et al. 2003) so that both basolateral and apical membrane would be accessible to biotin. After 24 hours the cells were washed 3x at 4°C with 5 ml of PBS (0.1M $NaH_2PO_4*2H_2O$, 0.1M $Na_2HPO_4*2H_2O$, 0.9% NaCl or 3mM KH_2PO_4, 22mM $Na_2HPO_4*2H_2O$, 0.7% NaCl with pH7.6-7.8). Sulfo-NHS-LC-Biotin (Pierce, Rockford, IL, USA) was dissolved in PBS to 1mg/ml. To each dish 1.5ml of biotin was added. After the 2 hours incubation at 4°C, during which dishes were carefully moved a bit 2 to 4 times, cells were washed three times with 100mM glycine in PBS to quench the ureacted biotin. The last wash was standing for 20 minutes after which the cells were scraped from the plate in 1 ml new PBS glycine. The cells were moved on ice out of the cold room but were kept on ice. By centrifugation for 2min at 0.8g cells were collected and were washed twice with PBS. 200µl of lysis buffer with protease inhibitors (150mM NaCl, 10mM HEPES, 1% Triton X-100 pH 7.5-7.7 and 1%(v/v) Sigma-Aldrich protease inhibitor cocktail) was added. Cells were scraped to a tube and incubated on ice for 1 hour while vortexing every 10 minutes. Meanwhile neutravidin agarose resin (Pierce, USA) was washed 5 times with lysis buffer with centrifugation of 2 min. at 2500g. Samples were centrifuged at 4°C and 13000rpm (Biofuge fresco, Heraeus) and supernatants were transferred to a new tube. The OD_{280} was measured and the samples were diluted with lysis buffer containing protease inhibitor (Sigma-Aldrich, Hamburg, Germany) so all samples had similar OD´s. Same amounts of sample were added to 150µl 50% slurry of washed neutravidin agarose resin and were incubated rolling slowly for 2 hours at 4°C. The OD was around 100 and about 130µl was used. The samples and resin were transferred to 2ml tubes with a filter containing support (Hande Centrifuge columns, Pierce, Rockford, IL, USA) and were washed 6x with 700µl lysis buffer. Elution was performed 4x with 35µl of 2xSDS loading buffer and the fifth time with 70µl, each time centrifuged for 2min at 700g. Eluate 2 was loaded on a 6-15% gradient gel for analysis with a fluorescence scanner (Typhoon, GE Healthcare, Munchen, Germany), as was the cleared lysate. Eluate 2 contained more protein than eluate 1, both for wild type barttin as for E88X barttin. These gels were analysed for the amount of YFP ClC-Kb and were western blotted to check for actin in the eluates and measure the amounts in the cleared lysate.

Membrane YFP ClC-Kb was either normalized to the amount of actin present in the cleared lysate or to the amount of YFP ClC-Kb present in the cleared lysate. These data were normalized to the amount present when expressed with WT barttin, this was done to account for differences in the settings of the photomultiplier and loading differences between experiments. This resulted in either the absolute or relative channel membrane insertion per barttin mutant. The experiment was done three times, though only ones for ClC-Kb without barttin and twice for ClC-Kb with the calcium channel beta subunit.

2.8.6.2 Basolateral or apical cell membrane biotinylation

MDCK cells were grown confluent on polycarbonate membrane Transwell inserts, filters with 0.4µm pore size and 24mm in diameter (Corning Costar) in 6 well plates, and were transfected with lipofectamine after one day on growth (see Fig. 2.2). One well of the six well plate contained no filter but the same amount of cells, to see when the cells were confluent. After 24 hours the cells were washed at 4°C with PBS (0.1M $NaH_2PO_4*2H_2O$, 0.1M $Na_2HPO_4*2H_2O$, 0.9% NaCl or 3mM KH_2PO_4, 22mM $Na_2HPO_4*2H_2O$, 0.7% NaCl and 0.1mM $CaCl_2$, 1mM $MgCl_2$ with pH7.6-7.8) three times on both sides. Sulfo-NHS-LC-Biotin (Pierce, Rockford, IL, USA) was dissolved in PBS to 1.5mg/ml. To one side of the filter 1ml of PBS was added, to the other side PBS with biotin. This way only the apical membrane (top) or basolateral membrane (bottom) proteins can be accessed. After 1 hour incubation at 4°C, buffers were removed and measured for their OD_{280} to check for leak and correct application of the biotin, both sides were washed three times with 100mM glycine in PBS to quench the unreacted biotin. The last wash was standing for 20 minutes and was followed by 2 washes with PBS. Filters were carefully removed from their support and placed in small dishes where 300µl of lysis buffer with protease inhibitors (150mM NaCl, 10mM HEPES, 1% Triton X-100 pH 7.5-7.7 and 1%(v/v) Sigma-Aldrich protease inhibitor cocktail) was added.

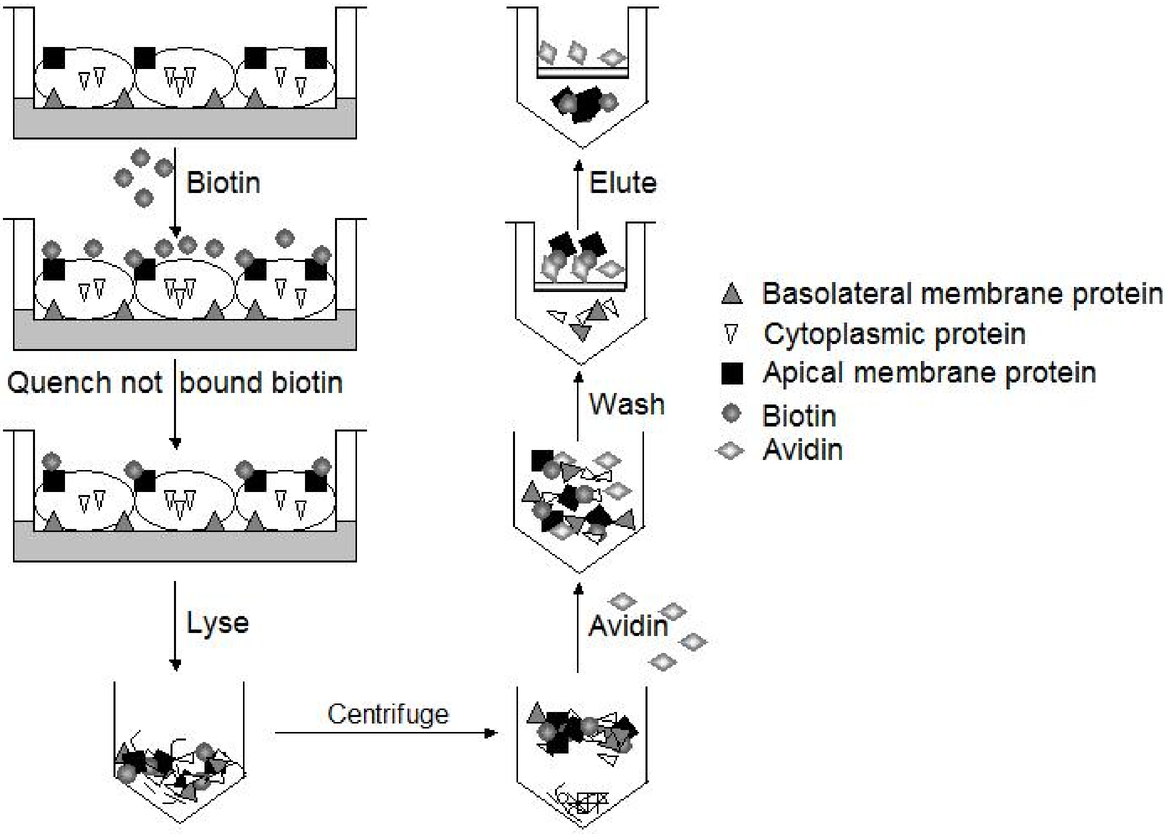

Figure 2.2 Scheme of apical biotinylation of MDCKII cells grown on filters.

The cells were moved out of the cold room but were kept on ice. Cells were scraped to a tube and incubated on ice for 1 hour while vortexing every 10 minutes. Meanwhile neutravidin agarose resin (Pierce, Rockford, IL, USA) was washed 5 times with lysis buffer with centrifugation of 2min at 2500g. The samples were centrifuged 10min at 4°C and 13000rpm (Biofuge fresco, Heraeus) and supernatants were transferred to a new tube. OD_{280} was measured and the samples were diluted with lysis buffer containing protease inhibitor that they all had similar OD´s. Same amounts of sample were added to 150-250µl or 50% slurry of washed neutravidin agarose resin and were incubated rolling slowly for 2 hours at 4°C. Usually the OD was around 230 and 180µl was used. The samples and resin where transferred to 2ml tubes with a filter containing support (Hande Centrifuge columns, Pierce, Rockford, IL, USA) and washed 6 times with 700µl lysis. Elution was performed 4 times with half a bed volume (35-60µl) of 2xSDS loading buffer and the fifth time with one bed volume, each time centrifugating for 2 min. at 700g. Eluate 2 was loaded on a 6-15% gradient gel for analysis with a fluorescence scanner (Typhoon, GE Healthcare, Munchen, Germany), as was the cleared lysate. Eluate 2 contained more protein than eluate 1, both for the wild type barttin as for E88X barttin. These gels were analysed for the amount of YFP ClC-Kb and were western blotted to check for actin in the eluates and measure the amounts in the cleared lysate.

The measured amount of membrane YFP-ClC-K was normalized to the amount of actin present in the cleared lysate, thus to the amount of cells used. The apical or basolateral purified amount of ClC-Kb fluorescence was devided by the total amount of purified channel, so both apical and basolateral, for WT and E88X barttin separately (Warner, Lew et al. 2005). In these experiments a stable cell line of WT or E88X barttin CFP was used two times, three times these barttins were transfected.

3. Results

3.1 The amino acid sequence is conserved in the amino terminal part of barttin

There are many mutations known to affect the barttin protein, as mentioned in the introduction (chapter 1.5.2). This thesis focuses on six published mutations inside the *BSND* gene which result in Bartter Syndrome type IV. R8L, R8W, G10S, Q32X, G47R and E88X are all present in the N-terminal part of barttin as shown in the representation of barttin in figure 3.1A. This region is also the most conserved amongst species (Fig. 3.1C) and comprises two putative transmembrane domains.

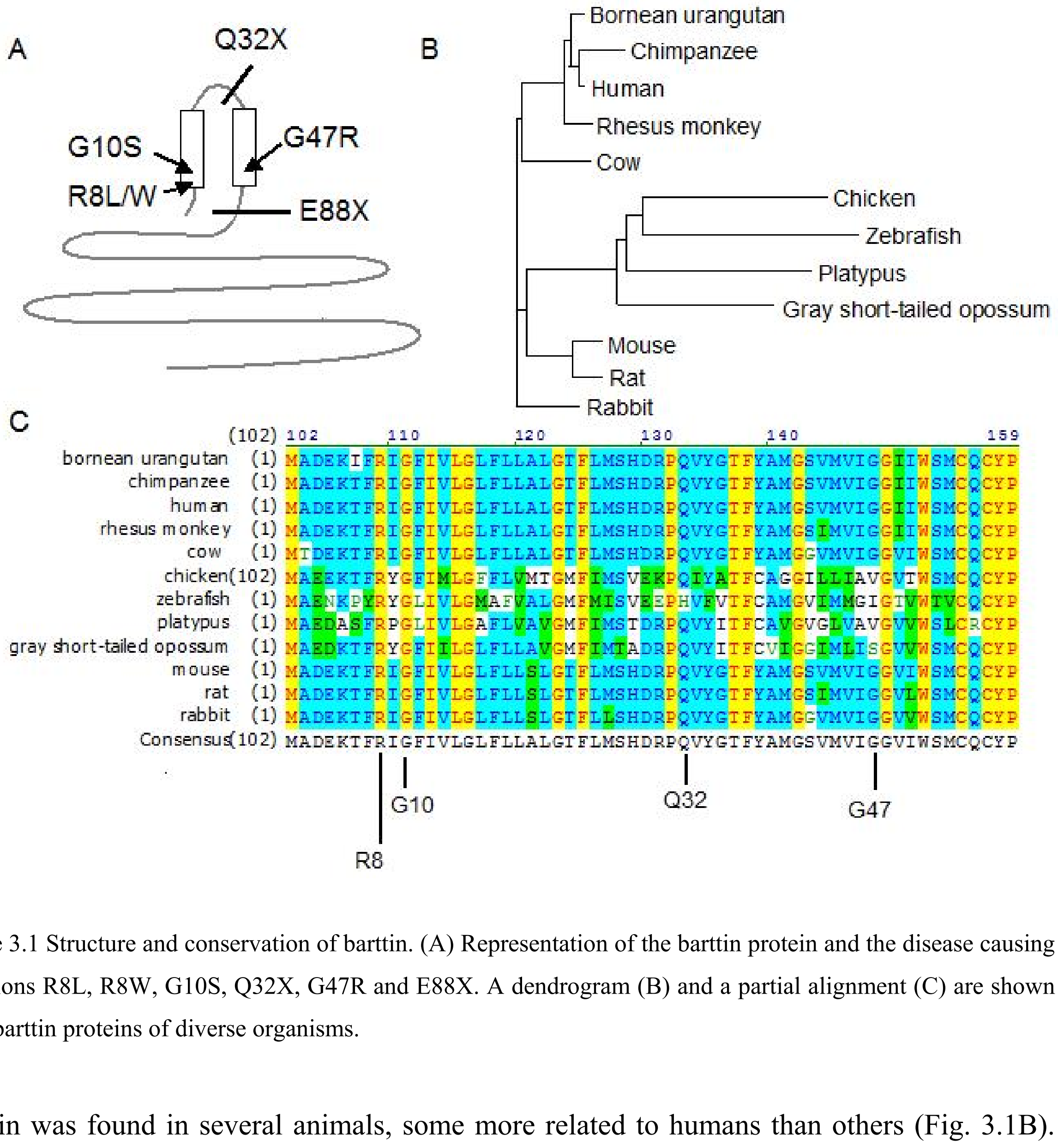

```
                (102) 102     110       120       130       140              159
bornean urangutan  (1) MADEKIFRIGFIVLGLFLLALGTFLMSHDRPQVYGTFYAMGSVMVIGGIIWSMCQCYP
       chimpanzee  (1) MADEKTFRIGFIVLGLFLLALGTFLMSHDRPQVYGTFYAMGSVMVIGGIIWSMCQCYP
            human  (1) MADEKTFRIGFIVLGLFLLALGTFLMSHDRPQVYGTFYAMGSVMVIGGIIWSMCQCYP
    rhesus monkey  (1) MADEKTFRIGFIVLGLFLLALGTFLMSHDRPQVYGTFYAMGSIMVIGGIIWSMCQCYP
              cow  (1) MTDEKTFRIGFIVLGLFLLALGTFLMSHDRPQVYGTFYAMGGVMVIGGVIWSMCQCYP
     chicken(102) MAEEKTFRYGFIMLGFFLVMTGMFIMSVEKPQIYATFCAGGILLIAVGVTWSMCQCYP
        zebrafish  (1) MAENKPYRYGLIVLGMAFVALGMFMISVEEPHVFVTFCAMGVIMMGIGIVWTVCQCYP
         platypus  (1) MAEDASFRPGLIVLGAFLVAVGMFIMSTDRPQVYITFCAVGVGLVAVGVVWSLCRCYP
gray short-tailed opossum  (1) MAEDKTFRYGFIILGLFLLAVGMFIMTADRPQVYITFCVIGGIMLISGVVWSMCQCYP
            mouse  (1) MADEKTFRIGFIVLGLFLLSLGTFLMSHDRPQVYGTFYAMGSVMVIGGVIWSMCQCYP
              rat  (1) MADEKTFRIGFIVLGLFLLSLGTFLMSHDRPQVYGTFYAMGSIMVIGGVLWSMCQCYP
           rabbit  (1) MADEKTFRIGFIVLGLFLLSLGTFLLSHDRPQVYGTFYAMGGVMVIGGVVWSMCQCYP
   Consensus(102) MADEKTFRIGFIVLGLFLLALGTFLMSHDRPQVYGTFYAMGSVMVIGGVIWSMCQCYP
```

Figure 3.1 Structure and conservation of barttin. (A) Representation of the barttin protein and the disease causing mutations R8L, R8W, G10S, Q32X, G47R and E88X. A dendrogram (B) and a partial alignment (C) are shown from barttin proteins of diverse organisms.

Barttin was found in several animals, some more related to humans than others (Fig. 3.1B). An alignment was made with use of Vector NTI Advance 10 (Invitrogen), the respective dendrogram (Fig. 3.1B) and N-terminal part of the sequences (Fig. 3.1C) is shown. Chicken, zebrafish, platypus and the gray short-tailed opossum are the most different while the bornean urangutan, chimpanzee, rhesus monkey and cow are more homologue to human. Human barttin has 320 amino acids while chicken has 102 additional amino acids at its N-terminus and the chimpanzee 82 at the c-terminus. R8 and G10 are conserved in all these species though Q32 and G47 are also quite conserved.

3.2 Barttin mutants enable ClC-Kb exit from the endoplasmic reticulum

3.2.1 WT and mutant barttin enable complex glycosylation of ClC-Kb

To examine the effect of wild type (WT) barttin on the intracellular trafficking of the hClC-Kb chloride channel, MDCK cells were transiently transfected either with a yellow fluorescent protein (YFP) tagged hClC-Kb alone or cotransfected with WT barttin. Figure 3.2 shows a denaturing SDS protein gel of the cleared lysates as an untreated sample, or it was treated either with endoglycosidase H (endo H) or N-glycosidase F (PNGase F).

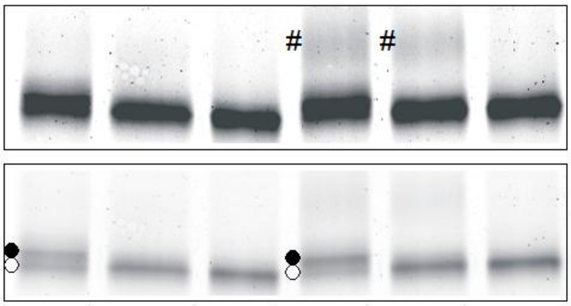

ClC-Kb	+	+	+	+	+	+
barttin	-	-	-	+	+	+
endo H	-	+	-	-	+	-
PNGase F	-	-	+	-	-	+

Figure 3.2 ClC-Kb is complex glycosylated only in the presence of barttin. A denaturing SDS protein gel of a deglycosylation analysis of YFP tagged hClC-Kb. The same gel is shown twice at different intensities to visualise all bands. Endo H is endoglycosidase H and PNGase F is N-glycosidase F. Protein bands susceptible to both glycosidases are core glycosylated while bands only deglycosylated by PNGase F are complex glycosylated. A double band is marked with dots, the additional third band is appearing when ClC-Kb is expressed in the presence of barttin and is displayed at the hash mark.

Endo H only cleaves sugars that are added during the start of N-glycosylation in the endoplasmic reticulum (ER) but not of mature chains, so there is only cleavage of high mannose structures that indicate core glycosylation which is performed in the ER. PNGase F is able to cleave core and complex glycosylated sugars of which the latter is processed in the medial part of the golgi apparatus during the maturation process of N-glycosylation. EndoH resistence of N-glycosylation thus occurs after Golgi-localized modification (Maley, Trimble et al. 1989; Petäjä-Repo, Hogue et al. 2000; Parker, Gergely et al. 2004; Plaut and Carbonetti 2008). This deglycosylation analysis supplies information on the trafficking abilities of ClC-Kb out of the ER to the golgi apparatus. In the absence of barttin a double band was detected at approximately 90 and 92kDa (respectively the black and white dots in Fig. 3.2), while the calculated mass is 103kDa. This difference in the calculated mass and molecular weight detected on the SDS gel might be due to anomalous protein migration on the gel (Uchida, Sasaki et al. 1995). The upper band was shown to be sensitive to both endo H and PNGase F, thus this band represents core glycosylated ClC-Kb. In the presence of barttin a third band appeared at 107kDa which was only deglycosylated by PNGase F, indicating complex glycosylated ClC-Kb (hash mark in Fig. 3.2). Barttin is shown to induce ClC-Kb exit out of the ER and facilitating the trafficking of the channel to the Golgi apparatus.

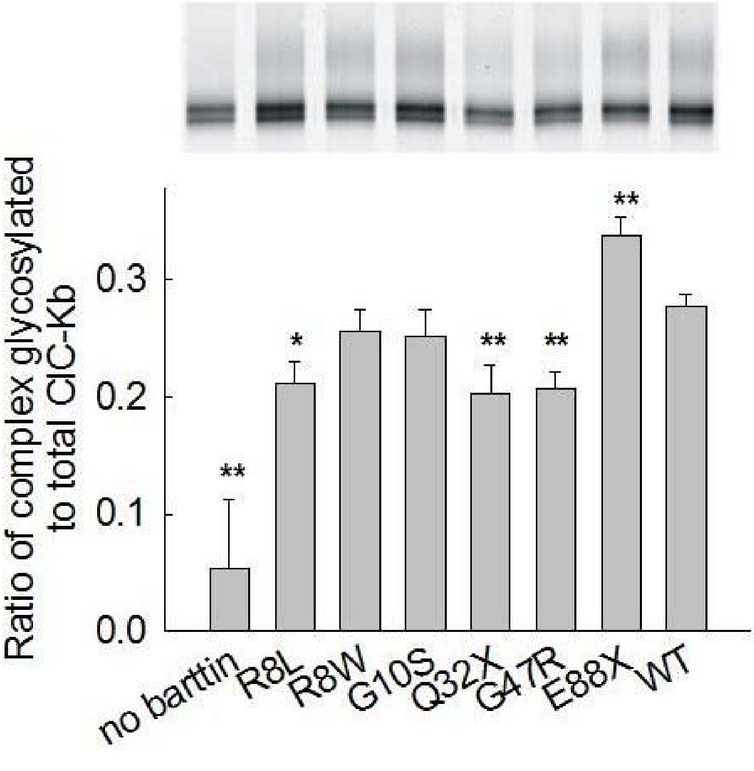

Figure 3.3 All barttin mutants induce complex glycosylation of ClC-Kb. A denaturing SDS protein gel of the cleared lysate of MDCK cells expressing either YFP-ClC-Kb alone or coexpressing mutant or WT barttin. The graph shows the ratio of the complex glycosylated amount of ClC-Kb fluorescence divided by the total ClC-Kb fluorescence (core+complex+not glycosylated) detected per coexpressed barttin mutant. * $0.01<p<0.05$, ** $p<0.01$ compared to the ratio in the presence of WT barttin. The number of experiments (n) is 5 or more.

The effect of the mutations in barttin on the trafficking of ClC-Kb was analysed by coexpressing YFP-ClC-Kb together with different mutant barttins in MDCK cells. Cells were lysed in triton. Figure 3.3 shows the cleared lysate on an SDS gradient gel and the graph of the analysis. For each mutant the fluorescence of the complex glycosylated ClC-Kb channel was divided by the sum of fluorescence detected for core + complex + not glycosylated YFP tagged ClC-Kb channel. This ratio indicated that E88X mutated barttin results in a higher ratio of complex glycosylated ClC-Kb than in the presence of WT barttin. Only R8W and G10S gave similar ratio´s as WT barttin. R8L, Q32X and G47R resulted in lower complex glycosylation of the ClC-Kb channel than in the presence of WT barttin and were not significantly different to the ratio detected when the channel was expressed without barttin. However, all barttin mutants were able to induce ClC-Kb complex glycosylation, while the complex glycosylated ClC-Kb band was detected in the SDS gel. The ratio of ClC-Kb without barttin should be considered as background value since colouring of the lane in the absence of a complex glycosylated band is probably due to the coomassie staining present in the loading buffer.

3.2.2 Q32X and G47R barttin decrease ClC-Kb channel expression

Mutations in barttin could have an effect on expression or stability of the ClC-Kb protein, the latter might be due to changed glycosylation. To investigate this, a comparison was made of the total amount of fluorescent YFP ClC-Kb in the absence or presence of the various barttin mutants to the total fluorescence of the channel when coexpressed with WT barttin. This analysis of the cleared lysate is displayed in figure 3.4.

G47R and Q32X gave significantly less YFP ClC-Kb fluorescence than in the presence of WT barttin though Q32X is the only mutant not significantly different from YFP channel fluorescence in the absence of barttin. The lower amount of channel fluorescence present in these three samples can be due to decreased expression, either by lower transfection efficiency or an effect of barttin on the expression level of the channel, or by a lower stability of the channel which could be proteolysed more easily.

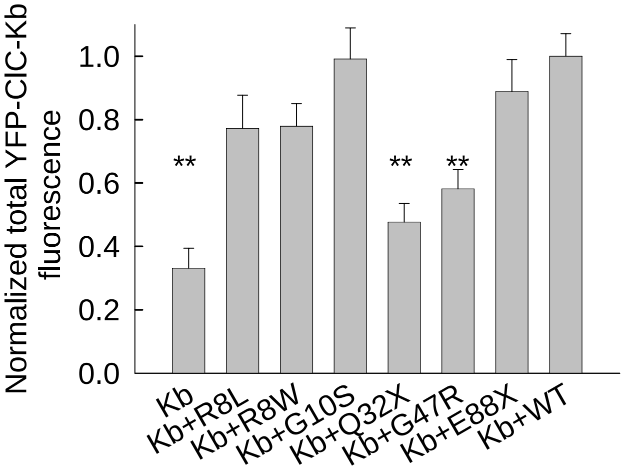

Figure 3.4 G47R and Q32X lower the amount of ClC-Kb opposed to WT barttin. The fluorescence of YFP ClC-Kb alone or in the presence of WT or mutant barttin was measured. This fluorescence in the starting material was normalized to the total amount of fluorescence in the presence of WT barttin. ** $p<0.01$ compared to fluorescence of ClC-Kb YFP in the presence of WT barttin, $n \geq 7$.

3.3 Most barttin mutants transport ClC-Kb to the plasma membrane

3.3.1 G10S, E88X and WT barttin stimulate ClC-Kb insertion into the plasma membrane

Confocal imaging is often used to show trafficking properties of proteins and (co-) localization. Figure 3.5 shows confocal images of MDCK cells expressing WT barttin and mutant barttins tagged with a cyan fluorescent protein (CFP). MDCK cells were fixed with paraformaldehyde and scanned for fluorescence with a confocal microscope. WT barttin

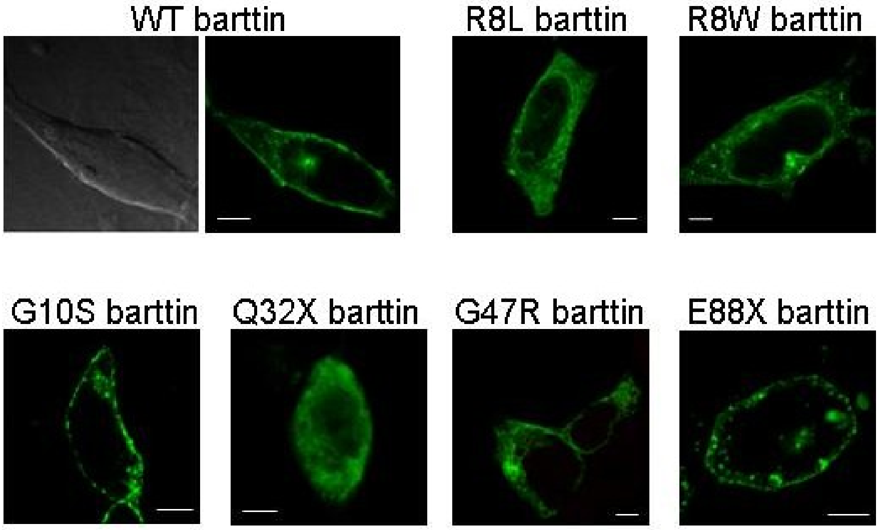

Figure 3.5 Confocal images of fixed MDCK cells expressing WT or mutated CFP tagged barttin. Cells were transiently transfected. WT barttin is shown as differential interference contrast and fluorescent confocal image, while mutant barttins were shown only as fluorescent pictures. White bar is 5µm.

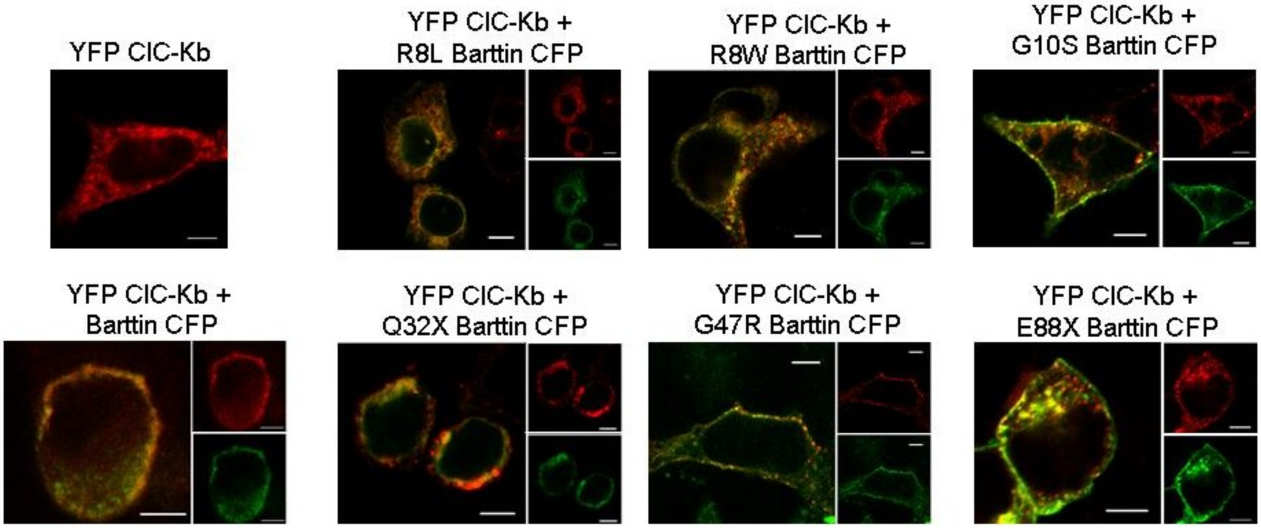
YFP ClC-Kb
YFP ClC-Kb + R8L Barttin CFP
YFP ClC-Kb + R8W Barttin CFP
YFP ClC-Kb + G10S Barttin CFP
YFP ClC-Kb + Barttin CFP
YFP ClC-Kb + Q32X Barttin CFP
YFP ClC-Kb + G47R Barttin CFP
YFP ClC-Kb + E88X Barttin CFP

Figure 3.6 Confocal images of fixed MDCK cells expressing YFP tagged ClC-Kb alone or with WT or mutant barttin CFP. YFP is shown in red and CFP in green, a colocalization gives a yellow/orange staining. MDCK cells were transiently transfected and fixed. White bar is 5µm.

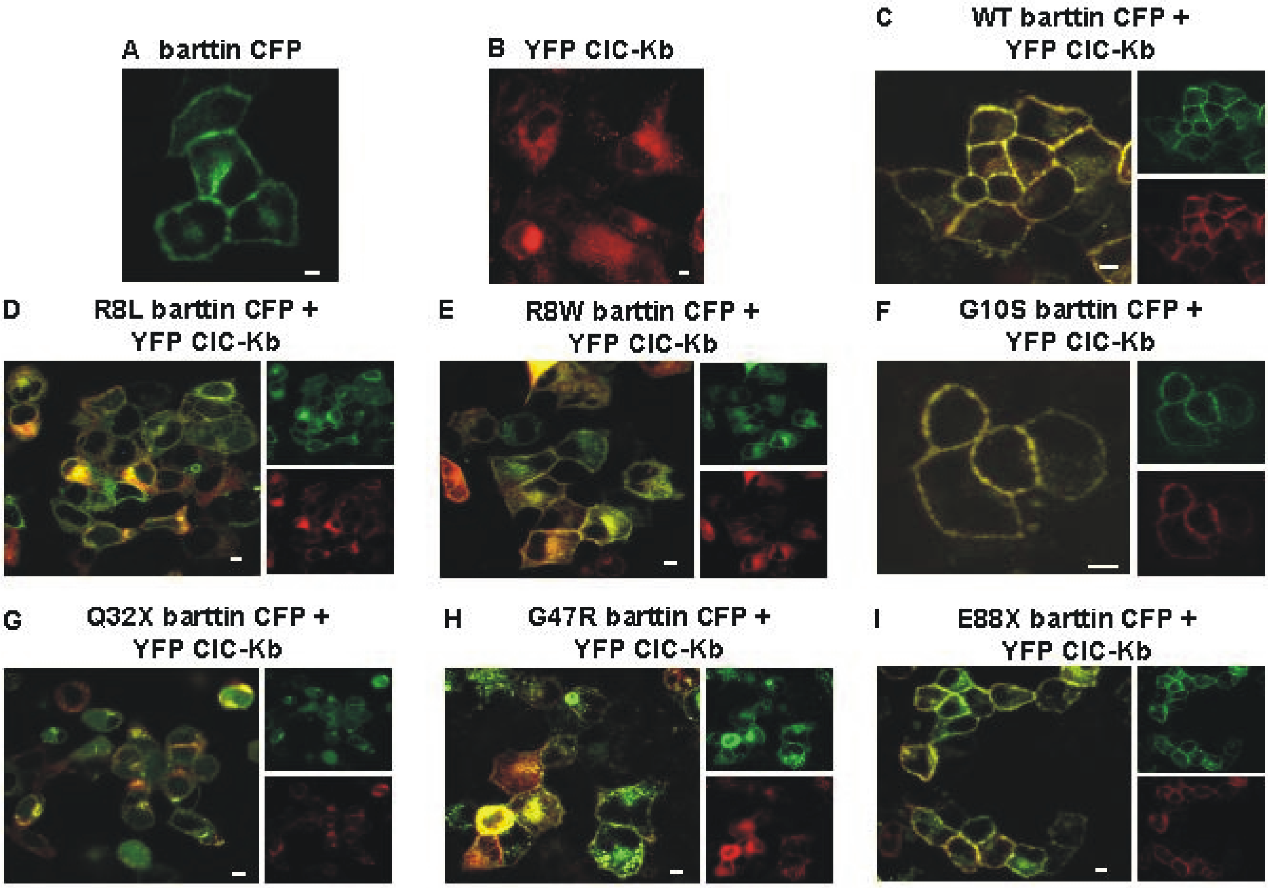
A barttin CFP
B YFP ClC-Kb
C WT barttin CFP + YFP ClC-Kb
D R8L barttin CFP + YFP ClC-Kb
E R8W barttin CFP + YFP ClC-Kb
F G10S barttin CFP + YFP ClC-Kb
G Q32X barttin CFP + YFP ClC-Kb
H G47R barttin CFP + YFP ClC-Kb
I E88X barttin CFP + YFP ClC-Kb

Figure 3.7 Confocal images of living MDCK cells. Cells either expressed only WT barttin CFP or YFP ClC-Kb or a coexpression was performed with YFP ClC-Kb and WT or mutant barttin CFP. Cells were transiently transfected. YFP is shown in red and CFP in green, a colocalization gives a yellow/orange staining. On the right side pictures are shown from either CFP or YFP while on the left an overlap is shown. The white bar is 5µm.

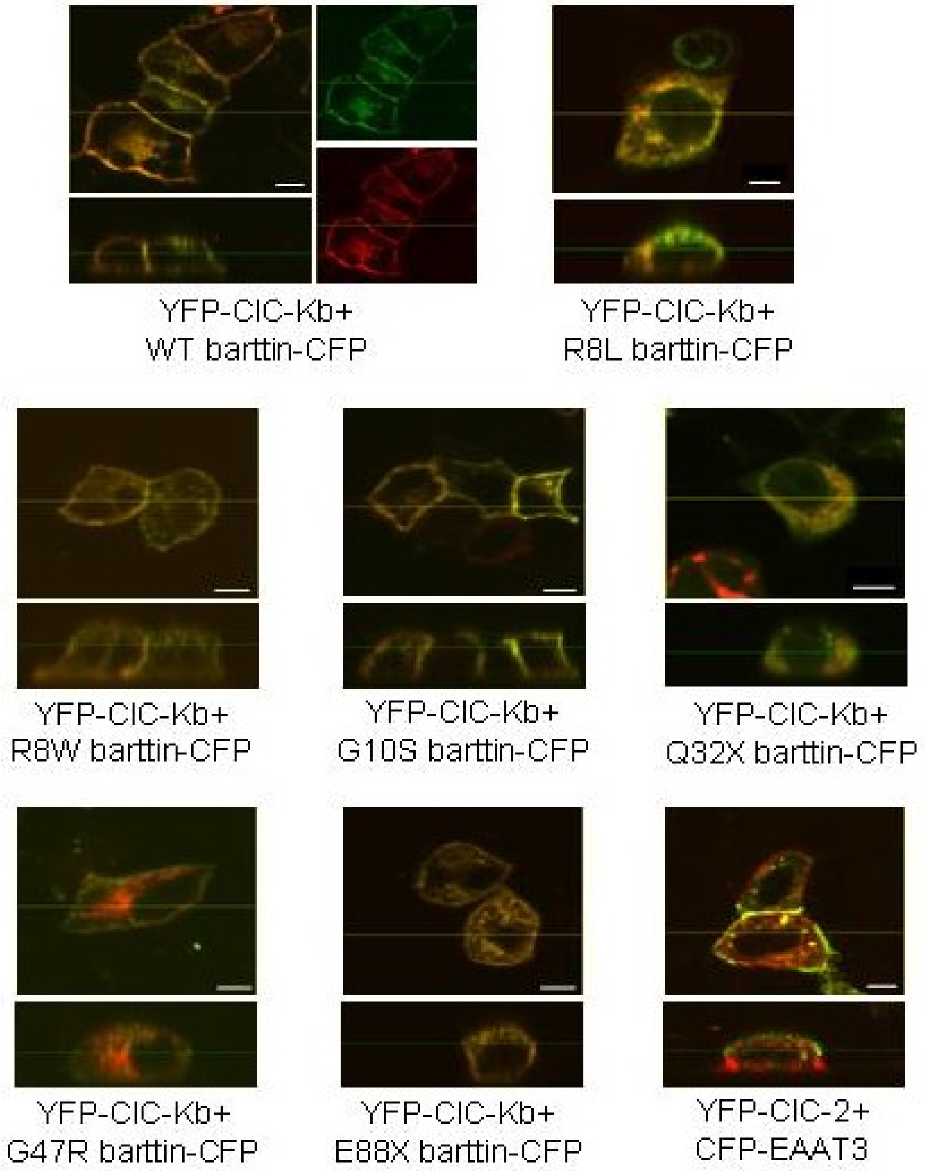

YFP-ClC-Kb+
WT barttin-CFP

YFP-ClC-Kb+
R8L barttin-CFP

YFP-ClC-Kb+
R8W barttin-CFP

YFP-ClC-Kb+
G10S barttin-CFP

YFP-ClC-Kb+
Q32X barttin-CFP

YFP-ClC-Kb+
G47R barttin-CFP

YFP-ClC-Kb+
E88X barttin-CFP

YFP-ClC-2+
CFP-EAAT3

Figure 3.8 Horizontal and vertical confocal images of living MDCK cells grown on dishes. Cells were transiently transfected with YFP tagged ClC-Kb and WT or mutant barttin CFP and were grown on dishes suitable for confocal imaging. Horizontal slides were made of which a vertical slides was created. EAAT3 and ClC-2 are shown as examples of apical and basolateral membrane staining, respectively. YFP is shown in red and CFP in green, a colocalization gives a yellow/orange staining. White bar is 5μm.

showed membrane staining, as did G10S and E88X. R8L, R8W, Q32X and G47R gave much more intracellular staining. Especially Q32X stained the complete cell, often even the nucleus. This showed that at least some barttin mutants exhibit some impairment of their trafficking properties.

In fixed MDCK cells coexpression of YFP tagged ClC-Kb channels with barttin CFP, resulted in similar membrane staining as in the absence of ClC-Kb (Fig 3.5 and 3.6). WT, G10S and E88X barttin resulted in colocalisation and membrane staining with ClC-Kb, though E88X also gave intracellular staining. Membrane staining was more difficult to distinguish for R8L, R8W, Q32X and G47R barttin that exhibited a lot of intracellular staining. Since artifacts due to fixation of tissue have been noticed before (Ziemer, Diaz-Cascajo et al. 2000), confocal images of living cells were obtained (Fig. 3.7). A more profound membrane staining was observed for living cells.

In figure 3.8 living cells were scanned horizontally at different heights so that a vertical slide could be reconstructed, this way apical and basolateral sections of the plasmamembrane could be distinguished in a monolayer of MDCK cells. In order to check the ability of cultured MDCK cells, grown on dishes, to perform the physiological distribution of proteins to the apical and basolateral membrane EAAT3 and ClC-2 were cotransfected. EAAT3 is reported to be expressed solely apical (Cheng, Glover et al. 2002) and ClC-2 is present on the basolateral side in MDCK cells (Peña-Münzenmayer, Catalán et al. 2005). Although there has been some controversy on ClC-2 localization (Mohammad-Panah, Gyomorey et al. 2001; Dhani, Mohammad-Panah et al. 2003; Catalán, Niemeyer et al. 2004), it is shown that ClC-2 is sorted to the basolateral membrane by a di-leucine motif (Peña-Münzenmayer, Catalán et al. 2005). These results show the capability of MDCK cells, grown confluently on dishes, to differentiate in basolateral and apical plasmamembranes. R8L, Q32X and G47R barttin gave less membrane staining and not always a colocalization of both barttin and ClC-Kb. R8W barttin was present in the membrane but also intracellular. WT, G10S and E88X gave clear membrane staining. WT and G10S were more basolateral than apical though E88X seemed to give an overall staining. However, although usually MDCK cells are grown on filters for polarization, these confocal images suggest growth of confluent monolayer of MDCK cells on dishes give similar results. Stable WT or E88X barttin CFP transfected MDCK cells were grown on filters, and gave similar protein distribution as transiently transfected cells. Figure 3.9 shows these confocal images.

Confocal imaging has the disadvantage that it is difficult to detect low amounts of protein in the membrane when there is also intracellular retainment. ClC-K1 is the only ClC-K channel known to traffick to the plasma membrane without barttin since it is able to give ion conductances in the absence of barttin. Though this β-subunit increases the channels ion conductance and membrane insertion (Scholl, Hebeisen et al. 2006). As we have shown previoulsy (Scholl *et al.* (2006)) figure 3.10 shows no membrane staining in the absence of barttin indicating the limitations of this technique. Coexpression of ClC-K1 with WT barttin results in clear membrane staining as does R8W barttin, however Q32X gives overall intracellular staining.

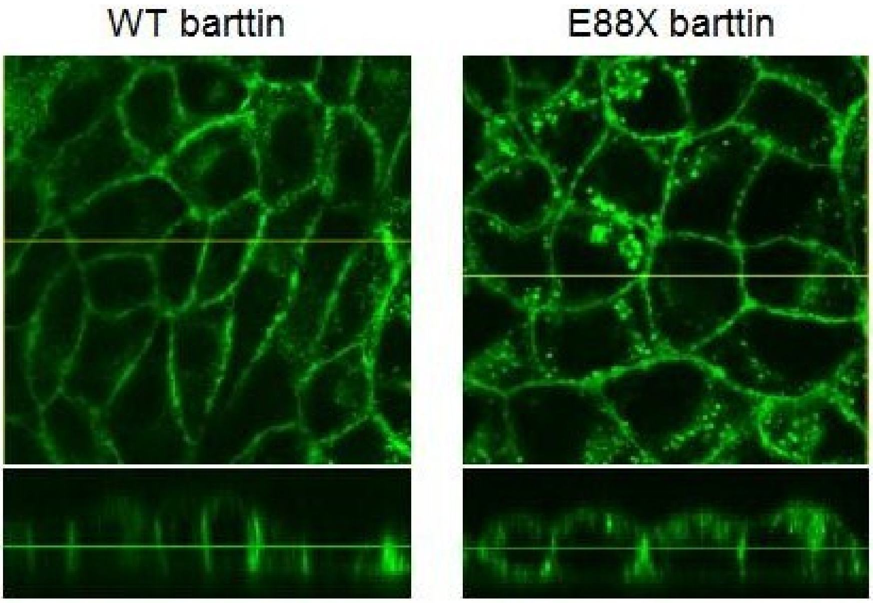
WT barttin
E88X barttin

Figure 3.9 Confocal images and vertical slides of stably WT or E88X barttin CFP transfected polarized MDCK cells. MDCK cells expressed either WT or E88X barttin CFP, were grown on filters and were fixed before imaging. The line in the upper part shows where the vertical slide was created and in the lower part the line indicates the hight of the horizontal slide.

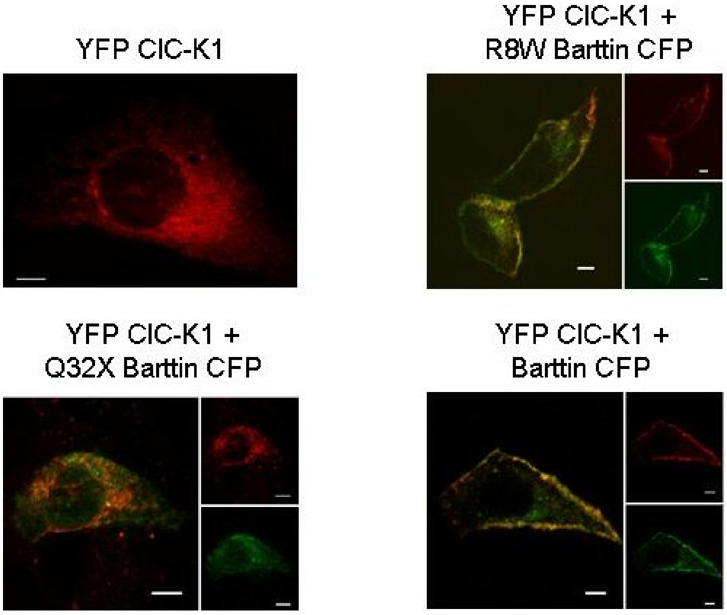
YFP ClC-K1
YFP ClC-K1 +
R8W Barttin CFP
YFP ClC-K1 +
Q32X Barttin CFP
YFP ClC-K1 +
Barttin CFP

Figure 3.10 Q32X does not colocalise in the membrane with rClC-K1. Confocal images of fixed MDCK cells expressing rClC-K1 YFP alone or with CFP tagged WT, R8W or Q32X barttins. Images were made from fixed cells. CFP is shown in green, YFP in red. White bar is 5µm.

3.3.2 Only Q32X barttin is inable to induce ClC-Kb membrane insertion

Since confocal imaging showed whether the ClC-K channel is located close to the membrane but not if it is really inserted into the membrane, biotinylation was performed. A non confluent plate of transfected MDCK cells was used and medium without calcium, decreasing the possibility of formation of tight junctions, so that both the apical and basolateral sides of the cell could be accessed by biotin (Daniels and Amara 1998). Biotin bound to the membrane proteins and was purified with avidin. After elution the samples were placed on an SDS gradient gel and could be analysed. Only experiments were used with no detection of actin in the membrane purified fraction, which was a control of the disruption of cells and internalisation of biotin during the experiment.

The data in both graphs in figure 3.11 was normalised to the ratio of membrane ClC-Kb YFP found in the presence of WT barttin. This calculation was performed to account for varying photomultiplier settings, SDS protein gel backgrounds and loading conditions per experiment. The calcium channel β-subunit was used as a negative control in these experiments since it should not have an effect on cellular distribution of ClC-Kb channels but the transfection efficiency might be higher in the presence of this second plasmid. This subunit might be involved in endocytosis (Gonzalez-Gutierrez, Miranda-Laferte et al. 2007; Hidalgo and Neely 2007), however it did not elevate the actin detection in purified membrane fractions, maybe because of limiting the endocytosis by performing the experiment at 4ºC. No difference to ClC-Kb alone was given since this experiment was only performed once. Figure 3.11 the graph on the top represents the fluorescence of membrane inserted YFP ClC-Kb that is devided by the amount of actin present in the starting material, to account for the different cell amounts per sample. Significant higher ratios were found in the presence of WT or G10S barttin than in the presence of the calcium channel β-subunit. Less membrane inserted ClC-Kb than induced by WT barttin was found for G10S, Q32X and G47R mutants. Differences in the presence of R8L, R8W and E88X were not significant. The lower ratio for G47R barttin is due to a lowered expression, as can be concluded from the graph on the bottom. Graph 3.11 bottom displays the amount of membrane inserted channel fluorescence devided by the total amount of channel fluorescence. Only Q32X barttin and the calcium channel β-subunit induced lower channel membrane insertion than WT barttin. R8L, G10S, G47R, E88X and WT barttin were different to the membrane insertion in the presence of the calcium channel β-subunit. No differences were found for R8W because of too large variances. There seems to be a higher detection of channel in the membrane when coexpressed with the calcium channel β-subunit compared to when ClC-Kb is expressed alone, this looks like an effect of a higher expression or transfection level of ClC-Kb in the presence of this second transfected plasmid.

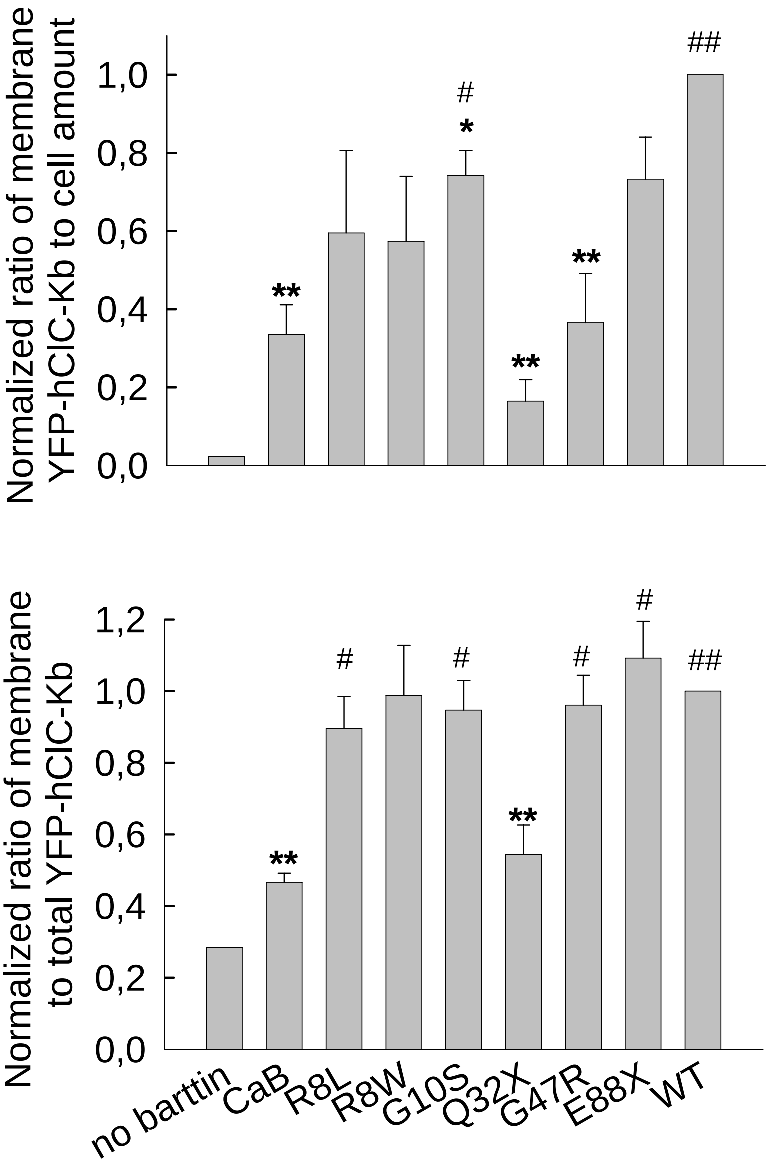

Figure 3.11 Only Q32X barttin is impaired in ClC-Kb membrane insertion. A biotinylation assay of the complete cell membrane was performed. The fluorescence of purified biotinylated membrane inserted YFP ClC-Kb was analysed in two ways. Either the fluorescence was divided by the amount of actin present in the starting material (which stands for the amount of cells) and was normalized to WT barttin (shown on top), or (bottom) the fluorescence was divided by the amount of total YFP ClC-Kb fluorescence present in the starting material per mutant and was normalized to WT barttin. n=3 except for without barttin which was 1 and the calcium channel β-subunit (CaB) which was 2. * $0.01<p<0.05$, ** $p<0.01$ compared to the ratio in the presence of WT barttin while # is compared to the ratio in the presence of the calcium channel β-subunit.

3.3.3 E88X barttin lacks the sorting mechanism of WT barttin

The vertical slides from the confocal images in figure 3.8 and 3.9 seemed to show an overall staining of the membrane of MDCK cells when E88X barttin CFP was expressed, opposed to WT barttin. To investigate this in more detail a bioninylation assay was performed on confluently grown MDCK cells. These were grown on a filter so that either the apical or basolateral membrane could be accessed with biotin. A confluent monolayer was grown and buffers with calcium were used, to keep tight junctions intact.

Only experiments with no detected actin in the purified membrane fraction were used. Data obtained for this biotinylation assay are displayed in figure 3.12 in which fluorescence of biotinylated membrane inserted ClC-Kb was devided by the amount of actin in the starting material. The apical or basolateral purified amount of ClC-Kb fluorescence was devided by the total amount of purified channel, so both apical and basolateral, for WT and E88X barttin separately. Less basolateral but more apical membrane insertion of YFP ClC-Kb is observed in the presence of E88X barttin than with WT barttin. Coexpression of YFP ClC-Kb with WT

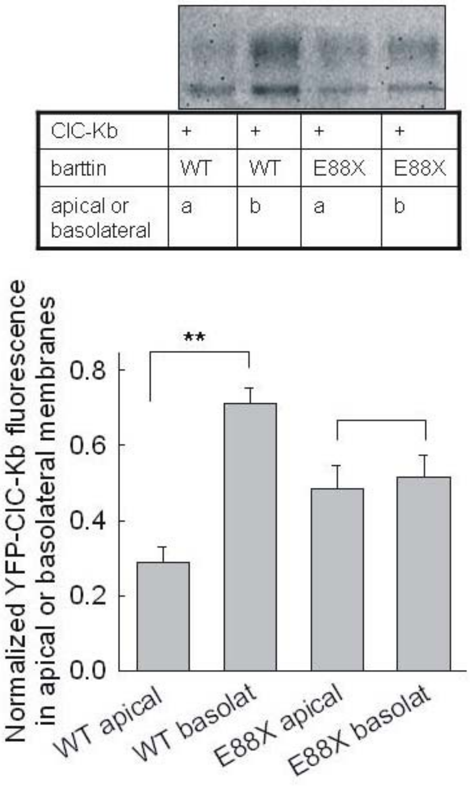

Figure 3.12 E88X barttin lacks epithelial sorting. An SDS protein gel is shown, as is the graph of the analysis of the biotinylation assay of separated apical or basolateral membranes. YFP-ClC-Kb was either expressed together with WT or E88X barttin. Biotin was added to the apical or basolateral side of the cells, purified, placed on a gel and was analysed. Fluorescence was normalized to the amount of actin present in the cleared lysate. Apical or basolateral purified fluorescent channel was devided by fluorescence optained from apical+basolateral biotin application, for WT and E88X barttin separately. n=5.

barttin gave significantly (p=0.0001) more ClC-Kb insertion into the basolateral membrane than into the apical membrane. For E88X barttin no difference (p=0.74) between apical and basolateral ClC-Kb membrane insertion was detected. This implicates a sorting problem induced by the E88X barttin mutation. The amount of channel purified in the absence of barttin was often too low to detect and was thus not used in this analysis.

3.4 Loss of protopore activation by most barttin mutants

3.4.1 Only E88X induces currents like WT barttin in human ClC-K isoforms

The fact that most mutated barttin proteins traffick to the membrane does not necessarily mean that they also activate ClC-K channels. To investigate the activating capability of mutant barttin, tsA201 cells were transiently transfected and analysed using whole cell patch clamp electrophysiology.

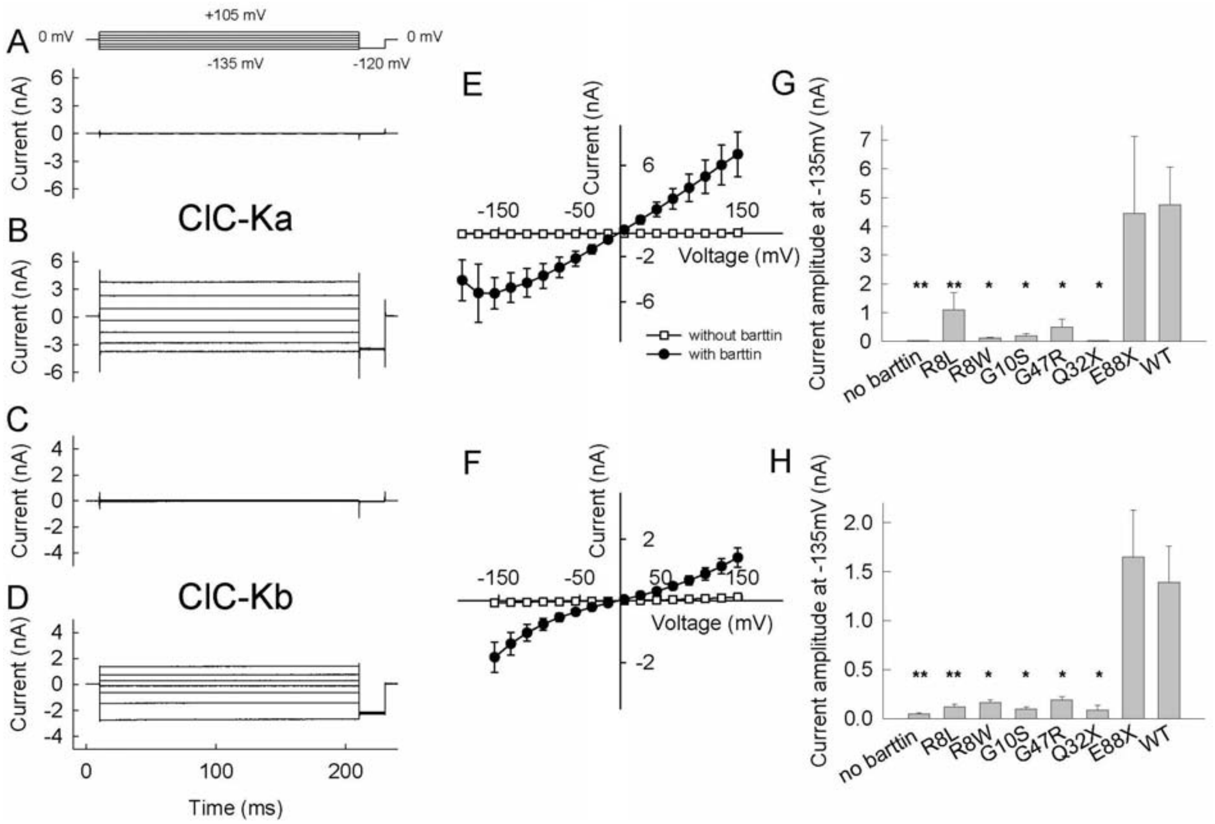

Figure 3.13 Only E88X barttin induces currents in human ClC-K channels as WT barttin. ClC-Ka and ClC-Kb expressed either alone or together with WT or mutant barttin. Representative current recordings of ClC-Ka (A,B) or ClC-Kb (C,D) alone (A,C) or coexpressed with WT barttin (B,D). The voltage protocol is shown in A. Voltage / current relationship of ClC-Ka (E) or ClC-Kb (F) with or without WT barttin. Current amplitudes at -135mV of ClC-Ka (G) or ClC-Kb (H) expressed alone or together with WT or mutant barttin. * $0.01<p<0.05$, ** $p<0.01$ compared to the current in the presence of WT barttin.

Both ClC-Ka and ClC-Kb do not produce currents in the absence of barttin (Fig. 3.13A-D). The current voltage relationship is linear over a large voltage range except at the very negative voltages where ClC-Ka currents decrease (Fig. 3.13E). ClC-Kb has a slightly increased conductance at more positive and negative voltages (Fig. 3.13F). E88X is the only barttin mutant able to induce hClC-K currents like WT barttin, other mutants gave dramatic decreases of the current amplitudes (Fig. 3.13G, H).

So far it was not clear whether the lack of current of the human ClC-K isoforms in the presecense of barttin mutants was caused by a disruption of transport or an activation deficiency. To separate these two functions of barttin, a concatamere was constructed from ClC-1 and ClC-Kb. This concatamere was able to transport ClC-Kb to the plasma membrane using ClC-1 as a vehicle. This way, it was possible to investigate the activating properties of barttin on membrane inserted CLC-Kb proteins.

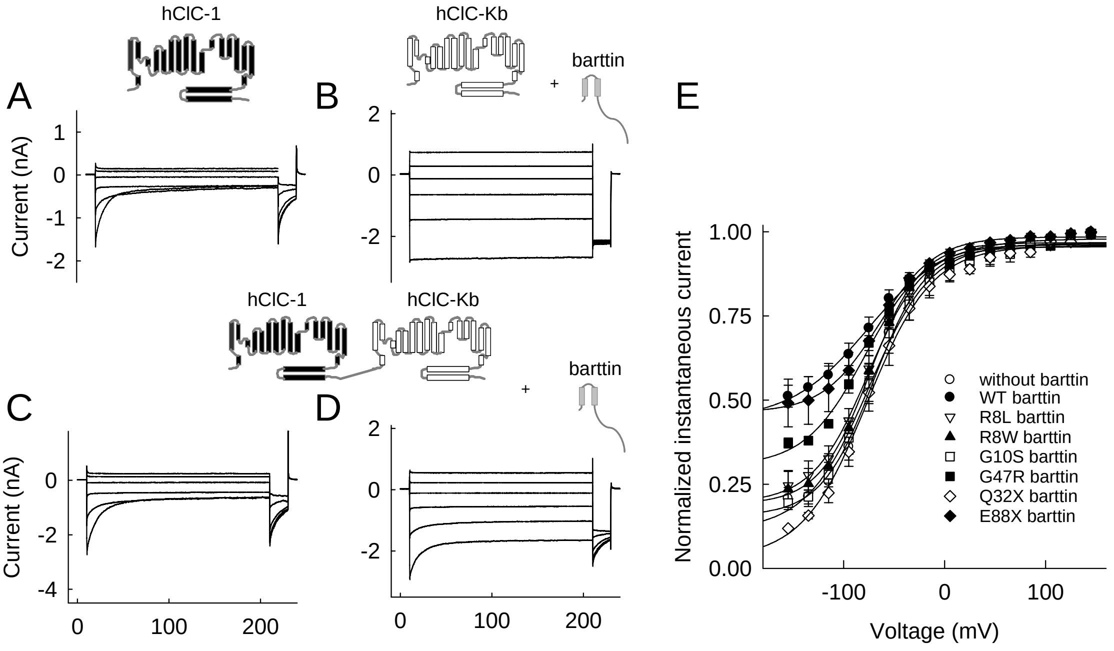

Figure 3.14 Activation of the ClC-Kb protopore by WT, E88X and G47R barttin. Representative current recordings of CLC-1 (A), ClC-Kb with barttin (B), ClC-1/ClC-Kb concatamere with (D) and without barttin (C). Measurement of the instantaneous current amplitude at -120mV after application of several different voltages. The ClC-1/ClC-Kb concatamere was expressed alone or together with WT or mutant barttin (E).

Figure 3.14A shows a representative current recording of ClC-1. In the absence of barttin, the ClC-1/ClC-Kb concatamer displays very similar currents as ClC-1 (Fig. 3.14C) indicating that only the ClC-1 protopore is functional. An additional voltage independent component is present when the concatamere is expressed with the accesory subunit (Fig. 3.14D). This is due to the additionally functional CLC-Kb protopore, seen as a superposition of currents from ClC-1 and ClC-Kb with barttin (Fig. 3.14A-D).

The instantaneous current amplitude of the tail current at a fixed voltage step to -120mV was measured after long prepulses of voltages between +145 and -155mV. Currents were normalized to the most extreme value and plotted versus the applied voltages. The graph shows a lower value upon hyperpolarisation when only the ClC-1 protopore is active while the addition of barttin gives an increase to about 50% because of the additional voltage independent component that represents the activated ClC-Kb protopore. Almost all of the barttin mutations failed to activate the ClC-Kb protopore. Measurement at the -135mV prepulse showed that E88X barttin was the only mutant able to activated ClC-Kb like WT barttin. G47R was the only mutant different to both concatamere activation in the absence or presence of WT barttin and thus seemed to be able to partially activate the ClC-Kb protopore (Fig. 3.14 E).

3.4.2 All barttin mutants but Q32X invert the voltage dependence of activation of rat V166E ClC-K1

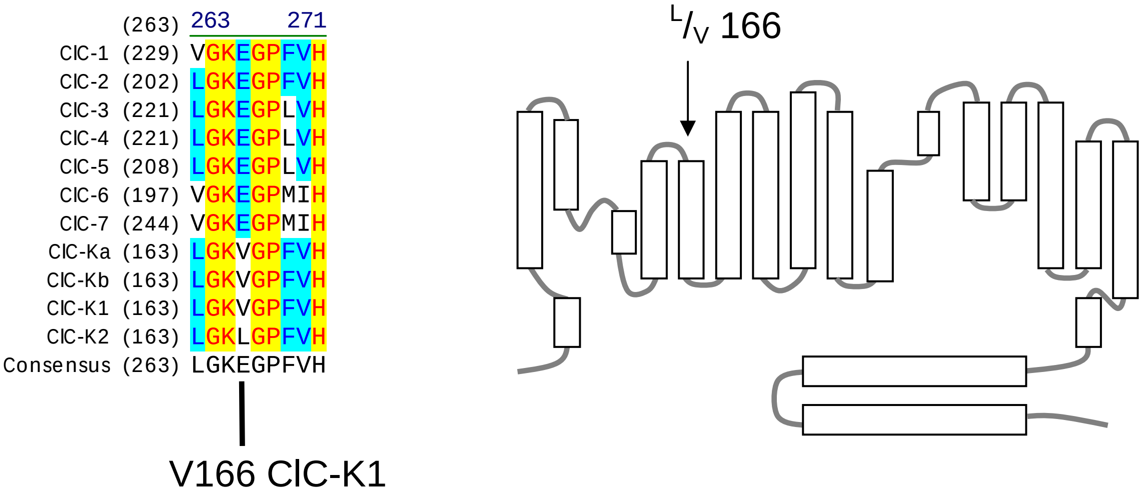
(263) 263 271
ClC-1 (229) VGKEGPFVH
ClC-2 (202) LGKEGPFVH
ClC-3 (221) LGKEGPLVH
ClC-4 (221) LGKEGPLVH
ClC-5 (208) LGKEGPLVH
ClC-6 (197) VGKEGPMIH
ClC-7 (244) VGKEGPMIH
ClC-Ka (163) LGKVGPFVH
ClC-Kb (163) LGKVGPFVH
ClC-K1 (163) LGKVGPFVH
ClC-K2 (163) LGKLGPFVH
Consensus (263) LGKEGPFVH
V166 ClC-K1
L/V 166

Figure 3.15 GK$^{V}/_{L}$GP motif in ClC-K channels. Alignment of human ClC proteins and rat ClC-K1 and K2. The amino acid at position 166 in rat ClC-K1 is in ClC-K channels either a valine or a leucine while in other human ClC proteins this is a conserved glutamatic acid residue. On the right side a representation of a ClC-K channel is shown, amino acid 166 in rClC-K1 is marked.

CLC-K channels are the only ClC proteins that, in either rat or human, do not contain a GKEGP motif but a GK$^{V}/_{L}$GP amino acid sequence (Fig. 3.15). This missing glutamic acid is thought to function as a fast gate in other ClC proteins (see introduction 1.4.3), acting on the individual protopores independly. Human ClC-K channels are not functional without barttin however rat ClC-K1 is. Restoring this motif in rClC-K1, by a V166E substitution, gives a major change in the channels behaviour.

Figure 3.16 shows V166E rClC-K1 activation by membrane hyperpolarization in the absence of barttin (Fig. 3.16A). The addition of barttin (Fig. 3.16E) inverts this voltage dependence of activation. Representative current recordings of V166E rClC-K1 in the presence of the disease causing barttin mutants show a similar induced change of activation for all barttin mutants with one exception, Q32X (Fig. 3.16B-D, F-H). This indicates that most barttin mutants are able to bind rClC-K1 and influence or activate its ion conduction, which could not be detected for the human ClC-K isoforms in figure 3.13.

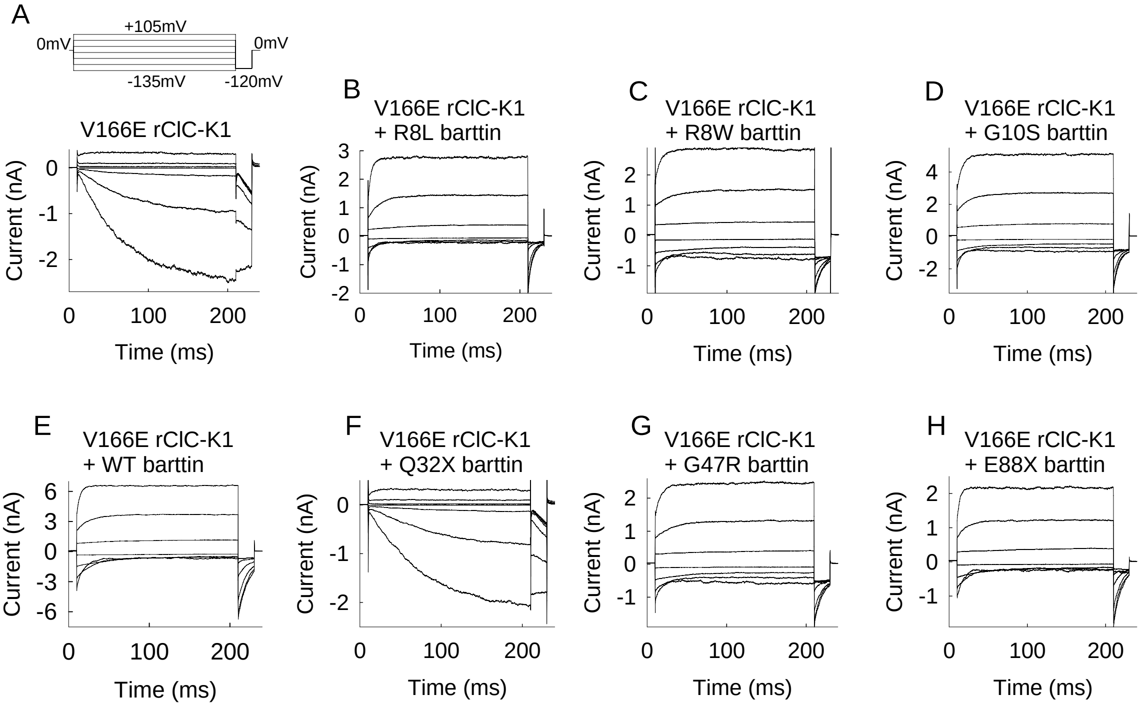

Figure 3.16 All barttin mutants but Q32X invert rat V166E ClC-K1 voltage dependence of activation. Representative whole cell current recordings of V166E rClC-K1. The channel was expressed alone (A) or coexpressed with WT (E) or mutant barttin (B-D, F-H). The voltage protocol is shown on the left.

Figure 3.17 shows the macroscopic current amplitude of V166E rClC-K1 at the end of a 200ms pulse at +105mV. Mutants R8L, R8W, Q32X and G47R reduced anion currents opposed to the measured current in the presence of WT barttin. G10S and E88X increased currents like WT barttin and only coexpression of Q32X barttin with V166E rClC-K1 did not significantly increase currents compared to expression of the channel alone.

Non-stationary noise analysis was used to obtain the single channel amplitude and the absolute open probability of V166E rClC-K1 in the absence of barttin or in the presence of WT or some of the mutant barttins. The analysis of this channel coexpressed with WT barttin is shown in figure 3.18. Several pulses to different voltages from –100 to –200mV were applied after a prepulse to +75mV. Figure 3.18A displays the current to time graph and the variance of the current to the time. The variance of the current was plotted against the current and was than fitted so that the absolute open probability at +75mV and the single channel amplitudes between –100 to –200mV (Fig. 3.18B) could be calculated. To obtain the absolute activation curves (Fig. 3.18C), first a relative activation curve was obtained by measurement of the instantaneous current amplitude of the tail current at a fixed voltage step to –120mV after several long prepulses of voltages between +145 and -155mV. These currents were normalized to their most extreme value. These relative activation curves could than be adjusted to absolute activation curves by adjusting the open probability at +75mV to the calculated absolute open probablity for each mutant at +75mV.

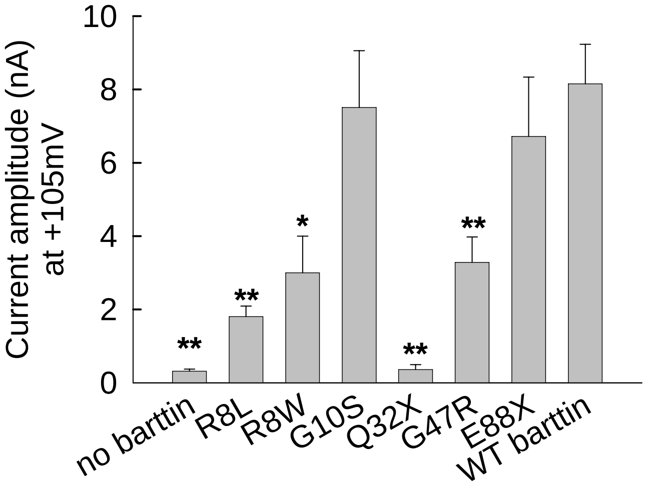

Figure 3.17 Barttin mutatations, except G10S and E88X, affect the current amplitude of V166E ClC-K1. Current amplitudes of V166E rClC-K1 in the absence or presence of WT or mutant barttin. Macroscopic current amplitudes at the end of a 200ms long pulse to +105mV were measured.

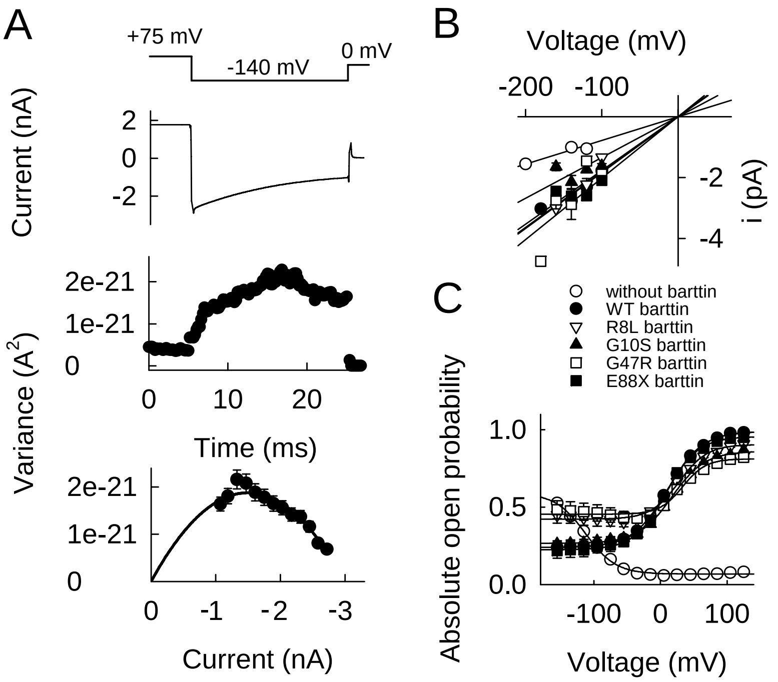

Figure 3.18 Non-stationary noise analysis of V166E rClC-K1 alone or in the presence of WT, R8L, G10S, G47R or E88X barttin. (A) Non-stationary noise analysis of V166E rClC-K1 coexpressed with WT barttin. From top to bottom is displayed; A voltage protocol, the current to time and variance to time graph and the variance to current graph. The fit of the variance to current graph gives the number of channels and the single channel conductance which are neccesary to calculate the open probability at +75mV. In B the single channel amplitudes and in C the absolute activation curves of V166E rClC-K1 alone or with WT or mutant barttin are shown.

Figure 3.18C indicates that the addition of WT barttin changes the voltage dependence of V166E rClC-K1 dramatically. WT barttin increases the single channel amplitude (Fig. 3.18B) while inverting the open probability in the positive and negative voltage range (as has been shown previously (Scholl, Hebeisen et al. 2006)). Barttin mutants do not seem to change the single channel amplitude compared to WT barttin. E88X barttin affects the absolute open probability like WT barttin. G10S lowers the absolute probability of the channel in the positive voltage range compared to WT barttin, while R8L and G47R have an additional increase in the negative voltage range.

4. Discussion

Barttin is a β-subunit of ClC-K chloride channels. Mutations in the BSND gene encoding for barttin result in Bartter syndrome type IV, a disease manifested with renal salt wasting and sensorineural deafness. Disease-causing mutations are present in the amino-terminal part of barttin, which is also the most conserved among species. These mutations were analysed for their effects on the two known functions of barttin; transport ClC-K channels to the plasma membrane and activating their protopores.

4.1 Effect on endoplasmatic reticulum exit and channel stability

In this thesis barttin is shown to be involved in the ER exit of the ClC-Kb channel and its trafficking to the Golgi apparatus. Deglycosylation analysis showed that in the absence of barttin, hClC-Kb is core or not glycosylated while in the presence of barttin there is also complex glycosylation (Fig. 3.2). Although the ratios of complex glycosylated to total ClC-Kb differ for some of the mutant barttins, they are all able to induce complex glycosylation and thus ClC-Kb exit out of the ER and its trafficking to the Golgi apparatus (Fig. 3.3).

The lower ratio of complex glycosylation of ClC-Kb channel in the presence of the R8L, Q32X and G47R mutation in barttin could imply trafficking impairment. G10S and R8W barttin induced the same ratio of complex glycosylated ClC-Kb compared to WT barttin while E88X resulted in a higher ratio. This could be due to channel internalisation by normal turnover mechanisms but the inability of breaking down the protein. A lack of the c-terminal PY motif in the E88X mutant could be the reason of this since it is involved in the ubiquitinylation of barttin and probably regulating its proteolysis and internalisation. There is also the possibility that due to overexpression there is more intracellular retainment which might not be the same for each barttin mutant. This could lead to a lower ratio of complex glycosylated ClC-Kb. Or in the contrary, a lower retainment to a higher ratio as for the E88X mutant barttin.

Other members of the ClC channel / transporter family have been shown to undergo glycosylation. ClC-K channels from *Xenopus leavis* kidney tissue were glycosylated as was shown by deglycosylation with PNGaseF. Two conserved asparagines in the ClC family have been demonstrated to be effectively glycosylated in ClC-0, ClC-1, ClC-K1 and ClC-K2 (Kieferle, Fong et al. 1994; Uchida, Sasaki et al. 1995; Maulet, Lambert et al. 1999). ClC-3 undergoes differential tissue specific N-glycosylation (Schmieder, Lindenthal et al. 2001) and ClC-5 is N-glycosylated on asparagines at the amino acid positions 169 and 470 (Schmieder, Bogliolo et al. 2007).

Previous research showed some ClC proteins to gain protection against proteolysis due to their glycosylation. ClC-7 is the only mammalian ClC protein lacking N-linked glycosylation sides. Somewhat like barttin and ClC-Kb, ClC-7 is required for Ostm-1 to leave the ER and reach the lysosomes. ClC-7 could be shielded from lysosomal proteases by Ostm-1 which is highly glycosylated. Ostm-1 seems to stabilise ClC-7, when absent there is a decline of ClC-7 to a pathogenic level and it has been suggested that the pathogenesis of OSTM-1 mutations can be completely explained by this large reduction in ClC-7 protein levels (Lange, Wartosch et al. 2006). ClC-5 glycosylation decreased the protein susceptibility to ubiquitin and proteasomal degradation. Disruption of this post-translational modification reduced the cell surface pool and the protein was retrieved faster from the cellmembrane though glycosylation was not required for targeting to the surface membrane (Schmieder, Bogliolo et al. 2007). The expression of ClC-K2 reported to be consistently weaker in the absence of barttin than in its presence which was also observed for ClC-Kb in this thesis (Fig. 3.4). ClC-K2 was shown to rapidly degrade without barttin coexpression, showing higher stability in its presence (Hayama, Rai et al. 2003).

In stable MDCK cell lines, ClC-K2 was retained in the Golgi in the absence of barttin while in its presence the channel was transported to the plasma membrane (Hayama, Rai et al. 2003). However, we (Scholl, Hebeisen et al. 2006) have showed an ER retainment of ClC-Kb and ClC-K1 in transiently transfected MDCK cells. Results in this thesis are more consistend with the latter finding. ER retainment would explain the lack of N-glycosylation of ClC-Kb in the absence of barttin, however the channel could also be transported to the golgi apparatus where it was not further processed and was then retained. When expressed in oocytes, barttin resided in the plasma membrane while human ClC-Ks were in cytosolic compartments. Coexpression led to colocalisation of barttin with the channel in the membrane (Waldegger, Jeck et al. 2002). Barttin was co-precipitated with ClC-K2 suggesting a protein-protein interaction. R8L was reported to be retained in the ER but to be still able to bind ClC-K2 (Hayama, Rai et al. 2003). Results in this thesis suggest there is an influence of R8L barttin on ClC-Kb that enables transport to the golgi apparatus. This difference in results could be due to the channels to be derived from different species.

Barttin seems neccesary for ClC-Kb exit out of the ER and for its trafficking to the golgi apparatus where N-glycosylation is finished. Glycosylation might protect the protein from proteolysis. This is in agreement with the measured decrease in the amount of channel fluorescence that is detected when expressed alone or in the presence of G47R or Q32X barttin compared to WT barttin (Fig. 3.4), which could be due to decreased expression or increased proteolysis. The expression level could be affected either by a lower transfection efficiency or an effect of barttin on the expression level of the channel, while a lower stability of the channel might be due to less glycosylation resulting in increased proteolysis. A lower transfection efficiency for Q32X and G47R barttin is not likely since the G47R barttin containing plasmid is of the same length as the other missense mutations and Q32X is even shorter, making transfection easier. In figure 3.3 these two constructs already have been shown to give a reduced ratio of complex glycosylated ClC-Kb channel. Though this does not explain the same amount of fluorescent ClC-Kb in the presence of R8L barttin compared to WT barttin coexpression, since this mutation also leads to less complex glycosylation.

4.2 Insertion into the surface membrane

Transport of ClC-Kb channels to the golgi apparatus does not mean there is also insertion into the plasma membrane. This localisation was visualised by confocal imaging and measured by cell biotinylation.

4.2.1 Intracellullar versus Membrane localisation

R8L, G10S, G47R, E88X were shown to insert ClC-Kb channels into the plasma membrane like WT barttin. Q32X was impaired in its chaperone function while E88X is disturbed in channel sorting, inserting same ClC-Kb amounts in apical and basolateral membranes opposed to a basolateral preference by WT barttin.

For detection of ClC-Kb in the membrane, both confocal imaging and whole cell biotinylation were performed. The reason for this was that in the case of rClC-K1 channels no membrane staining could be detected in the absence of barttin though these channels give currents in tsA201 cells in the absence of barttin (Fig. 3.10 and (Scholl, Hebeisen et al. 2006)). Clear membrane staining was observed in confocal images of WT, G10S and E88X barttin expressed either alone or together with ClC-Kb though there was some intracellular staining, which was less for G10S barttin (Fig. 3.5-3.8).

R8L, R8W and G47R gave much more intracellular staining in confocal images, which might prohibit the detection of membrane fluorescence. However, all three mutant barttins gave similar amounts of ClC-Kb membrane insertion as WT barttin. Q32X did not seem to traffick to the membrane in confocal images and was shown not to induce ClC-Kb membrane insertion. G47R and Q32X barttin gave less ClC-Kb membrane insertion than induced by WT barttin (Fig. 3.11) however, the decrease by the G47R mutation was found to be a result of less total amount of channels. Only Q32X is really impaired in its chaperone function in the transport of ClC-Kb into the plama membrane.

These findings are not completely in agreement with previous reports. Hayama *et al.* (2003) reported WT barttin transport to the surface membrane and intracellular staining probably due to overexpression while Estevez et al. (2001) reported that the surface expression of ClC-Ka was dramatically increased with the addition of barttin opposed to almost no membrane insertion in its absence. This is in agreement with the findings in this thesis. However, the rat ClC-K2 channel was also shown not to be transported to the plasma membrane in the presence of R8L barttin while G10S showed an intermediate phenotype between WT and R8L barttin (Hayama, Rai et al. 2003). R8L and R8W did not increase the surface expression of ClC-Ka (Estévez, Boettger et al. 2001). Immunoprecipitation showed direct interaction between barttin and ClC-Ka, ClC-Kb and rClC-K1, in oocyte lysates (Waldegger, Jeck et al. 2002).

A mutant barttin, Y98A, results in a disrupted PY motif and has been reported to give intense staining of the plasma membrane and no intracellular staining opposed to WT barttin which showed intracellular staining, The mutant was implicated to be more stable than WT barttin (Hayama, Rai et al. 2003). This linkage of protein stability to observed intracellular staining in confocal images also applies to data in this thesis. Intracellular staining of ClC-Kb alone or with R8L, G47R or Q32X were the most profound and these mutants also gave a smaller ratio of complex ClC-Kb glycosylation which suggests a decreased stability.

4.2.2 Apical versus basolateral membrane insertion

E88X is distorted in its epithelial sorting ability. WT barttin inserts more ClC-Kb channel into the basolateral than in the apical membrane while E88X gives similar amounts in both apical and basolateral membranes.

Vertical confocal images from cells expressing E88X barttin gave an overall staining of both apical and basolateral membrane while for WT barttin this was more basolaterally located (Fig. 3.8 and 3.9). Though the sorting of EAAT3 and ClC-2 showed the polarisation capability of transiently transfected MDCK cells grown confluently on plates (like (Burnham, Amlal et al. 1997; Li, Worrell et al. 2004; Li, Li et al. 2007)), to make absolutely sure WT and E88X barttin were stably or transiently transfected in MDCK cells which were grown on filters (Deen, van Balkom et al. 2002; Kamsteeg, Bichet et al. 2003) and fixed with paraformaldehyde before confocal imaging. The biotinylation assay in figure 3.12 confirmed the lack of sorting by E88X barttin compared to WT barttin, the latter having a preference for the basolateral membrane. The amount of apical or basolateral purified ClC-Kb in the presence of E88X barttin was in the range of apical membrane inserted channel in the presence of WT barttin, this was much less than in the basolateral membrane with WT barttin. This reduced amount of membrane inserted ClC-Kb due to the E88X barttin mutation opposed to the same amount of insertion as with coexpression of WT barttin for the complete cell biotinylation, could be due to the polarisation and the confluency of the cells for the apical/basolateral experiment opposed to not polarised not confluently grown cells for the complete cell biotinylation. The lack of the PY motif in E88X barttin could have an important effect on this mutants behaviour (also see Chapter 4.6). This motif is thought to be an ubiquitinylation site and ubiquitin has been shown to possibly play a role in sorting mechanisms (Soetens, De Craene et al. 2001).

Many motifs are known that, depending on surrounding amino acids, can lead to ER retention or targeting like KDEL, KKXX, KXKXX, RR, RXR (Zerangue, Malan et al. 2000; Parker, Gergely et al. 2004). Barttin might cover such a signal of ClC-Kb channels, thus allowing its transport out of the ER. There has also been a report on a basolateral sorting signal, YED (Lopez, Métral et al. 2005). NBC1 is a cotransporter of Na^+ and HCO^-_3 that is exclusively in the basolateral membrane, but when 23 aa at the c-term is deleted sorts to the apical membrane (Li, Worrell et al. 2004). In an autosomal dominant form of nephrogenic diabetes insipidus, aquaporin 2 is missorted to the basolateral membrane instead of the apical one (Kamsteeg, Bichet et al. 2003; Robben, Knoers et al. 2006; Sohara, Rai et al. 2006). Possibly the cytoplasmic tail of barttin contains a sorting motif that is deleted in the E88X mutant, causing the sorting disability.

4.3 Channel activation by WT and mutant barttin

4.3.1 Human isoforms

Most barttin mutants were inable to activate ClC-Kb. E88X barttin activates like WT barttin and G47R was able to partially activate the ClC-Kb protopores (Fig. 3.14). No currents were detected for ClC-Ka or ClC-Kb for all but the E88X mutated and WT barttin (Fig. 3.13). At least for R8L, R8W, G10S and Q32X this is due to a lack of activation of the ClC-Kb protopores. Though G47R was able to partially activate the channel it also resulted in a decreased channel stability. This combination seems to dramatically decrease the ClC-Kb current in the presence of WT barttin.

ClC-Ka, Kb or barttin were previously shown to give currents like uninjected oocytes while coexpressing human ClC-K in the presence of barttin did result in different currents

(Estévez, Boettger et al. 2001; Waldegger, Jeck et al. 2002). ClC-Ka gave higher currents than ClC-Kb in oocytes (Estévez, Boettger et al. 2001) which was also observed in the human cells used in this thesis. ClC-Ka, ClC-Kb, rClC-K1 and V166E rClC-K1 currents look different in oocytes (Waldegger and Jentsch 2000; Estévez, Boettger et al. 2001; Waldegger, Jeck et al. 2002; Picollo, Liantonio et al. 2004) than in mammalian cell lines. Similar to results mentioned here for ClC-Kb currents in human cells, R8W dramatically diminished while R8L and G47R completely abolished the stimulatory effect of barttin on ClC-Ka currents in oocytes. However, G10S is reported to induce much higher ClC-Ka currents in oocytes compared to WT barttin (Estévez, Boettger et al. 2001). This difference of G10S effect reported in oocytes compared to results presented in this thesis might be due to the different expression systems. G47R abolishes the stimulatory effect on ClC-Ka (Estévez, Boettger et al. 2001) as reported here on both ClC-Ka and Kb.

4.3.2 Rat ClC isoform

Rat ClC-K1 is the only ClC-K channel known to both traffick to the plasma membrane and conduct ions in the absence of barttin. This made it a good candidate to look for barttins effect on the channels properties. ClC-K channels have a lack of voltage-dependent gating which is gained by insertion of a glutamic acid instead of a neutral amino acid in the GKEGP motif. This absence of voltage dependence might be important for their role in transepithelial transport (Waldegger and Jentsch 2000), and mutating this motif back in the rat ClC-K1 channels created a channel with gating properties highly influenced in the presence of barttin.

Representative current recordings from V166E mutated ClC-K1 with mutated or WT barttin showed all mutants, except for Q32X, able to bind the channel and invert its voltage dependence. Currents measured at +105mV showed that G10S and E88X barttin induced V166E rClC-K1 current amplitudes like WT barttin while R8L, R8W and G47R gave intermediate amplitudes. Q32X barttin did not increase the channels current amplitude and was not detected at the membrane (Fig. 3.10). In oocytes, barttin R8L and R8W almost completely abolished the ClC-K1 activation by barttin though G10S still activated like WT barttin (Waldegger, Jeck et al. 2002) which is comparable to the results in this thesis.

Non-stationary noise analysis showed that E88X barttin gave similar channel properties as WT barttin while R8L, G10S and G47R gave slightly decreased absolute open probabilities in the positive voltage range while R8L and G47R have an additional increase in the negative voltage range. All tested mutants resulted in a similar single channel amplitude of V166E rClC-K1 as WT barttin.

4.4 Conclusions

WT and mutant barttin induce ClC-Kb exit from the ER to the golgi apparatus where complex glycosylation is finished. This could have a stabilizing effect on the channel, protecting it from proteolysis. As we have previously shown (Scholl, Hebeisen et al. 2006), the N-terminal part of barttin that contains the two transmembrane domains is very important for barttins ability to traffick to the membrane and activate ClC-K channels. The mutations in the gene encoding for barttin, leading to Bartter syndrome type IV, all reside in this area. Thus most mutated barttins are able to traffick to the plasmamembrane but are unable to activate the ClC-Kb protopores. G47R gives less membrane insertion of ClC-Kb channels due to less total amount of ClC-Kb and only activates the protopore partially, this might not be enough to give visible activation of ClC-Kb. The current amplitude measurement for ClC-Ka was similar as for ClC-Kb, since only E88X barttin induced currents like WT barttin. This might suggest the same inability of activating the ClC-Ka protopore as for ClC-Kb. Q32X is the only tested barttin mutant that is dramatically affected in its trafficking and maybe binding abilities. E88X results in a sorting disability.

The symptoms of Q32X induced Bartter syndrome are the most severe, consistent with its failure in both the trafficking as well as the activating properties of barttin. G10S is discovered early however, does not lead to renal end stage failure while G47R is detected later in life. The late detection of the G47R mutation could be due to its partial functionality, while G10S is severely affected though still able to traffick to the membrane. The E88X patient was also diagnosed early, though only channel sorting seems to be affected.

4.5 Further research

The barttin protein is still not completely understood. The use of a cell line derived from the inner ear (Teixeira, Viengchareun et al. 2006) instead of kidney could give more insights in the function of barttin. Barttin exhibits a CQC motif at the boundary of the second membrane helix and the cytoplasmic tail. This is the same position as the CQC motif found to be nessecary for plasma membrane targeting of the epithelial Mucin MUC1 (Pemberton, Rughetti et al. 1996).

ER retention of ClC-Kb could be due to a lack of export signal, expression of a retention signal or it is actively retrieved from the golgi apparatus. The retention of CLC-Kb either in the ER or the golgi apparatus in the absence of barttin, could suggest a retention motif in the channel protein and maybe an export signal in barttin. Barttin could cover a retention signal in the ClC-Kb channel. Further, barttin might only be nessecary for ClC-Kb trafficking to the golgi apparatus and the glycosylation of ClC-Kb could target the channel to membrane or barttin is also needed to transport the channel there. There also has to be a reason for barttin E88X to loose its sorting ability. Though it is more likely for ClC-Ka and Kb to contain a sorting motif than for barttin, since ClC-Ka resides on apical and basolateral sides of the cell and ClC-Kb only basolateral.

E88X barttin might also lead to Bartter syndrome type IV because of a lack of regulation, due to loss of the PY motif. This motif is involved in regulation of diverse proteins. Liddle's channels are beta-ENaC channels that lack a PY motif and exhibit impaired Na^+-feedback regulation (Kamynina and Staub 2002). Its absence could inhibit the endoplasmatic reticulum degradation machinery, that degrades misfolded proteins of the ER in a ubiquitin and proteasome dependent manner. It could lead to a stagnation of protein production due to clogged ER and lack of usable amino acids in the cell or result in higher cell surface expression of the protein due to the lack of internalisation. In this thesis is shown that there is a similar amount of ClC-Kb in the plasma membrane as induced by WT barttin in not polarized cells or even less in polarized cells. The PY motif is a regulatory domain, when it is mutated it gives more plasma membrane detection and higher ClC-K currents. This is not the case for E88X barttin, which also lacks this PY motif. It would be interesting to know if there is a stimulating motif that is lost in the E88X deleted protein.

A difference in calcium sensitivity in the presence or absence of barttin was previously suggested to show a direct modification of ClC-K1 channels by barttin. Barttin dramatically increased the current amplitude of ClC-K1 (Waldegger and Jentsch 2000; Waldegger, Jeck et al. 2002) and was co-precipitated with ClC-K2 suggesting a protein-protein interaction (Hayama, Rai et al. 2003). Interaction studies of barttin with ClC-Kb could show the interaction domains of both proteins and possible defects in disease causing barttin or ClC-Kb mutants.

5. Abstract

5.1 Abstract, Englisch

Bartter syndrome type IV is an inherited human disease combining severely reduced renal salt absorption and sensorineural deafness. The affected gene, *BSND*, encodes barttin, which is an accessory subunit of ClC-K chloride channels. These channels are present in the kidney and the inner ear. Barttin modifies stability, surface insertion and function of ClC-K channels. Distinct mutations cause disease symptoms of diverse severity. To define the molecular basis of this diversity, six disease-causing mutations – R8L, R8W, G10S, Q32X, G47R, and E88X – were examined. The functional consequences of these mutations on ClC-K channel properties were examined using a combination of heterologous and stable expression in renal cell lines, electrophysiology, confocal imaging and biochemical analysis. Three missense mutations, R8L, R8W and G10S abolish the function of human ClC-K/barttin channels, but have only minor effects on subcellular trafficking. Another mutant with mild renal phenotype, G47R, is capable of performing all functions of WT barttin but binds less effectively to ClC-K channels or only partially activates the ClC-K protopore. E88X influences epithelial sorting, disabling barttins preference for the basolateral membrane. Q32X barttin associates with ClC-K channels but fails to promote surface membrane insertion and channel activation. This is the only tested mutation that leads to renal failure. These results demonstrate that Bartter syndrome type IV is not always caused by an impaired scaffolding function of barttin, but by various affected functions of barttin, most importantly its effect on anion conduction by human ClC-K channels.

Keywords:
Bartter Syndrome type IV
ClC-K chloride channels
barttin

5.2 Zusammenfassung, German

Bartter Syndrom Typ IV ist eine erbliche Erkrankung des Menschen, die eine deutliche Reduktion der renalen Salzresorption mit sensorisch-neuraler Taubheit kombiniert. Das beeinträchtigte Gen, BSND, kodiert für Barttin, eine akzessorische Untereinheit von ClC-K Chloridkanälen. Diese Kanäle werden sowohl in der Niere als auch im Innenohr exprimiert. Barttin modifiziert die Stabilität, den Oberflächeneinbau in die Plasmamembran und die Funktion des ClC-K Kanals. Verschiedene Mutationen verursachen Krankheitssymptome von unterschiedlichem Schweregrad. Um die molekulare Basis dieser Diversität herauszufinden, wurden sechs krankheitsverursachende Mutationen – R8L, R8W, G10S, Q32X, G47R, und E88X – untersucht. Die funktionelle Beinträchtigung der ClC-K Kanaleigenschaften durch diese Mutationen wurde mit einer Kombination aus heterologer und stabiler Expression in Nierenzelllinien untersucht, sowie mit Verfahren der Elektrophysiologie, Konfokalmikroskopie und mit biochemischen Analysen. Drei Mutationen, R8L, R8W und G10S, blockieren die Funktion humaner ClC-K Kanäle, haben aber nur einen geringen Einfluss auf subzelluläre Kanaltransportvorgänge. Eine andere Mutante mit einem milden Nierenphenotyp, G47R, ist in der Lage alle Funktionen des WT Barttins aus zu üben, bindet aber weniger effizient an ClC-K Kanäle oder aktiviert die ClC-K-Protoporen nur teilweise. Die Mutation E88X beeinflusst die epitheliale Verteilung, indem sie die den vorzugsweisen Einbau des Barttins in die basolaterale Membran aufhebt. Q32X Barttin assoziiert mit ClC-K Kanälen, fördert aber weder den Einbau in die Oberflächenmembran noch die Kanalaktivierung. Dies ist die einzige getestete Mutation, die bei Patienten zum Nierenversagen führt. Diese Ergebnisse zeigen, dass krankheits-verursachende Barttin-Mutationen nicht immer den Einbau von ClC-K Kanälen in die oberflächliche Membran verhindern, sondern eine Vielzahl anderer Funktionen beeinträchtigen können

Stichwörter:
Bartter Syndrom Typ IV
ClC-K Chlorid Kanälen
barttin

6. References

Akizuki, N., S. Uchida, et al. (2001). "Impaired solute accumulation in inner medulla of *Clcnk1-/-* mice kidney." American Journal of Physiology - Renal Physiology **280**: F79-F87.

Alvarez, O., C. Gonzalez, et al. (2002). "Counting channels: A tutorial guide on ion channel fluctuation analysis." Advances in Physiology Education **26**(4): 327-341.

Barlassina, C., C. Dal Fiume, et al. (2007). "Common genetic variants and haplotypes in renal CLCNKA gene are associated to salt-sensitive hypertension." Human Molecular Genetics **16**(13): 1630-1638.

Bartter, F. C., P. Pronove, et al. (1962). "Hyperplasia of the Juxtaglomerular Complex with Hyperaldosteronism and Hypokalemic Alkalosis." American Journal of Medicin **33**: 811-828.

Birkenhager, R., E. Otto, et al. (2001). "Mutation of BSND causes Bartter syndrome with sensorineural deafness and kidney failure." Nature Genetics **29**: 310-314.

Blanz, J. and A. Zdebik (2004). "Krankheiten durch Mutationen in Chloridkanälen der ClC-familie." Biospektrum (Heidelberg) **10**: 507-509.

Brennan, T. M. H., D. Landau, et al. (1998). "Linkage of infantile Bartter syndrome with sensorineural deafness to chromosome 1p." The American Journal of Human Genetics: 355-361.

Briet, M., R. Vargas-Poussou, et al. (2005). "How Bartter´s and Gitelman´s Syndromes, and Dent´s Disease have provided important insights into the function of three renal chloride channels: ClC-Ka/b and ClC-5." Nephron Physiology **103**: 7-13.

Brum, S., J. Rueff, et al. (2007). "Unusual adult-onset manifestation of an attenuated Bartter's syndrome type IV renal phenotype caused by a mutation in BSND." Nephrology Dialysis Transplantation **22**: 288.

Burnham, C. E., H. Amlal, et al. (1997). "Cloning and functional expression of a human kidney Na^+:HCO^-_3 cotransporter." The Journal of Biological Chemistry **272**(31): 19111-19114.

Catalán, M., M. I. Niemeyer, et al. (2004). "basolateral ClC-2 chloride channels in surface colon epithelium: regulation by a direct effect of intracellular chloride." Gastroenterology **126**: 1104-1114.

Cheng, C., G. Glover, et al. (2002). "A novel sorting motif in the glutamate transporter excitatory amino acid transporter 3 directs its targeting in Madin-Darby Canine Kidney cells and hippocampal neurons." The Journal of Neuroscience **22**(24): 10643-10652.

Daniels, G. M. and S. G. Amara (1998). "Selective labelling of neurotransmitter transporters at the cell surface." Methods in Enzymology **296**: 307-318.

Deen, P. M. T., B. W. M. van Balkom, et al. (2002). "Aquaporin-2: COOH terminus is necessary but not sufficient for routing to the apical membrane." American Journal of Physiology - Renal Physiology **282**: F330-F340.

Dhani, S. U., R. Mohammad-Panah, et al. (2003). "Evidence for a functional interaction between the ClC-2 chloride channel and the retrograde motor dynein complex." The Journal of Biological Chemistry **278**(18): 16262-16270.

D'Souza-Li, L. (2006). "The calcium-sensing receptor and related diseases." Arquivos Brasileiros de Endocrinologia & Metabologia **50**(4): 628-639.

Dutzler, R. (2006). "The ClC family of chloride channels and transporters." Current Opinion in Structural Biology **16**: 439-446.

Dutzler, R., E. B. Campbell, et al. (2002). "X-ray structure of a ClC chloride channel at 3.0A reveals the molecular basis of anion selectivity." Nature **415**: 287-294.

Embark, H. M., C. Böhmer, et al. (2004). "Regulation of ClC-Ka/barttin by the ubiquitin ligase Nedd4-2 and the serum- and glucocorticoid-dependent kinases." Kidney International **66**: 1918-1925.

Estévez, R., T. Boettger, et al. (2001). "Barttin is a Cl^- channel ß-subunit crucial for renal Cl^- reabsorption and inner ear K^+ secretion." Nature **414**: 558-561.

Fahlke, C. (2001). "Ion permeation and selectivity in ClC-type chloride channels." American Journal of Physiology - Renal Physiology **280**: F748-F757.

Fahlke, C., H. T. Yu, et al. (1997). "Pore-forming segments in voltage-gated chloride channels." Nature **390**: 529-532.

Fava, C., M. Montagnana, et al. (2007). "The functional variant of the CLC-Kb channel T481S is not associated with blood pressure or hypertension in Swedes." Journal of Hypertension **25**(1): 111-116.

Fischer, M., A. G. H. Janssen, et al. (2008). "Fast and slow gating of rat ClC-K1 channels." Acta Physiologica **192**(663): 53.

Fong, P. (2004). "ClC-K Channels: If the Drug fits, use it." EMBO Reports **5**(6): 565-566.

Frey, A., A. Lampert, et al. (2006). "Influence of gain of function epithelial chloride channel ClC-Kb mutation on hearing thresholds." Hearing Research **214**(1-2): 68-75.

Fukuyama, S., M. Hiramatsu, et al. (2004). "Novel mutations of the chloride channel Kb gene in two Japanese patients clinically diagnosed as Bartter Syndrome with hypocalciuria." J. Clin. Endocrinol. Metab. **89**(11): 5847-5850.

García-Nieto, V., C. Flores, et al. (2006). "Mutation G47R in the *BSND* gene causes Bartter syndrome with deafness in two Spanish families." Pediatric Nephrology **21**: 643-648.

Gonzalez-Gutierrez, G., E. Miranda-Laferte, et al. (2007). "The Src homology 3 domain of the ß-subunit of voltage-gated calcium channels promotes endocytosis via dynamin interaction." The Journal of Biological Chemistry **282**(4): 2156-2162.

Haug, K., M. Warnstedt, et al. (2003). "Mutations in ClCN2 encoding a voltage-gated chloride channel are associated with idiopathic generalized epilepsies." Nature Genetics **33**: 527-532.

Hayama, A., T. Rai, et al. (2003). "Molecular mechanisms of Bartter syndrome caused by mutations in the BSND gene." Histochem Cell Biol **119**: 485-493.

Hebeisen, S., A. Biela, et al. (2004). "The role of the carboxy terminus in ClC chloride channel function." The Journal of Biological Chemistry **279**(13): 13140-13147.

Hebert, S. C. (2003). "Bartter syndrome." Current opinion in Nephrology and Hypertension **12**: 527-532.

Hidalgo, P. and A. Neely (2007). "Multiplicity of protein interactions and functions of the voltage-gated calcium channel ß-subunit." Cell Calcium **42**: 389-396.

Hunter, M. (2001). "Accessory to kidney disease." Nature **414**: 502-503.

Icking, A., M. Amaddii, et al. (2007). "Polarized transport of Alzheimer amyloid precursor protein is mediated by adaptor protein complex AP1-1B." Traffic **8**: 285-296.

Jeck, N., S. C. Reinalter, et al. (2001). "Hypokalemic salt-losing tubulopathy with chronic renal failure and sensorineural deafness." Pediatrics **108**(1).

Jeck, N., P. Waldegger, et al. (2004). "A common sequence variation of the *CLCNKB* gene strongly activates ClC-Kb chloride channel activity." Kidney International **65**: 190-197.

Jeck, N., S. Waldegger, et al. (2004). "Activating mutation of the renal epithelial chloride channel ClC-Kb predisposing to hypertension." Hypertension **43**: 1175-1181.

Jentsch, T. J., T. Friedrich, et al. (1999). "The ClC chloride channel family." Pflügers Archives - European Journal of Physiology **437**: 783-795.

Jentsch, T. J., K. Steinmeyer, et al. (1990). "Primary structure of *Torpedo marmorata* chloride channel isolated by expression cloning in *Xenopus* oocytes." Nature **348**: 510-514.

Jurman, M. E., L. M. Boland, et al. (1994). "Visual identification of individual transfected cells for electrophysiology using antibody-coated beads." Biotechniques **17**(5): 876-881.

Kamsteeg, E.-J., D. G. Bichet, et al. (2003). "Reversed polarized delivery of an aquaporin-2 mutant causes dominant nephrogenic diabetes insipidus." The Journal of Cell Biology **163**(5): 1099-1109.

Kamynina, E. and O. Staub (2002). "Concerted action of ENaC, Nedd4-2, and Sgk1 in transepithelial Na^+ transport." American Journal of Physiology - Renal Physiology **283**: F377-387.

Kieferle, S., P. Fong, et al. (1994). "Two highly homologous members of the ClC chloride channel familiy in both rat and human kidney." Proceedings of the National Academy of Sciences **91**: 6943-6947.

Kitananka, S., U. Sato, et al. (2006). "A compound heterozygous mutation in the BSND gene detected in Bartter syndrome type IV." Pediatric Nephrology **21**: 190-193.

Kobayashi, K., S. Uchida, et al. (2002). "Human ClC-Kb gene promoter drives the EGFP expression in the specific distal nephron segments and inner ear." Journal of the American Society of Nephrology **13**: 1992-1998.

Koivisto, U.-M., A. L. Hubbard, et al. (2001). "A novel cellular phenotype for familial hypercholesterolemia due to a defect in polarized targeting of LDL receptor." Cell **105**: 575-585.

Kokubo, Y., N. Iwai, et al. (2005). "Association analysis between hypertension and *CYBA*, *CLCNKB*, and *KCNMB1* functional polymorphisms in the Japanese population." Circulation Journal **69**: 138-142.

Konrad, M., M. Vollmer, et al. (2000). "Mutations in the chloride channel gene ClCNKB as a cause of classic Bartter Syndrome." Journal of the American Society of Nephrology **11**: 1449-1459.

Krämer, B. K., T. Bergler, et al. (2008). "Mechanisms of disease: the kidney-specific chloride channels ClCKA and ClCKB, the barttin subunit, and their clinical relevance." Nature Clinical Practice - Nephrology **4**(1): 38-46.

Kutub Ali, M. and C. Bergson (2003). "Elevated Inracellular calcium triggers recruitment of the receptor cross-talk accessory protein calcyon to the plasma membrane." The Journal of Biological Chemistry **278**(51): 51654-51663.

Landau, D., H. Shalev, et al. (1995). "Infantile variant of Bartter syndrome and sensorineural deafness: a new autosomal recessive disorder." American Journal of Medical Genetics **59**(4): 454-459.

Lange, P. F., L. Wartosch, et al. (2006). "ClC-7 requires Ostm1 as ß-subunit to support bone resorption and lysosomal function." Nature **440**: 220-223.

Lei, J., S. Nowbar, et al. (2003). "Thyroid hormone stimulates Na-K-ATPase activity and its plasma membrane insertion in rat alveolar epithelial cells." American Journal of Physiology - Lung Cellular and Molecular Physiology **285**: L762-L772.

Li, H. C., E. Y. Li, et al. (2007). "Identification of a novel signal in the cytoplasmic tail of the Na^+:HCO^-_3 cotransporter NBC1 that mediates basolateral targeting." American Journal of Physiology - Renal Physiology **292**(F1245-F1255).

Li, H. C., R. T. Worrell, et al. (2004). "Identification of a carboxyl-terminal motif essential for the targeting of Na^+-HCO^-_3 cotransporter NBC1 to the basolateral membrane." The Journal of Biological Chemistry **279**(41): 43190-43197.

Liantonio, A., A. Picollo, et al. (2006). "Activation and inhibition of kidney ClC-K chloride channels by fenamates." Molecular Pharmacology **69**: 165-173.

Liantonio, A., A. Picollo, et al. (2008). "Molecular switch for ClC-K Cl^- channel block/activation: optimal pharmacophoric requirements towards high-affinity ligands." Proceedings of the National Academy of Sciences **105**(4): 1369-1373.

Liantonio, A., M. Pusch, et al. (2004). "Investigations of pharmacologic properties of the renal ClC-K1 chloride channel co-expressed with barttin by the use of 2-(p-chlorophenoxy)propionic acid derivates and other structurally unrelated chloride channel blockers." Journal of the American Society of Nephrology **15**: 13-20.

Lopez, C., S. Métral, et al. (2005). "The ammonium transporter RhBG, requirement of a tyrosine-based signal and ankyrin-G for basolateral targeting and membrane anchorage in polarized kidney epithelial cells." The Journal of Biological Chemistry **280**(9): 8221-8228.

Lui, W., T. Morimoto, et al. (2002). "Analysis of NaCl transport in thin ascending limb of Henle's loop in ClC-K1 null mice." American Journal of Physiology - Renal Physiology **282**: F451-F457.

Maley, F., R. B. Trimble, et al. (1989). "Characterization of glycoproteins and their associated oligosaccharides through the use of endoglycosidases." Analytical Biochemistry **180**: 195-204.

Matsuda, J. J., M. S. Filali, et al. (2008). "Overexpression of ClC-3 in HEK293T cells yiels novel currenct that are pH dependent." American Journal of Physiology - Cell Physiology **294**: C251-C262.

Matsumura, Y., S. Uchida, et al. (1999). "Overt nephrogenic diabetes insipidus in mice lacking the ClC-K1 chloride channel." Nature Genetics **21**: 95-98.

Maulet, Y., R. C. Lambert, et al. (1999). "Expression and targeting to the plasma membrane of xClC-K, a chloride channel specifically expressed in distinct tubule segments of Xenopus laevis kidney." Biochemical Journal **340**: 737-743.

Meyer, S. and R. Dutzler (2006). "Crystal structure of the cytoplasmic domain of the chloride channel ClC-0." Structure **14**: 299-307.

Miller, C. (1982). "Open-state substructure of single chloride channels from Torpedo electropax." Philos. Trans. R. Soc. Lond. B. Biol. Sci. **299**(1097): 401-411.

Miyamura, N., K. Matsumoto, et al. (2003). "Atypical Bartter Syndrome with sensorineural deafness with G47R mutation of the ß-subunit for ClC-Ka and ClC-Kb chloride channels, barttin." The Journal of Clinical Endocrinology & Metabolism **88**(2): 781-786.

Mohammad-Panah, R., K. Gyomorey, et al. (2001). "ClC-2 contributes to native chloride secretion by a human intestinal cell line, caco-2." The Journal of Biological Chemistry **276**(11): 8306-8313.

Nozu, K., T. Inagaki, et al. (2008). "Molecular analysis of digenic inheritance in Bartter syndrome with sensorineural deafness." J. Med. Genet. **45**: 182-186.

Ozlu, F., H. Yapicioglu, et al. (2006). "Barttin mutations in antenatal Bartter syndrome with sensorineural deafness." Pediatric Nephrology.

Parker, A. K. T., F. V. Gergely, et al. (2004). "Targeting of inositol 1,4,5,-triphosphate receptors to the endoplasmatic reticulum by multiple signals within their transmembrane domains." The Journal of Biological Chemistry **279**(22): 23797-23805.

Pemberton, L. F., A. Rughetti, et al. (1996). "The epithelial mucin MUC1 contains at least two discrete signals specifying membrane localization in cells." The Journal of Biological Chemistry **271**(4): 2332-2340.

Peña-Münzenmayer, G., M. Catalán, et al. (2005). "Basolateral localization of native ClC-2 chloride channels in absorptive intestinal epithelial cells and basolateral sorting encoded by a CBS-2 domain di-leucine motif." Journal of Cell Science **118**: 4243-4252.

Petäjä-Repo, U., M. Hogue, et al. (2000). "Export from the endoplasmatic reticulum represents the limiting step in the maturation and cell surface expression of the human [delta] optoid receptor." The Journal of Biological Chemistry **275**(18): 13727-13736.

Picollo, A., A. Liantonio, et al. (2004). "Molecular determinants of differential pore blocking of kidney ClC-K chloride channels." EMBO Reports **5**(6): 584-589.

Plaut, R. D. and N. H. Carbonetti (2008). "Retrograde transport of pertussis toxin in the mammalian cell." Cellular Microbiology.

Pusch, M., G. Zifarelli, et al. (2006). "Channel or transporter? The ClC saga continues." Experimental Physiology **91**: 149-152.

Robben, J. H., N. V. A. M. Knoers, et al. (2006). "Cell biological aspects of the vasopressin type-2 receptor and aquaporin 2 water channel in nephrogenic diabetes insipidus." American Journal of Physiology - Renal Physiology **291**: F257-F270.

Schlingmann, K. P., M. Konrad, et al. (2004). "Salt wasting and deafness resulting from mutations in two chloride channels." The New England Journal of Medicine **350**(13): 1314-1319.

Schmieder, S., S. Bogliolo, et al. (2007). "N-glycosylation of the Xenopus laevis ClC-5 protein plays a role in cell suface expression, affecting transport activity at the plasma membrane." Journal of Cellular Physiology **210**: 479-488.

Schmieder, S., S. Lindenthal, et al. (2001). "Tissue-specific N-glycosylation of the ClC-3 chloride channel." Biochemical and Biophysical Research Communications **286**: 635-640.

Scholl, U., S. Hebeisen, et al. (2006). "Barttin modulates trafficking and function of ClC-K channels." Proceedings of the National Academy of Sciences **103**(30): 11411-11416.

Shalev, H., M. Ohali, et al. (2003). "The neonatal variant of Bartter Syndrome and Deafness: Preservation of renal function." Pediatrics **112**(3): 628-633.

Sile, S., N. B. Gillani, et al. (2007). "Functional *BSND* variants in essential hypertension." American Journal of Hypertension **20**: 1176-1182.

Sile, S., C. G. Vanoye, et al. (2006). "Molecular physiology of renal ClC chloride channels/transporters." Current Opinion in Nephrology and Hypertension **15**: 511-516.

Simon, D. B., R. S. Bindra, et al. (1997). "Mutations in the chloride channel gene, ClCNKB, cause Bartter's syndrome type III." Nature Genetics **17**: 171-178.

Soetens, O., J.-O. De Craene, et al. (2001). "Ubiquitin is required for sorting to the vacuole of the yeast general amino acid permease, Gap1." The Journal of Biological Chemistry **276**(47): 43949-43957.

Sohara, E., T. Rai, et al. (2006). "Pathogenesis and treatment of autosomal-dominant nephorgenic diabetes insipidus caused by an aquaporin 2 mutation." Proceedings of the National Academy of Sciences **103**(38): 14217-14222.

Teixeira, M., S. Viengchareun, et al. (2006). "Functional I_{sk}/KvLQT1 potassium channel in a new corticosteroid-sensitive cell line derived from the inner ear." The Journal of Biological Chemistry **281**(15): 10496-10507.

Traverso, S., L. Elia, et al. (2003). "Gating competence of constitutively open ClC-0 mutants revealed by the interaction with a small organic inhibitor." The Journal of General Physiology **122**: 295-306.

Uchida, S. (2000). "In vivo role of ClC chloride channels in the kidney." American Journal of Physiology - Renal Physiology **279**: F802-F808.

Uchida, S. and S. Sasaki (2005). "Function of chloride channels in the kidney." Annual Review of Physiology **67**: 759-778.

Uchida, S., S. Sasaki, et al. (1995). "Localization and functional characterization of rat kidney-specific chloride channel, ClC-K1." Journal of Clinical Investigation **95**: 104-113.

Vandewalle, A., F. Cluzeaud, et al. (1997). "Localization and induction by dehydration of ClC-K chloride channels in the rat kidney." American Journal of Physiology **272**(5 Pt 2): F678-F688.

Vollmer, M., N. Jeck, et al. (2000). "Antenatal Bartter syndrome with sensorineural deafness: refinement of the locus on chromosome 1p31." Nephrology Dialysis Transplantation **15**: 970-974.

Waldegger, S., N. Jeck, et al. (2002). "Barttin increases surface expression and changes current properties of ClC-K channels." European Journal of Physiology **444**: 411-418.

Waldegger, S. and T. J. Jentsch (2000). "Functional and structural analysis of ClC-K chloride channels involved in renal disease." The Journal of Biological Chemistry **275**(32): 24527-24533.

Warner, F. J., R. A. Lew, et al. (2005). "Angiotensin-converting enzyme 2 (ACE2), but not ACE, is preferentially localized to the apical surface of polarized kidney cells." The Journal of Biological Chemistry **280**(47): 39353-39362.

Zaffanello, M., A. Taranta, et al. (2006). "Type IV Bartter syndrome: report of two new cases." Pediatric Nephrology **21**: 766-770.

Zelikovic, I. (2003). "Hypokalaemic salt-losing tubulopathies: an evolving story." Nephrology Dialysis Transplantation **18**: 1696-1700.

Zerangue, N., M. J. Malan, et al. (2000). "Analysis of endoplasmatic reticulum trafficking signals by combinatorial screening in mammalian cells." Proceedings of the National Academy of Sciences **98**(5): 2431-2436.

Ziemer, M., C. Diaz-Cascajo, et al. (2000). ""Tubular Spitz's nevus"-an artifact of fixation?" Journal of Cutaneous Pathology **27**: 500-504.

7. Acknowledgements

I would like to thank Prof. Dr. Christoph Fahlke for his guidance over the last few years. The project which resulted in this thesis was financed by the Deutsche Forschungsgemeinschaft (DFG). Furthermore, I owe thanks to PD. Dr. Anaclet Ngezahayo and Prof. Dr. rer. nat. Symeon Papadopoulos, for taking the time and effort to read this thesis and take part in the exam. Symeon, also thank you for granting me access to your confocal microscope. Dr. Rudolf Bauerfeind and Alexander Polster, thanks for your help with the fluorescent microscopy. Thanks to all the people in the lab at the RWTH Aachen and MH Hannover for accepting me as I ran around the lab. Special thanks to Dr. Patricia Hidalgo, Dr.-med. Ute Scholl, Dr. Simon Hebeisen, Dr. Martin Fischer and Dr. Alexi Alekov for helpful discussions and the last three also for proofreading parts of this thesis. Birgit Begemann, Toni Becher, Hannelore Heidtmann and Barbara Poser thank you very much for technical assistance. Every lab should have a Barbara, to keep things organised. Burkhard Berkelmann, thank you for keeping the lab running in Hannover. Labs run on technical assistants, a force of nature often ignored.

Sonja Meyer zu Berstenhorst thank you for being there. Ivanna Shcherbyna, thank you for taking me to the movies, eating and chatting. You were the friend I needed. Thanks to my friends at home who have seen too little of me the last few years but were always very understanding about this and kept believing in me. Of course, I am grateful to my brother and parents, always making it a pleasure to go home. Keeping faith aside from their worries. And Bart... nobody can understand these last few years better than you. Thank you for always believing in me, standing by me when things were very difficult.

8. Curriculum vitae

Audrey Gertruda Huberdina Janssen

July 8th 1980	Born in Venray, The Netherlands, as daughter of Herman Janssen and Petronella Poels
1992-1997	Raayland College, Venray (NL), B-levels
1997-1999	Raayland College, Venray (NL), A-levels
1999-2004	Radboud University Nijmegen (NL), M.Sc. in (medical) microbiology and biochemistry. Guest research apprenticeship at the University of Sussex (UK).
2004-present	PhD position at the Department from Prof. C. Fahlke. First at the RWTH Aachen than at the MH Hannover. Guest researcher at the Research Centre in Jülich (D).

9. List of publications

Under revision	**Janssen A.G.H.**, Scholl U., Domeyer C., Begemann B., Nothmann D., Fahlke C. Disease-causing dysfunctions of barttin in Bartter Syndrome type IV. Journal of the American Society of Nephrology.
2008	**Janssen A.G.H.**, Domeyer C., Fahlke C. (2008). Barttin mutations in Bartter syndrome type IV. Acta Physiologica 192, (663): 60. Conf. Proceedings.
2008	Fischer M., **Janssen A.G.H.**, Fahlke C. (2008). Fast and slow gating of rat ClC-K1 channels. Acta Physiologica 192, (663): 53. Conf. Proceedings.
2007	**Janssen A.G.H.**, Domeyer C., Fahlke C. (2007). Functional consequences of barttin mutations causing Bartter´s syndrome type IV. Acta Physiologica 189, (653): 46. Conf. Proceedings.
2007	Boroumand M., **Janssen A.G.H.**, Fahlke C., Fischer M. (2007). Barttin modifies fast and slow gating of ClC-K channels. Acta Physiologica 189, (653): 99. Conf. Proceedings.
2006	Scholl U., Hebeisen S., **Janssen A.G.H.**, Müller-Newen G., Alekov A., Fahlke C. (2006). Barttin modulates trafficking and function of ClC-K channels. Proceedings of the National Academy of Sciences 103, (30): 11411-11416.